ADSORPTION OF CARBON DIOXIDE USING CHEMICALLY TREATED FLY ASH

BY

ALI LAWAN YAUMI

A Thesis Presented to the
DEANSHIP OF GRADUATE STUDIES

KING FAHD UNIVERSITY OF PETROLEUM & MINERALS

DHAHRAN, SAUDI ARABIA

In Partial Fulfillment of the
Requirements for the Degree of

MASTER OF SCIENCE

In

CHEMICAL ENGINEERING

MAY 2012

KING FAHD UNIVERSITY OF PETROLEUM & MINERALS

DHAHRAN 31261, SAUDI ARABIA

DEANSHIP OF GRADUATE STUDIES

This thesis, written by **ALI LAWAN YAUMI** under the direction of his thesis advisor and approved by his thesis committee, has been presented to and accepted by the Dean of Graduate Studies, in partial fulfillment of the requirements for the degree of **MASTER OF SCIENCE IN CHEMICAL ENGINEERING**.

Thesis Committee

Dr. Reyad A. Shawabkeh (Advisor)

Dr. Ibnelwaleed A. Hussein (Member)

Dr. Nadhir A. H. Al Baghli (Member)

Dr. Usamah A. Al-Mubaiyedh
Department Chairman

Dr. Salam A. Zummo
Dean of Graduate Studies

13/5/12
Date

ii

DEDICATION

This work is dedicated to my beloved parents, wife and daughter.

ACKNOWLEDGEMENT

ALHAMDULILLAH, all praises are due to Allah, Most Beneficent Most Merciful, Master of glory and Honour for giving me the life, health and opportunity to complete this program and research. I acknowledge King Fahd University of Petroleum and Minerals for giving me the opportunity to undertake this graduate studies program.

I express my profound gratitude to my competent and patient advisor, Dr. Reyad A. Shawabkeh for his tireless efforts, dedication and valuable contribution in making the research successful and my committee members Dr. Ibnelwaleed A. Hussein and Dr. Nadhir A. Al Baghli for their valuable contributions and suggestion towards this research.

My sincere appreciation goes to the Chairman of Chemical Engineering Department Dr. Usamah A. Al-Mubaiyedh and all the staff for their support and encouragement

My special thanks to the entire Nigerian community for always making me feel at home

My profound appreciation goes to my dearest and beloved father, mother, wife, brothers, sisters and friends for their prayers, encouragement and advice throughout my studies and daily undertakings. May Almighty Allah reward you abundantly.

Finally, my special thanks go to all relations, friends and well-wishers.

Table of Content

List of Tables

List of Figures

THESIS ABSTRACT (ENGLISH)

Name: **Ali Lawan Yaumi**

Tittle: **Adsorption of Carbon Dioxide Using Chemically Treated Fly Ash**

Department: **Chemical Engineering**

Date: **01-05-2012**

The aim of this research is to treat two major environmental problems in the Saudi industrial sector in the Kingdom by chemically modifying waste fly ash to a useful material for adsorption of Carbon dioxide (CO_2) from gas stream. Adsorption is considered as one of the potential options because of its low energy requirement, cost advantage, and ease of applicability over a relatively wide range of temperatures and pressures. The chemically treated fly ash was characterized using several techniques such as EDXA, FTIR, XRD, SEM and BET in order to know the chemical composition and physical properties of the ash. Several kinetic parameters for adsorption of CO_2 were studied to obtain the best rate of adsorption. The results revealed that the surface morphology was quite different as a result of the chemical treatment of the fly ash surface. The maximum adsorption capacity of the amine functionalized ash was found to be 240 mg/g. The kinetic studies showed that adsorption capacity increases with increase in flow rate, concentration, low humidity and temperature. Thermodynamic studies showed that the heat of adsorption was 80 and 178 KJ/mol at low and high relative humidity's suggesting that the process is endothermic. The experimental data was modeled using Langmuir, Freunlich, BET and dispersion model. It was found that BET and dispersion models best fits the experimental data.

MASTER OF SCIENCE DEGREE

KING FAHD UNIVERSITY OF PETROLEUM AND MINERALS, SAUDI ARABIA

ملـخص الرســالة

الاســــــــــم: **على لاوان يومي.**

عنوان الرسالة: **امتصاص ثاني أكسيدالكربون باستخدام الرمادالمتطايرالمعالج كيميائيا.**

التخصـــــص: **الهندسة الكيميائية.**

تاريخ التخـرج: **مايو 2012.**

الهدف من هذا البحث التعامل مع اثنين من المشاكل البيئية الرئيسية في القطاع الصناعي السعودي في المملكة بتعديل الرماد المتطاير كيميائيا إلى مادة مفيدة لامتصاص ثاني أكسيد الكربون الامتزاز. ويعتبر الامتصاص كأحد الخيارات المحتملة نظراً للاحتياجات من الطاقة منخفضة، وميزة التكلفة، وسهولة التطبيق على نطاق واسع نسبيا من درجات الحرارة والضغط. تم التحقق من الرماد المتطاير المعالج كيميائيا باستخدام العديد من الأساليب مثل (SEM, XRD, FTIR, EDXA, BET) بغية معرفة التركيب الكيميائي والخصائص الفيزيائية من الرماد. تمت دراسة عدة عوامل حركيه للحصول على أفضل سعه للامتصاص. كشفت النتائج عن خواص سطحيه مختلفة تماما نتيجة للعلاج الكيميائي لسطح الرماد المتطاير. قدرة الامتصاص الحد الأقصى من الرماد المعاج بالأمين هي240 مغ/غ. وأظهرت الدراسات الحركية أن معدل الامتصاص يزيد مع زيادة في معدل التدفق، وتركيز وانخفاض الرطوبة ودرجات الحرارة. الدراسات أظهرت أن حرارة الامتزاز 80 و 178 كيلوجول/مول في ارتفاع وانخفاض الرطوبة النسبية مما يوحي بأن العملية اندوثيرميه. وكان على غرار البيانات التجريبية استخدام طراز لانغمويز، فريونليتش، والتشتت. ووجد أن نموذج التشتت يلائم البيانات التجريبيه.

درجة الماجستير في العلوم

جامعة الملك فهد للبترول والمعادن، المملكة العربية السعودية

CHAPTER ONE

1.0 INTRODUCTION

The gradual increase in the atmospheric concentration of Carbon dioxide (CO_2) is becoming a serious environmental problem [1]. The concentration of CO_2 in the atmosphere is promoted by the combustion of fossil fuels for the generation of electricity, combustion of heavy oil, coal, oil shale, and exhausts from automobiles as this leads to the depletion of the ozone which results in global warming. CO_2 as a greenhouse gas has a major impact on the environment and climate change which causes global warming [2]. The ecological systems, sea levels and the atmosphere are generally being affected by the rising level of CO_2. Currently, humans are emitting around 29 billion tons of CO_2 into the atmosphere per year. Around 43% remains in the atmosphere while the rest is absorbed by vegetation and the oceans [3]. For the past ten years (2002 – 2012), the average annual rate of increase is 2.07 ppm. This rate of increase is more than double the increase in the 1960s. Presently, the concentration of CO_2 in the atmosphere is 394.45ppm [4].

The consequences of CO_2 emission include reduction in productivity in agriculture, melting of ice caps due to rise in sea level, and reduction in ozone layer. Chemical reaction is also given a platform in the atmosphere due to increase in high cloud cover in winter causing the depletion of the ozone layer [5], weather systems of the earth changes, resulting in more climatic changes causing more drought, flood and stronger storms which facilitates the spread of diseases to areas which were too cold for them to survive. The effects on ecosystems could be many and varied as both plants and animals are sensitive to changes in the climate. The resulting diseases ranging from plants and animals would change with overall effects of most of the organism moving towards the north and south poles respectively [6].

The stabilization of CO_2 in the atmosphere can be potentially achieved by capture and sequestration from the main source of emission. Separation and recovery of CO_2 emitted by power plants can be achieved by processes such as liquid solvent absorption, membrane separation, pressure/temperature swing adsorption and cryogenic techniques [7, 8]. However, amine based processes and wet scrubbing systems are currently in use to separate in plants to commercially separate CO_2, due to the large amount of water needed in these systems, they are energy intensive [1]. These processes also have high regeneration energy, large equipment size, and solvent leakage from piping systems leading to corrosion of process equipment [9].

Adsorption is a potential technique used in the separation of CO_2 due to its low energy requirement, low cost, ease of applicability over wide range of

temperature and pressure. [1, 8, 10-15]. The classification of adsorption to be physical or chemical is based on the nature of bonding between the adsorbate and solid surface. Chemical adsorption involves electron transfer with high heat of adsorption while in physical adsorption; weak bonds are formed with low heat of adsorption [16]. However, the success of using adsorption as an efficient technique to separate CO_2 depends on the development of durable and easily regenerable adsorbent with high selectivity and adsorption capacity [2]. Among these materials are activated carbons, zeolites, fly ash and different metal oxides [17-19]. There are promising results from the use of zeolites in separating CO_2 from gas stream. It has been generally found that at lower temperature , the alumino - silicate based material have high adsorption capacity because of large internal pore volume, regularity in structure, molecular size of its pores and diverse framework in chemical composition, which enable them to be tailor-made into different structure and properties [20]. It has been shown by [17] that the CO_2 adsorption capacity of activated carbon, zeolite 13X and zeolite 4A were 110, 135 and 160mg/g at room temperature and 1atm CO_2 partial pressure. However, with increasing temperature, their adsorption capacity decreases rapidly. The adsorption capacities of zeolites are also affected by the presence of water. Activated carbons are known to be excellent adsorbents for the separation of CO_2, unlike zeolites, they do not require removal of moisture, they have large surface area, with easily modified pore structures and low cost, their used as an adsorbent for CO_2 separation is affected due to their high sensitivity to temperature associated with power plant flue gases [1].

The combustion of coal and fossil fuel results in a by- product called fly ash which are normally collected by means of cyclones(mechanical devices) or electrostatic precipitators to control air pollution [22]. Fly ash is used in different applications such as water pollution control [24], agriculture [25] and recovery of metals [26]. However, this material has no economical value and is one of the major wastes materials in the Kingdom that requires disposal. About 25% of fly ash produced is used annually worldwide with utilization of about 95% in Germany, Netherlands; Belgium in 1996 [27] and 50% utilization was reported in the United Kingdom in 1998. However, large quantities of fly ash is produced in united states and china with 32% and 40% utilization levels respectively [12, 28].

According to 2009 survey of American Chemical Society, united states produced more than 71 million tons of fly ash annually in and only 45% of the quantity were used in different applications[22], while the rest are dumped in landfills, such disposal is not economic and environmental unfriendly [29].

Particular attention has been given to fly ash as an economical adsorbent for its leachability of metals from waste water and removal of flue gases because of its readily availability and abundance [30], another advantage of using fly ash is its ability to easily solidify after the pollutants are adsorbed [31] .The components of fly ash are basically alumina, silica, iron oxide and residual carbon, but these constituents vary according to the coal type used and the degree of combustion [1]. The objective of this study is to use of a waste material, fly

ash, for the treatment of another waste gas such as CO_2. The surface of the ash will be chemically treated in order enhance its removal capacity and selectivity against CO_2.

1.1 OBJECTIVES

The aim of this research is to treat two major environmental problems in the Saudi industrial sector in the Kingdom by chemically modifying waste fly ash to a useful material for adsorption of CO_2 from gas stream. The ultimate goal in this work is to remove a pollutant using another pollutant as a raw material according to the following objectives:

1. Chemical activation of fly ash surface. During this step the target functional group such as amine functional group will be mounted onto the surface of the ash, the treatment will increase the surface area because of the enhanced pore structure
2. Characterization of the resulting chemically treated fly ash will be performed using Energy Dispersive X-ray Analysis (EDX), Fourier Transformation infrared (FTIR), Brunauer-Emmett-Teller (BET), Scanning Electron Microscope (SEM), and X-ray diffraction (XRD).
3. Study the adsorption of CO_2 by treated fly ash were several kinetic parameters for adsorption such as effect of CO_2 concentration, temperature, gas flow rate, and relative humidity to obtain the best rate of adsorption.
4. Development of mathematical model that simulates the obtained results and predicts the optimum adsorption capacity.

1.2 ORGANIZATION OF THE THESIS

There are five chapters in the thesis, which indicates the goal of this work, literature pertaining to similar work is shown in chapter two which presents a review of related literature. It is divided into two sections; the first section presents a general overview of fly, its physical and chemical properties while the second section presents brief reviews on related work by several researchers.

Chapter three covers the experimental part. This chapter is divided into three sections. The first section presents the materials and chemicals used in the experiments. The second section gives a general description, characterization of the adsorbent and experimental procedures. While the third section describes the model used. Chapter four presents the experimental results together with the discussion. Finally, chapter five gives the conclusions and recommendations of the thesis.

CHAPTER TWO

2.0 LITERATURE REVIEW

Fly ash is the powdery residue obtained by the separation of solids from flue gases and fossil fuel combustion. It is also known as a complex heterogeneous material and as the residue of combustion of coal, the finest 0.2-90μm formed by the change in mineral matter present in the particles of the coal after combustion [11].

It is spherical in shape which consists of fine powdery particles that are mainly amorphous, solid or hollow in nature. Fly ash as a carbonaceous material is composed of angular particles, the particle size distribution of most bituminous coal fly ash is common to that of silt, and sub-bituminous coal fly ash is also silt sized, though it's a bit coarser. The surface area of fly ash varies from 170-1000m^2/kg with specific gravity ranging from 2.1-3.0 [12]. Fly ash color differs from tan to gray to black depending on the amount of unburned carbon in the ash. The low level of carbon and calcium or lime in lignite and sub bituminous fly ash makes their color light tan to buff in color, while bituminous fly ash is usually

shade of grey, with lighter shade of grey indicating higher quality. Characteristics shapes and particle size of fly ash is dependent upon the source, uniformity of the coal, degree of pulverization before burning, uniformity of combustion, combustion environment and type collection systems used. Majority of pulverized fly ash are solid or hollow, glassy and spherical shaped, the finest is in the same order as ordinary Portland cement.

The chemical properties of fly ash are greatly affected by the technique used in handling and storage and the degree of combustion of the coal. Basically, there are four types of coal which varies in terms of its chemical composition, heating value, ash content and geological origin. The four types of coal are also classified according to the type of coal from which the ash is derived; the types are anthracite, bituminous, sub-bituminous and lignite. Fly ash is sometimes classified based on the type of coal from which it is obtained.

The main components of bituminous fly ash are alumina, silica, iron oxide and calcium with different amount of carbon. The fly ash characterized by higher concentration of calcium and magnesium oxide with reduced percentage of iron oxide and silica as well as lower carbon content are derived from sub bituminous and lignite coal [12].

2.1 CO_2 Capture Methods

The most important energy source is considered to be fossil fuel with no alternative to it and it is the main source of greenhouse gas emission that causes global warming. A decrease in fuel consumption; switching to lower carbon

content fuels which are renewable such as nuclear energy, biomass, wind. The use of naturel gas instead of coal is presently the reliable methods of reducing CO_2 in the atmosphere.

The technologies used to separate CO_2 include chemical solvent scrubbing, physical solvent absorption, membrane technology, cryogenic techniques, chemical looping combustion and adsorption.

Chemical solvent scrubbing

Over 60 years ago, chemical and oil industries have established a technology for the removal of hydrogen sulphide and CO_2 from gas streams. This is mostly experienced on natural gas streams and or with chemically reducing gases, although, there are many facilities in which amine is being used to separate CO_2 from gas streams. CO_2 recovery rates of over 90% capture are normally proposed and the purity of the product can be in the excess of 99% [1]. However, corrosion in the presence of O_2 and other impurities are the major concerns with MEA and other amine solvents, large amount of regeneration energy and large equipment size are needed because of the large volume of flue gases involved in the process.

Physical solvent scrubbing

It's preferable to use different solvents known as physical solvents in the pre combustion capture which combines less strongly with CO_2. CO_2 can be separated from them by in the stripper by reducing the pressure, resulting in lower energy consumption; this is the advantage of such solvent. Major physical solvents that

could be used in CO_2 capture are dimethyl ether of polyethylene glycol, propylene carbonate, cold methanol and sulpholane. Physical scrubbing for separation of sulfur compounds is being used on a large scale by commercial IGCC plant [13]. CO_2 separation by solvent scrubbing is established at large scale such as in ammonia production plants. [31]

Membranes technology

In membrane technology, separation is based on the physical or chemical interactions between the gases and the membrane material enabling one component to pass faster then the other through the membrane. Several types of membrane are in use now, which include polymeric materials, porous inorganic materials, palladium membrane and zeolite. Although they cannot readily achieve high degree of separation, so its necessary to use multiple stages or recycle one or more streams, these leads to complexity I the process and hence increases cost and energy consumption. To obtain ig purity CO_2, several membranes with different characteristics may be required. An improvement in the future possibly will be to combine inorganic membranes with operating temperature up to 1000^oC [31] with shift or reforming conversion reactions. At high pressure and CO_2concentration membranes are used commercially to remove CO_2 from natural gas. Much development is needed before membranes can be used on a large scale for the separation of CO_2 in power plants.

Cryogenics technique

Cryogenic technique is mostly used on commercial scale for CO_2 purification from streams with high CO_2 concentration (>90%) but not normally used for more dilute CO_2 streams. With cryogenic technique CO_2 can be separated by cooling and condensation from other gases. The most promising application of this technique s are separation of CO_2 from high pressure gases as in pre combustion capture processes or oxyfuel combustion the input gases contain high concentration of CO_2 . This separation technique has an advantage of directly producing liquid CO_2 used in ship transportation. However, the amount of energy needed to provide refrigeration necessary for the process to especially for dilute gas streams , and that some components such as water have to be removed before the gas is cooled to avoid blockages are some the disadvantages of cryogenic separation of CO_2 [31].

Chemical looping combustion

In chemical looping combustion, it does not require any expensive air separation unit, but rather it facilitates the production of a concentrated CO_2 stream. Development of a metal oxide that can with stand long term chemical cycling and resistant to chemical and physical degradation from flue generated impurities is the major developmental issue associated with chemical looping combustion. This technique can be applied at atmospheric pressure or at elevated pressure as part of gas turbine. The possible metal oxides used are nickel, manganese, iron and copper. The main problems associated with this technique include multiple handling of solid streams development of an efficient oxygen carrier material [31].

Absorption

Absorption is a post combustion capture method makes use of regenerable solid sorbents for the separation of CO_2 at high temperatures. Sorbents like lithium or calcium based oxides can react with CO_2 to form carbonates, and the carbonates can be regenerated to oxides by heating at higher a temperature [3]. The main problem associated with these processes are the use of natural solid sorbents such as dolomite and limestone whish deactivate rapidly which requires large make up flow for the sorbent, though deactivated sorbent may have application in cement industry. However, these processes have the potential to reduce efficiency penalties compared to wet absorption process.

Adsorption can be used to separate CO_2 from gas mixtures by using solid materials called adsorbents having high surface areas such as activated carbon and zeolites. The gas is fed to the bed containing the adsorbent which adsorbs the CO_2 and allows other gases to pass through. When the bed is saturated with CO_2, the feed gas is introduced to another adsorption column and the loaded column is regenerated to remove CO_2. Adsorption by pressure swing (PSA) involves regenerating the adsorbent by reducing the pressure, while temperature swing adsorption (TSA) involves regenerating the adsorbent by raising the temperature of the bed and in electric swing adsorption (ESA), low voltage electric current is passed through the bed to regenerate the adsorbent. Used commercially for gas separation and to some extent for the production of hydrogen and in CO_2 removal

from natural gas are pressure swing adsorption and temperature swing adsorption respectively [2]

Different adsorbents have been used for the separation of CO_2 using fly ash in aqueous solutions or flue gases from the literature.

Zou et al. [2001] studied the adsorption capacity of carbon dioxide using carbon based adsorbent having high surface area before and after chemical treatment at 28^{o}C and 300^{o}C. High adsorption capacity of the adsorbents was achieved at high temperature. It was found that their adsorption capacities for carbon dioxide were 0.28 and 0.22 mmol/g at 300^{o}C, 1 Bar, respectively. The results showed that at this temperature, adsorption of CO_2 without chemical treatment is very difficult [13].

Plaza, **et al. [2007**] investigated the adsorption of carbon dioxide on nitrogen enriched carbon. As preliminary support to study the effect of the impregnation, different alkyl amines were used as potential source of basic sites for CO_2 separation and commercially activated carbon was also used. The adsorption capacity of the raw carbon at room temperature as the microporous volume decreases which was responsible for the physiosorption process [14].

The effect of pre-oxidation of activated carbon modified with ammonia to enhance carbon dioxide adsorption was studied by **Shafeeyan, et al. [2010]** they

used ammonia without preliminary oxidation and treatment with ammonia. The Modified carbons materials were characterized by elemental analysis and Fourier transform infrared spectroscopy to study the impact and formation of specific functional groups on adsorption material. The results showed high temperature treatment with oxidation at 800^{o}C has improved the CO_2 capacity at higher temperature. It also revealed that the presence of nitrogen functional groups on carbon surfaces has increased the CO_2 adsorption capacity in both modification techniques [15].

A.Boonpoke1, et al. [2011] synthesized CO_2 adsorbents from locally available biomass (rice husk and bagasse), and investigated their adsorption capacity. The result showed that the BET surface area was found to be 927, 923 and 602 m^2/g for RAC, BAC and R-MCM-41 respectively. While the total pore volumes were found to be 0.53, 0.56 and 0.49 cm^3g^{-1}, and pore sizes were 0.8, 0.8, and 2.43 nm for BAC, RAC and R-MCM-41 respectively. At 30°C these materials were able to adsorb 76.89, 57.13 and 23.32 mg-CO_2 g^{-1} adsorbent respectively. When the adsorption temperature increased, adsorption capacity of BAC, RAC and R-MCM-41 was decreased. This indicates that physical adsorption is the dominated adsorption mechanism. BAC shows the highest capacity of CO_2 adsorption which is related to its high surface area, low ash and high carbon content. [17].

Grande, et al. [2008] employed activated carbon honey comb monolith as selective adsorbent with low electrical resistivity for CO_2 removal from flue

gases. They proposed and describe the electric swing adsorption using a mathematical model. The process comprises of desorption, electrification, feed and purge with all the regeneration steps counter current to the feed stream of the process. It revealed that about 89% or higher can be obtained, though with impurities of CO_2 around 16% has been revealed [18].

Belmabkhout, **et al. [2009]** studied the removal of CO_2 and H_2S over triamine-grafted mesoporous silica at room temperature. It was found that unlike physical adsorbents like activated carbon and zeolites, presence of moisture in the feed enhanced the CO_2 removal capability of TRI-PE-MCM-41 without altering its H_2S adsorption capacity. Thus, depending on the composition of the feed the two gases (CO_2 and H_2S) can be removed over the TRI-PE-MCM-41 simultaneously**.** The result also revealed that TRI-PE-MCM-41 exhibits high affinity toward both CO_2 and H_2S versus CH_4. It was also showed that TRI-PE-MCM-41 has extremely high CO_2 selectivity over methane [19].

Sanz, et al. [2010] studied the adsorption of CO_2 on functionalized SBA-15 over branched PEI prepared using impregnation technique. The result revealed that CO_2 adsorption increased in polythleneimine content favors the CO_2 adsorption, although the specific efficiency per unit content of adsorbent becomes lower. Chemisorption being the fundamental mechanism, CO_2 adsorption capacity increased with temperature [32].

For the removal of wide variety and range of organic and inorganic compounds, Fly ash has been proven to be an effective and excellent.

Shawabkeh, **et al. [2004]** used Jordanian oil shale ash for the removal of metal ions from solution. The adsorbent was treated with nitric acid and sodium hydroxide solution. The result showed that the sample treated with sulphuric acid have cation exchange capacity of 32 meq/100g while the sample treated with nitric acid showed the highest cation exchange capacity (CEC) of 146 meq/100 g. To fit the experimental data, Freundlich and BET models were used which revealed that the BET model best fitted the experimental result. An increase in the removal capacity for metals at high pH value was shown by batch adsorption isotherm for zinc and copper [33].

The adsorption abilities and influence of several parameters of fly ash and sepiolite for removal of Reactive Blue 21 from synthetic aqueous solutions was studied by **Demirbas, et al. [2009]**. Kinetic studies results showed that RB21 on to fly ash and sepiolite were been described by Results of the kinetic studies shows that RB21 dye onto FA and sepiolite were best described by the pseudo-second-order kinetic model the best correlation for RB21 dye on to fly ash and sepiolite was provided by Langmuir isotherm. The maximum adsorption capacities of RB21-FA and RB21- sapiolite from the Langmuir isotherm at 323K were 106 and 66 mg/g respectively. The enthalpy values for both adsorbents were found to be positive indicating that the process is endothermic [34].

Shawabkeh, et al. [2007] investigated the removal of H_2S from liquefied petroleum gas (LPG) using Jordanian oil shale ash as adsorbent. The effect of temperature, masses and particle size using dry and wet ash was also studied. The rate of H2S uptake was directly affected by the amount of gas passing through bed, temperature of the system and particle size of the ash. However, a sorption capacity of 30 mgH_2S/Liter of liquefied petroleum gas. This process is economical, safe and efficient [35].

FA substrate can be used for simultaneous removal of heavy metals and methylene blue from wastewater. **Maria Visa, et al. [2010]** investigated the effect of (methyl orange, methylene blue) on the removal efficiency of copper, cadmium and nickel ionic species from complex dye solutions using fly ash as adsorbents. The dyes adsorbed on the fly ash were found to be on the new copper surface having higher affinity for the active sites compared to nickel and cadmium. It was also found that the fraction of fly ash used does not depend on the efficiency of the heavy metal adsorbed. Fly ash substrate was recommended to be used for simultaneous removal of heavy metals and methylene blue from waste water. High adsorption efficiency was registered for heavy metal concentration up to 0.01mol/liter [36].

The effect of coal fly ash adsorption capacity and crystallinity toward lead was studied by **Astuti et al. [2011]**.the coal fly ash was treated at different sodium hydroxide concentration, temperature and reflux time to have solids of various

crystallinity. The result shows that the adsorption capacity of lead depends on the initial concentration, contact time and pH of the solution. The lower the crystallinity, the higher the adsorption capacity. The coal fly ash adsorption kinetics on to lead was found to be pseudo second order kinetic model [30].

Akgerman and Zardkoohi [1996] investigated the adsorption of phenol, 3-chlorophenol and 2, 4-dichlorophenol from wastewater onto fly ash. The result shows that phenol has the highest adsorption affinity for fly ash. The Freundlich isotherm was used to fit the experimental data. The adsorbed amount of phenol onto the fly ash was 67 mg/g, 20 mg/g for 3-chlorophenol and 22 mg/g for 2, 4-dichlorophenol respectively [37].

Mohan, et al. [2002] used a new low-cost activated carbon derived from fly ash for the removal of dyes from synthetic dye wastewater. The adsorption of the two dyes increases as the temperature increases indicating that the process is endothermic. The results showed that both the Freundlich and Langmuir models were used to fit the data. However, the data are better fitted with the nonlinear Freundlich adsorption isotherm. The adsorption capacities of crystal violet and basic fuchsine dyes on fly ash are higher than or comparable to those of other adsorbents used for the same or other cationic dyes [38].

The potential of fly ash and materials prepared from fly ash as a substitute for activated carbon and other adsorbents for the removal of CO_2 is being considered by many researchers.

Gray, **et al. [2004]** developed an economical amine-enriched sorbents based on fly ash carbon concentrate. Carbon enriched fly ash concentrates with a 3-chloroproylamine hydrochloride solution at 25^oC were used to generate initial fly ash carbon sorbents. Sample 95C was found to be the best sample with adsorption capacity of 175 mg/g. It was found that these amine-enriched fly ash carbon sorbents performed at a 9% CO_2 capture capacity based on commercially available sorbents for adsorption [39].

Arenillas, **et al. [2005]** prepared a low cost carbon material from fly-ash derived carbon, by impregnating with amine PEI. CO_2 adsorption capacities were relatively high especially at high temperatures for samples derived from a fly ash carbon concentrate. The addition of polyethylene glycol improves the adsorption capacity and reduced the time taken for the sample to reach equilibrium while the commercial active carbons relying on physiosorption have low capacities. [2].

Maroto-Valer, **et al. [2008]** developed activated fly ash derived sorbents for CO_2 capture. Significant increase in surface area was observed when the samples were steam heated at 850^oC. A decrease in surface area was achieved by impregnation process using different amine compounds, indicating a blockage of the porosity.

Amine impregnated samples has a CO_2 capacity higher than those previously published for fly ash carbon without activation. Adsorption capacity of the amine impregnated activated carbons was highest at 30 and 70^oC due to combination of physical adsorption inherent from the parent sample [16].

Bada and Potgieter-Vermaak, [2008] investigated the property of fly ash when subjected to chemical and heat treatment for adsorption purposes. The Chemical treatment was performed using one gram fly ash, one molar hydrochloric acid solution in the ratio 1g fly ash to 2M of acid and compared with untreated heat-treated samples. The analysis revealed that the chemically treated fly ash has a higher specific surface area of 5.4 m^2/g than the heat-treated fly ash with 3.0 m^2/g surface area. This was as a result of corrosion of the outer layer of the fly ash to ash which disintegrates its stable glassy layer [40].

Chandrasekar, et al. [2009] prepared a mesoporous silica of SBA-15 structure (FSBA-15) using fly ash as main silica source via a thermal fusion process for CO_2 adsorption. At 75^oC FSBA-15 and SBA-15 after polyethyleneimine impregnation showed a comparable CO_2 adsorption capacity of 110 and 120 mg CO_2/g, respectively. a surface area of 1,258 m^2/g and pore volume comparable to those of CMK-3 prepared using a pure SBA-15 template where shown. This shows that mesoporous silica SBA-15 and its carbon replicate CMK-3 can function effectively as an adsorbent for CO_2 adsorption [41].

A novel CO_2 capture material made of Li_4SiO^{4-} based sorbents from fly ash was developed by **Olivares-Marı´n et al. [2010]**. FA-1, FA-3 and FA-2 were the samples used and were subjected to calcination at 950oC in the presence of Li_2CO_3. For CO_2 sorption at different temperature both Li_4SiO_4 and fly ash based sorbent were tested. Both pure Li_4SiO_4 and fly ash-based sorbents were characterized and tested for CO_2 sorption at different temperatures between 400 and 650^oC and adding different amounts of K_2CO_3. When the sorption temperature increase; both the CO_2 sorption capacity and rate increases significantly. However, the CO_2 sorption capacity increases when the amount of K_2CO_3 increases; the maximum CO_2 sorption capacity for the sorbent derived from fly ash was 107 mg CO_2/g sorbent at optimal experimental conditions [42].

Reinika, et al. [2011] studied the preliminary tests on Alkaline modified oil shale fly ash and Optimal synthesis conditions for CO_2 adsorption at sodium hydroxide concentrations 1, 3, 5 and 8 M with 24 hour synthesis time and temperature of 130 and 160^oC. Characterization of the Original and activated ash samples were carried out using XRD, XRF, SEM, BET and TGA. TGA result showed that after alkaline hydrothermal treatment with sodium hydroxide, the physical adsorption of CO_2 on the oil shale ash sample decreases from 0.06 to 3-4 percent mass. CO_2 adsorption capacity is increased by alkaline treatment of the shale which depends on the reaction temperature, therefore, the treated material has the potential to be used in industrial processes for physical adsorption of CO_2 [43].

Liu et al. [2011] prepared mixture of A + X and pure A zeolites from fly ash and measured their CO_2 and N_2 adsorption capacity. The performance of the materials for CO_2 capture was synthesized from real process plant flue gas and the results was compared with standard 13X zeolite. The result revealed that around 330 m^2 surface area was found for the mixture which is higher than zeolites. However , both zeolite A and zeolite A+X showed better performance in CO_2 separation compared to zeolite 13 X at higher temperature from flue gases due to high selectivity of CO_2 and N_2. Therefore, for commercial process of CO_2 separation, less expensive, viable means of producing large quantities of adsorbent, zeolite prepared from waste fly ash can be used. [44].

Kumar, et al. [2012] studied the synthesis of alumino-silicates prepared from fly ash by varying and optimizing the parametric conditions for CO_2 capture. The alumino silicate fly ash based material was characterized and functionalized with 3-aminopropyl, triethoxysilane and 3-amino-2-methyl-1-propanol to impart basicity for carbon dioxide adsorption. It was observed that the fly ash alumino silicate has adsorption capacity of 6.62 mg/g which has improved by a factor of 4, while the AMP functionalized fly ash has a adsorption capacity of 26.5 mg/g with 15% CO_2 in N_2 at 55^oC. Furthermore, at 15% CO_2, 82% N_2 and 3% positive effect of water vapor was observed with an improvement in adsorption capacity to 34.8 mg/g. The synthesized alumino silicate material has excellent thermal stability making it a promising adsorbent for CO_2 adsorption [45].

Yi et al. [2012] studied the kinetics and equilibrium adsorption for NO, SO_2, CO_2 on LTA and FAU zeolites. Equilibrium model and henrys law were used to analyze the equilibrium data. The outcome indicate that adsorption affinity follows the trend of SO_2>CO_2>NO trend for the same adsorbent with stronger polar surface making it a promising adsorbent. It further shows that it is a micropore diffusion controlling mechanism. Minimum resistance to mass transfer was observed in NaY zeolite due to large pore amount and pore distribution, while the highest spatial hindered effect was observed in CaA zeolite. [46]

CHAPTER THREE

3.0 EXPERIMENTAL APPARATUS AND PROCEDURE

The reagents, chemicals and instrument used for the adsorption of CO_2 using chemically treated fly ash experiment is shown in table 3.1 and 3.2

3.1 CHEMICAL TREATMENT OF FLY ASH

The functionalization of the fly ash was performed using ammonium hydroxide. A sample of 100g of the ash was mixed with 300 ml of ammonium hydroxide in a 500 ml round bottom flask and refluxed at 120^{o}C for 24 hours. The mixture was cooled and 150 ml of ammonium hydroxide was added and allowed for 24 hours. It was later filtered, and half of the mixture was dried at 105^{o}C for 24hours in the oven while the other portion was dried at room temperature. FTIR analysis was carried out on the final product to confirm the presence of amine functional groups on to the surface.

3.2 CHARACTERIZATION OF CO_2 ADSORBENT

The techniques needed for the characterization of fly ash requires the knowledge of its chemical composition and physical properties of the ash, such as the particle size, specific surface area and phase composition. In order to obtain the best possible information the, functionalized CO_2 adsorbent was characterized using the following characterization techniques.

3.2.1 Brunauer-Emmett-Teller (BET) Nitrogen surface area determination

The BET technique has the ability to provide information on the total volume, specific surface area, pore size and pore volume distribution of the specified specimen, and as such, is used to determine the surface morphology of the sample. In BET analysis, characterization is done with gas adsorption, and of all readily available gases, nitrogen proved to be the superior adsorptive and is thus universally pre-eminent.

3.2.2 Scanning Electron Microscope (SEM)

The Scanning Electron microscope (JEOL model, JSM 6400) was used to determine the qualitative characteristics and morphological of the fly ash sample. The dried sample was fixed with double side masking tape. In order to make it surface conductive, the fly ash sample was carbon coated. It was then viewed on SEM at different magnification to see the surface topography of the sample.

Table 3.1: List of reagents and chemical used

Reagent and chemical	Manufacturing Source
Fly ash	Saudi Electricity company
ammonium hydroxide, 99.9%	Sigma Aldrich Company
Carbon dioxide,	National gas company, Dammam
Nitrogen gas	National gas company, Dammam
De-ionized water	KFUPM Chemical engineering laboratory

Table 3.2: List of apparatus and instruments used

Instrument	Manufacturer
TESTO CO_2 meter	PLATON
Relative humidity meter	PLATON
Water bath	C12CS LAUDA
Oven	FISHER ISOTEMP Oven
Heating mantle	KFUPM Chemical engineering laboratory
Brunauer-Emmet-Teller (BET)	Micrometric ASAP 2010
Temperature controller	C12CS LAUDA
Casio water resist Stop Watch	CASIO

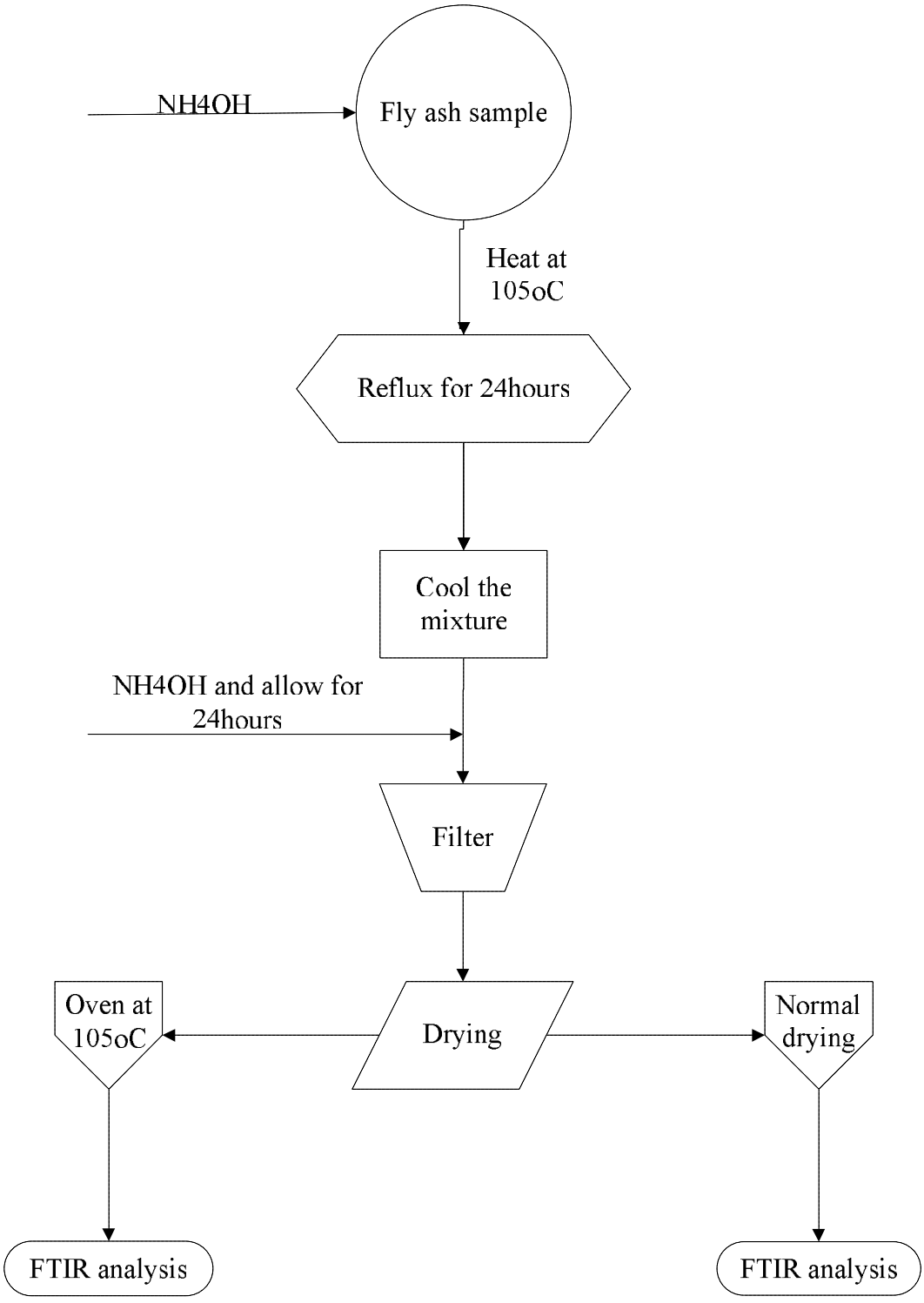

Figure 3.1: Chemical activation of fly ash

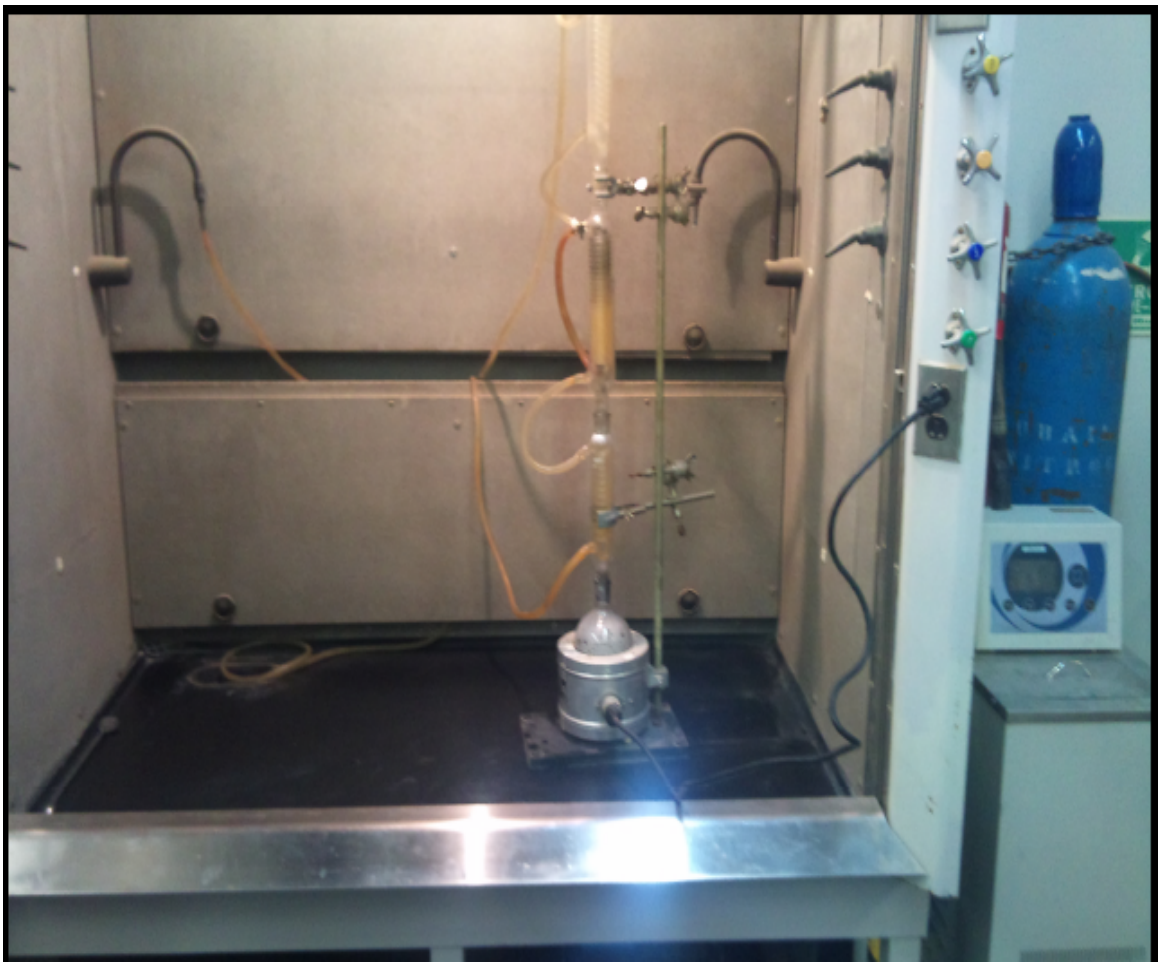

Figure 3.2: Functionalization of the fly ash

3.2.3 X-ray diffraction spectrometry (XRD)

The predominant phases in the functionalized ash sample was determined was determined using the X-ray diffraction spectrometry. The XRD can also determine the mineralogical composition of the ash sample. The phase identification of the fly ash sample which is in a powdery form, were determined by the X-ray diffractometry using a Phillips PW 1830 diffractometer with a Copper anode. It was operated at 40 kV and 40 mA for 1 h from 0^o to 80^o over the range of 2q and High Score Plus software was used for the identification of the phases present.

3.2.4 Energy Dispersive X-ray Analysis (EDX)

Energy Dispersive X-ray Analysis (EDX) was carried for the analysis of chemical composition of treated and untreated fly ash. The chemical composition of as-received fly ash is as 92.5% Carbon; 5.80% sulfur; 0.79% Magnesium; 0.09% Silicon and 0.61% vanadium. This analysis shows that the fly ash used in this research was mainly composed of carbon material with a very little amount of sulfur. Also, the presence of some heavy metals was observed in traces which are typical for heavy oil combustion residue.

3.2.5 Fourier Transform Infrared Spectroscopy (FTIR)

The Fourier transform infrared spectroscopy (FTIR) was used to identify the presence of functional groups attached to the functionalize fly ash. It is also used t identify either organic or inorganic compounds on surfaces of particles

3.3 ADSORPTION EXPERIMENT

The adsorption column was made of quartz glass, which is 18 cm in length and with inner diameter of 1.0 cm. The tube is surrounded by a glass jacket and a controlled- temperature water is circulating through the jacket to maintain isothermal condition [35]. The adsorption column was filled with 1.5g of the amine functionalized ash. Nitrogen gas is first introduced to the bed at the bottom of the column to free the surface of the ash followed. CO_2 gas enters the bed from the bottom of the column at different flow rates, while the CO_2 digital meter attached at the other end measures the CO_2 concentration as a function of time. The relative humidity was measured at the inlet and outlet of the column using the relative humidity meter. To raise the humidity of the inlet gas, the gas was passed through a water bath at 70^oC before passing to the column. The experiments were repeated at different CO_2 concentrations, flow rates and temperatures of the bed for low and high humidity. Desorption experiment was performed in a similar manner by passing Nitrogen to the column and the resulting CO_2 concentration was measured as a function of time.

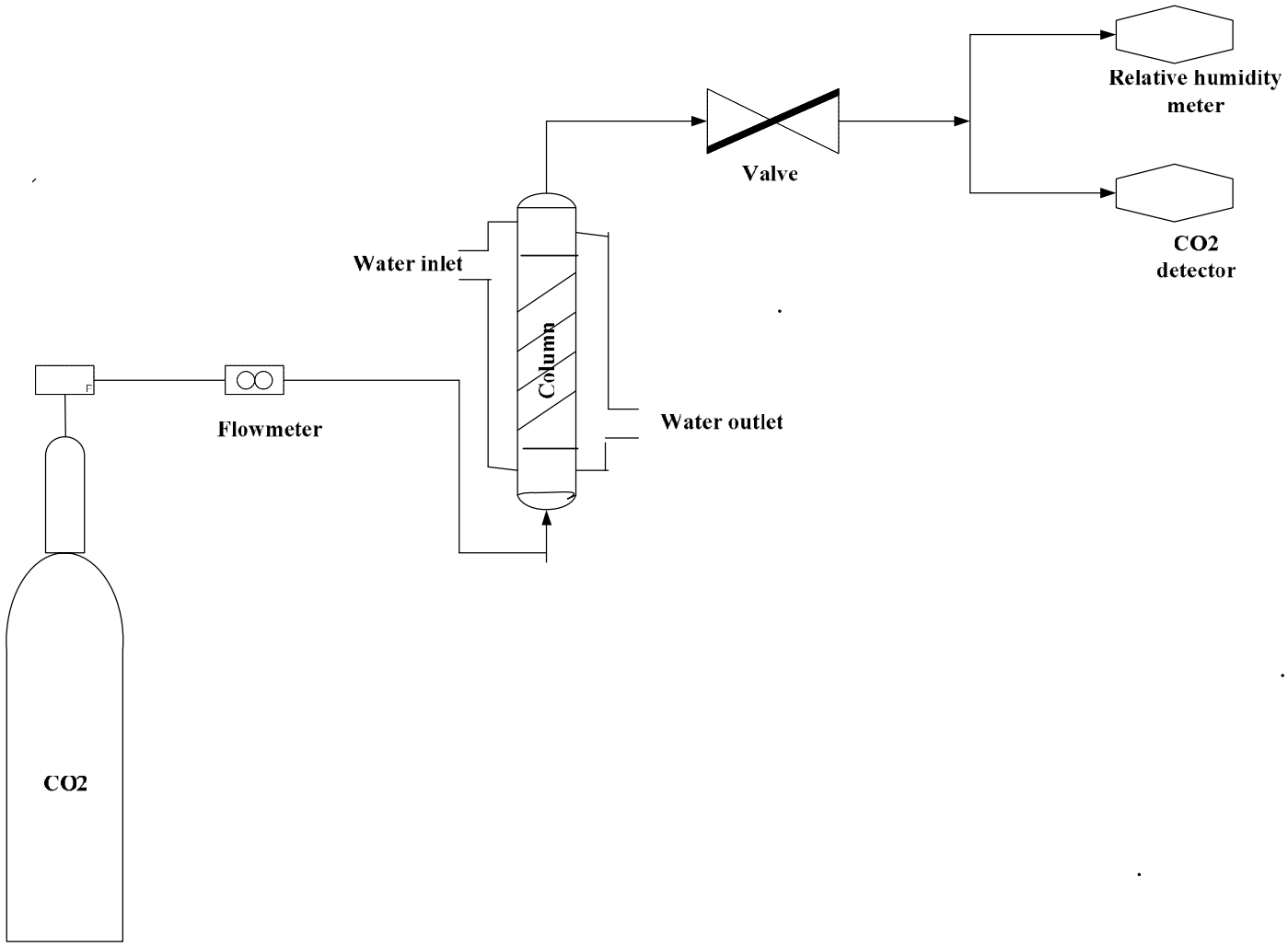

Figure 3.3: Carbon Dioxide Adsorption experiment

3.4 MODEL DEVELOPMENT

In order to estimate the breakeven point in term of mean residence time distribution of the non-adsorbed CO_2 molecules and hence to predict the axial diffusion of these gas molecules inside the ash column, the axial dispersion model was selected where a step change in CO_2 concentration from $C_A = 0$ to $C_A = C_A^o$ was used. Assuming only axial diffusion occurred, the PDE that describe the change in CO_2 concentration with respect to distance and time is

$$\frac{\partial C_A}{\partial t} = D_{eff}\left(\frac{\partial^2 C_A}{\partial r^2} + \frac{1}{r}\frac{\partial C_A}{\partial r}\right) - u\frac{\partial C_A}{\partial x} - kC_A^n \tag{1}$$

Where C_A is the concentration of carbon dioxide obtained at a distance r from the column entrance and D_{eff} and u are the axial diffusion and velocity of the gas of the gas inside the column, respectively.

The initial and boundary conditions for the above equation are

$$C_A = C_{Ao} \quad \text{at} \quad t = t\,, \quad r = R$$

$$C_A = 0 \qquad \text{at} \quad t = 0\,, \quad r = r$$

$$\frac{\partial C_A}{\partial r} = 0 \qquad \text{at} \quad t = t\,, \; r = 0$$

$$\frac{\partial C_A}{\partial x} = 0 \qquad \text{at} \quad t = 0\,, \; x = L$$

The above equations was solved using the MATHEMATICA V.8 to obtain the fraction of CO_2 concentration at the exit of the column, $r = L$, that has been in the column for a time less than t according to the finite difference equation.

$$\frac{C_{A\,i+1,j,k} + C_{A\,ij,k}}{\Delta t} = D_{eff}\left[\frac{C_{ij+1,k} - 2C_{ijk} + C_{ij-1,k}}{\Delta r^2} + \frac{1}{r_i}\left(\frac{C_{ij+1,k} - C_{ijk}}{\Delta r}\right)\right] - u_i \frac{C_{ijk+1} - C_{ijk}}{\Delta x} - KC_{ijk}^n \quad (2)$$

$$\frac{C_{i+1,jk}}{\Delta t} - \frac{C_{ijk}}{\Delta t} + 2D_{eff}\frac{C_{ijk}}{\Delta r^2} + \frac{D_{eff}}{r_i}\frac{C_{ijk}}{\Delta r} - \frac{u_i C_{ijk}}{\Delta x} = \left(D_{eff}\frac{C_{ij+1,k}}{\Delta r^2} + \frac{C_{ij+1,k}}{\Delta r\, r_i}\right) + D_{eff}\frac{C_{ij-1,k}}{\Delta r^2} - u_i\frac{C_{ij+1,k}}{\Delta x} - KC_{ijk}^n \quad (3)$$

$$\frac{C_{i+1,jk}}{\Delta t} - C_{ijk}\left(\frac{1}{\Delta t} - \frac{2D_{eff}}{\Delta r^2} - \frac{D_{eff}}{r_i\,\Delta r} + \frac{u_i}{\Delta x}\right) = C_{ij+1,k}\left(\frac{D_{eff}}{\Delta r^2} + \frac{1}{r_i\,\Delta r}\right) + \frac{D_{eff}\,C_{ij-1,k}}{\Delta r^2} - \frac{u_i}{\Delta x}C_{ijk+1} - KC_{ijk}^n$$

Let $\Omega = \frac{D_{eff}\,\Delta t}{\Delta r^2}$

Therefore,

$$C_{i+1,jk} = C_{ijk}\left(1 - 2\Omega - \Omega\frac{\Delta r}{r_i} - u_i\frac{\Delta t}{\Delta x}\right) + C_{ij+1,k}\left(\Omega + \frac{\Delta t}{r_i\,\Delta r}\right) + \Omega C_{ij-1,k} - C_{ijk+1} - K\Delta t C_{ijk}^n \quad (4)$$

CHAPTER FOUR

4.0 RESULTS AND DISCUSSION

4.1 SYNTHESIS AND CHARACTERIZATION OF FLY ASH

The process in which fly ash is mixed with certain alkaline activator such as ammonium hydroxide where the mixture is cured to make a solid material under certain temperature is known as alkaline activation of fly ash. The chemical analysis of oil fly ash used in this study was done elsewhere [22] as shown in table 1. In previous works [48, 49], it was found that an amorphous alumino silicate gel was the main reaction product formed during alkaline activation of fly ash and hence the resulting product is also known as zeolite precursor. On the other hand, the alkali activation of fly ash is a process narrowly related to the synthesis of zeolites [50].

The chemical activation was done using ammonium hydroxide solution. A sample of 100g of the ash was mixed with 300 ml of ammonium hydroxide in a 500 ml round bottom flask and refluxed at 120^{o}C for 24 hours. This will promote more interaction between ammonium hydroxide solution and the surface of the ash. The mixture was allowed to cool and 150 ml of ammonium hydroxide was added and

allowed for 24 hours. It was later filtered, and half of the mixture was dried at 105^{o}C for 24hours in the oven which was used for CO_2 adsorption at low relative humidity while the other portion was dried at room temperature for CO_2 adsorption at high relative humidity. As shown in previous works [51, 52], the alkaline activation of fly ash comprises of different stages such as Destruction–Coagulation and Coagulation–Condensation [50]. Experimental conditions employed in each synthesis process are the main difference between traditional zeolitic system and alkaline activated systems. The controlling mechanism for the chemical reaction producing the pre zeolite gel is associated with the dissolution process having high concentration of hydroxide ions in the system responsible for braking down the Si-O-Si, Al-O-Al and Si-O-Si bond forming part of the vitreous ash phase thereby forming Al-OH and Si-OH groups. The chemical species later get condensed leading to precipitation of zeolitic precursor [48, 51]. In addition, hydroxides open more micro and macropores in carbonaceous matrices in the process of chemical activation [52].

4.2 CHARACTERIZATION OF THE CHEMICALLY TREATED FLY ASH

The chemically treated fly ash was characterized using EDXA, FTIR, XRD, BET and SEM in order to obtain the best possible information. The characterization will also determine the physical properties of the ash, such surface morphology, particle size, specific surface area, surface morphology, phase composition and its chemical composition

Table 4.1: Chemical composition of fly ash

PARAMETER	QUANTITY	
pH @ 18^{o}C	2.8	
Moisture	0.33	wt%
unburned carbon @ 700^{o}C	90.2	wt%
Ash content	9.8	wt%
SO_3	3.6	wt%
Vanadium	4007 ppm	
Nickel	1021 ppm	
Iron	559 ppm	
Magnesium	1800 ppm	

4.2.1 Energy Dispersive X-ray Analysis

Table 4.2 shows the elemental analysis of the fly ash used in this study. From the elemental analysis, it shows that fly ash is composed mainly of carbon material with some heavy observed in traces and little amount of sulphur [22, 47].

4.2.2 Fourier Transform Infrared Spectroscopy (FTIR)

To determine whether a new functional group has been attached to the fly ash surface after chemical activation, the Fourier transform infrared spectroscopy was used. Figure 4.2(a and b) shows the FTIR spectra of the ash as received compared to the ash treated with NH_4OH solution over the range of 4000–400 cm^{-1}. The effect of chemical activation is strongly dependent upon the type of activation agent and the physical-chemical nature of the fly ash [53]. The OH- group will attack the surface of the fly ash at high alkaline pH during the activation as reported by sang et al [54]. More surface will area will be provided by the corroded surfaced for further attack by the activating agent resulting in the formation of amorphous alumino silicate material. [55].

The IR spectrum of the untreated ash is shown in fig 4.2a. The untreated ash has five major peaks at 1123, 1623, 2371, 3307 and 3772cm^{-1}. These broad peaks are related to C=C, C=O, C=C, H-C= and O-H functional groups respectively. For the chemically treated ash a broad peak at 3402 cm^{-1} shows the presence of $–NH_2$- [56], while the peak at 3186 cm^{-1} may be related to $–CONH_2$-. However, the intensity of the untreated ash at 3772 cm^{-1} and 3206 cm^{-1} were reduced after the

chemical activation to 3402 and 3186 as a result of the heat treatment on to the surface of the ash thereby attaching the amine functional group. A new peak was formed at 1097 cm^{-1} after the chemical treatment which may be related to C-O. There was a slight decrease in the intensity of the untreated ash at 2371 cm^{-1} to 2333 cm^{-1} for the treated ash. A minor peak was observed at 1386 cm^{-1} which is attributed to the presence of –O-H functional groups [57]. Therefore, the presence of amine on the surface of the ash is clearly indicated by the FTIR study. The study carried out on activated carbon prepared from rice straws reported similar results. [59].

4.2.3 X-ray diffraction spectrometry (XRD)

To determine the crystallinity and phases of the treated and untreated samples X-ray diffraction technique was used, In Fig. 4.1(a), XRD patterns show the presence of, zeolite, carbon, quartz, mullite, faujasite, sodalite and cancrinite [47, 58] for the untreated fly ash. Presence peak at $11^{o}\,2\theta$,$16^{o}\,2\theta$ and $18^{o}\,2\theta$ shows the presence of zeolite. A very broad peak was seen at $25^{o}\,2\theta$ which shows the presence of carbon and mullite. This shows the high concentration of crystalline carbon compared to other minerals. However, minor peaks at $27^{o}\,2\theta$, $33^{o}\,2\theta$ and $78^{o}\,2\theta$ were detected corresponding to carbon, mullite, and quartz respectively. This indicates that mullite and quartz are the two main phases of the crystalline components of the untreated fly ash [5].

Table 4.2: Elemental analysis of fly ash by EDXA

Element	Before treatment Weight, %	After treatment Weight, %
Carbon	45.37	73.05
Oxygen	26.46	12.33
Sodium	0.43	-
Magnesium	0.37	0.51
Aluminium	0.79	0.17
Silicon	9.25	0.48
Calcium	6.38	-
Vanadium	9.48	0.83
Iron	0.94	-
Sulphur	-	12.63

In Fig. 4.1(b), XRD patterns show that alkali-activated fly ash mainly consists of quartz and mullite as the major crystalline phases; the peaks at 11^{o} 2θ, 16^{o} 2θ and 18^{o} 2θ were reduced after the chemical treatment while the intensity of the mullite and carbon peaks at 25^{o} 2θ increased. There was a sharp increase in the peak at 78^{o} 2θ corresponding to quartz. However, the quartz and mullite peaks between 30 - 40^{o} 2θ decreased or were not visible after the treatment but the peak at 45^{o} 2θ increased suggesting the presence of mullite.

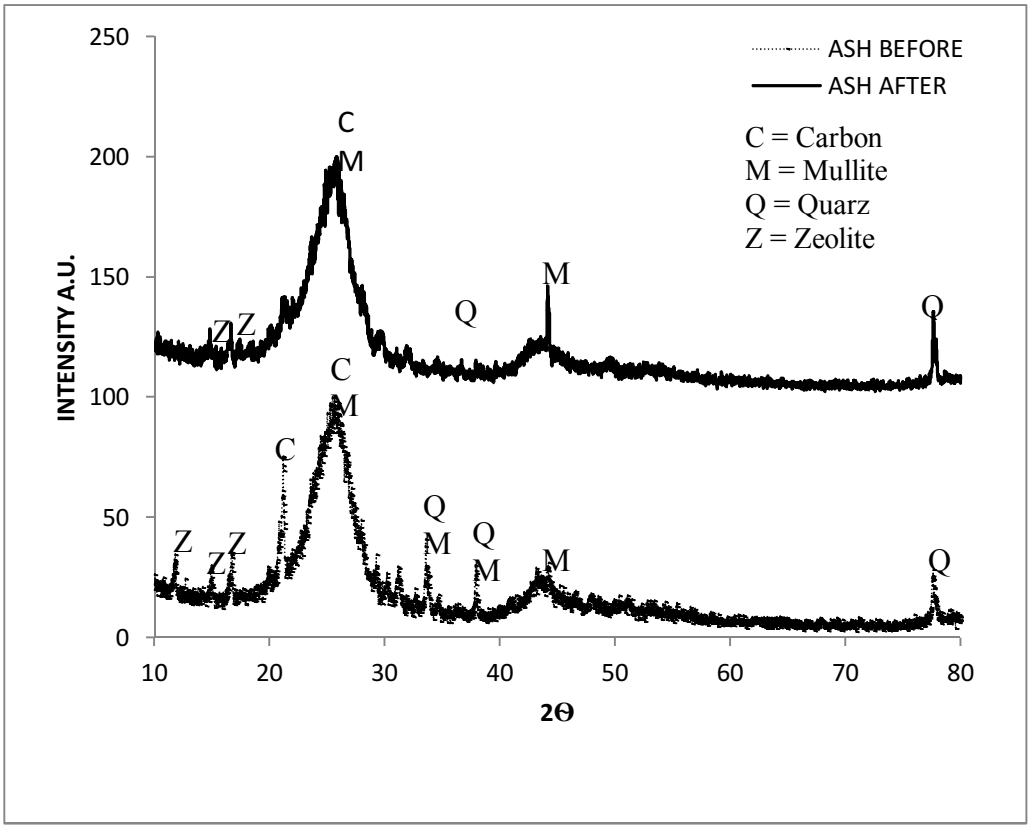

Figure 4.1: XRD spectrum (a) Fly ash before treatment (b) Fly ash after chemical treatment.

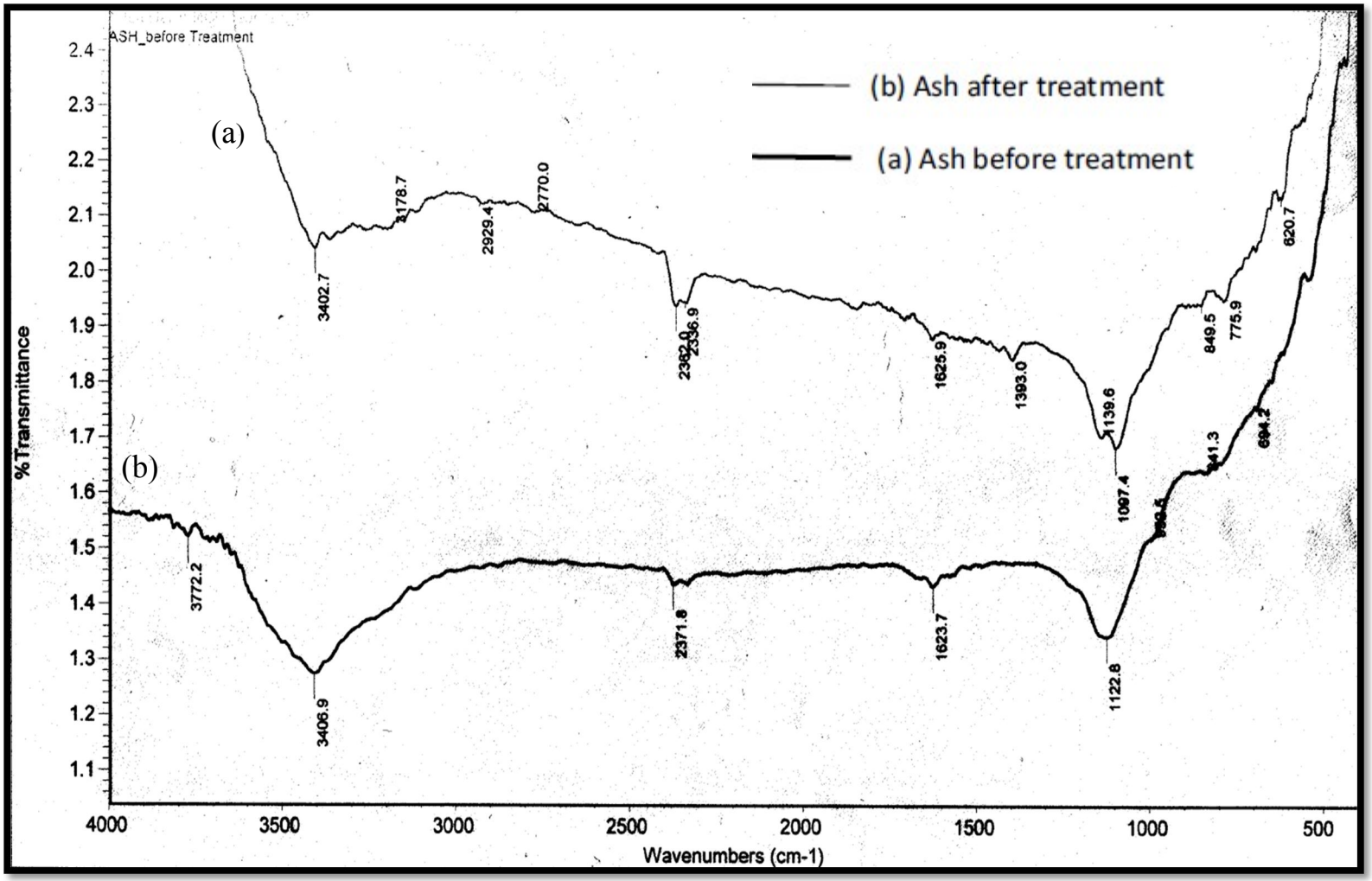

Figure 4.2: FTIR spectrum (a) Ash before treatment (b) Ash after chemical treatment.

4.2.4 Brunauer-Emmett-Teller (BET) surface area

The pore characteristics and surface area of the chemically treated and untreated ash samples are shown in Table 4.3. Figures 4.3 and 4.4 shows the adsorption–desorption isotherms of N_2 at 77 K for the chemically treated and untreated ash samples. The characteristics of the material is made of slit shaped pores, the distribution of the pore sized is principally micoporous. It can be seen that this isotherm belongs to type I in the IUPAC classification, The BET surface area increased from 59 m^2/g for untreated ash to 318 m^2/g after chemical activation. Also, the pore volume increase substantially from 0.036795 to 0.678627cm^3/g. hence the co2 adsorption capacity improved as a result of the improved characteristics. The high BET surface area and total pore volume of the treated fly ash was due to the activation process used, which involved chemical activation with NH_4OH. The average pore diameter varied from 132.8 **Å** 1for the untreated sample to 147.0658 **Å** for the treated ash. Pore development was also important in achieving large surface area and the or volume of the ash which promotes the diffusion of ammonium hydroxide into the pores and thus rerating more NH4OH carbon reactions which created more ores in the ash.as reported by[75]. It was shown by Stavropoulos and Zabaniotou [82] that KOH is dehydrated to K_2O, which reacts with co2 to produce water-shift reaction giving K_2CO_3 as a product. Drastic expansion of the carbon material creation of a large specific surface area and high pore volume is as a result of intercalation of metallic potassium. Mesoporous formation and enhanced surface area of activated carbon was found

to be promoted by CO_2 gasification as reported by Tseng et al. [83] as this would enhance the BET surface area and pore volume of the ash by promoting the diffusion of NH_4OH molecules into the pores and thereby increasing the NH_4OH - carbon reactions, which would then create more pores in the ash [75]. Similar observation was reported by where CO_2 gasification was found to promote the formation of mesopores and enhance the surface area of activated carbon.

4.2.5 Scanning Electron Microscope (SEM)

To determine the qualitative and morphological characteristics of the fly ash, Scanning Electron microscope was used. The dried sample was fixed with double side masking tape. Using double masking tape, the dried fly ash sample was fixed and carbon coated to make its surface conductive and was viewed on the SEM at different magnification to see the surface topography of the sample. Some scanning electron microscopy (SEM) images of the untreated and treated fly ash are shown in Fig 4.5(a-d). From the surface morphology of the ash samples, most of the ash particles were found to be spherical in shape with high porosity. For the untreated ash, the surfaces are blocked with some particles of calcium and having less porosity. The particles size is in the range of 10–100 μm. [47]. In Fig. 4.5(e-h), the morphology of the chemically treated fly ash shows more opened micropores with well-defined particle sizes and porous structure resulting from the alkaline activation. It is seen that well developed pores led to the large surface area and porous structure of the due to chemical treatment of the fly ash.

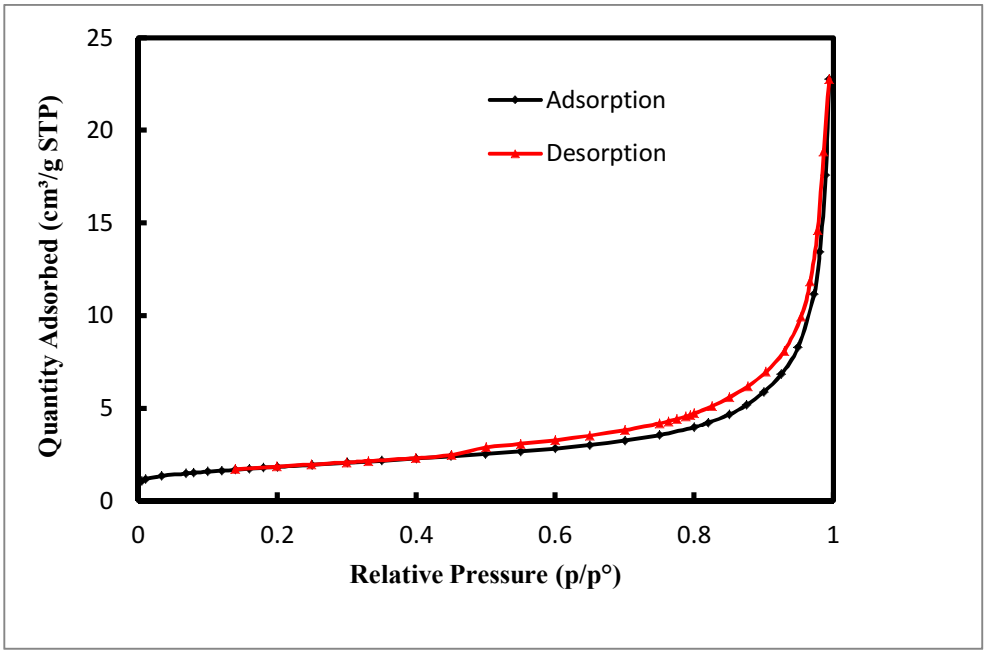

Figure 4.3: BET surface area analysis before treatment

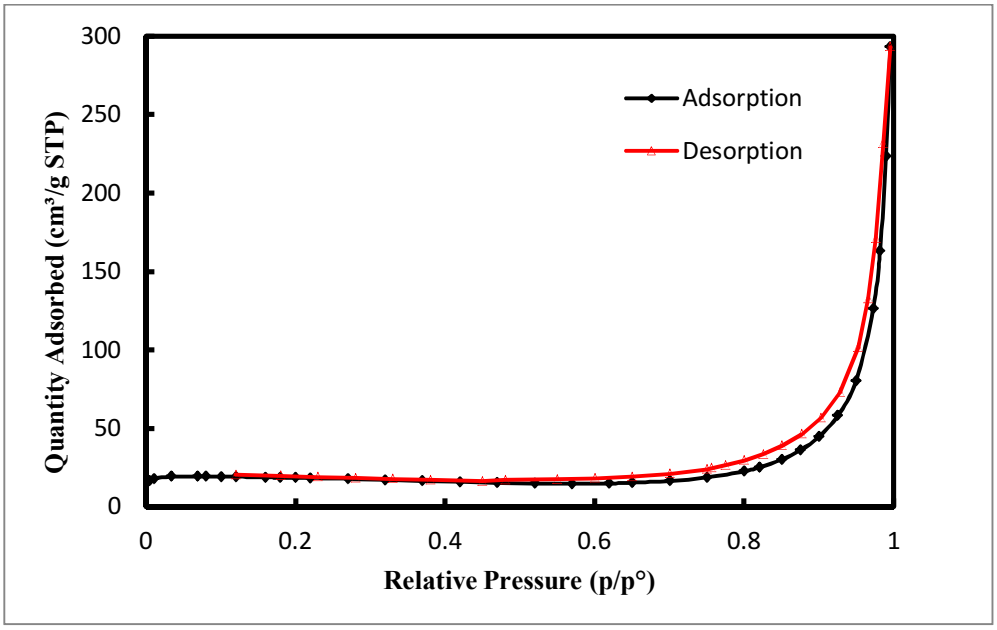

Figure 4.4: BET surface area analysis after treatment.

Table 4.3: Fly ash properties from N_2 adsorption

sample	BET surface area (m^2/g)	Langmuir surface area (m^2/g)	Average pore width (4v/A)(Å)	t-plot micropore volume (cm^3/g)
Ash before treatment	59	78	133	0.038
Ash after treatment	318	391	147	0.678

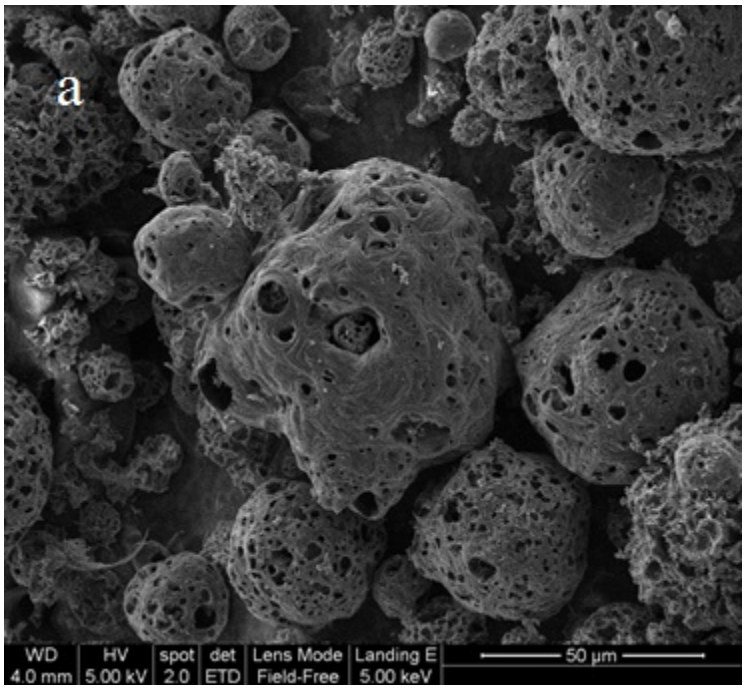

Figure 4.5: (a) SEM before chemical treatment.

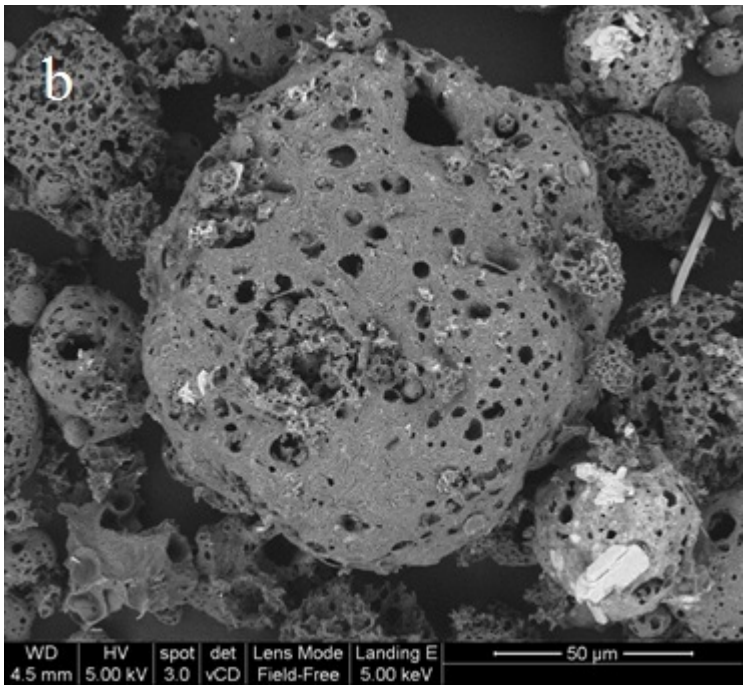

Figure 4.5: (b) SEM before chemical treatment.

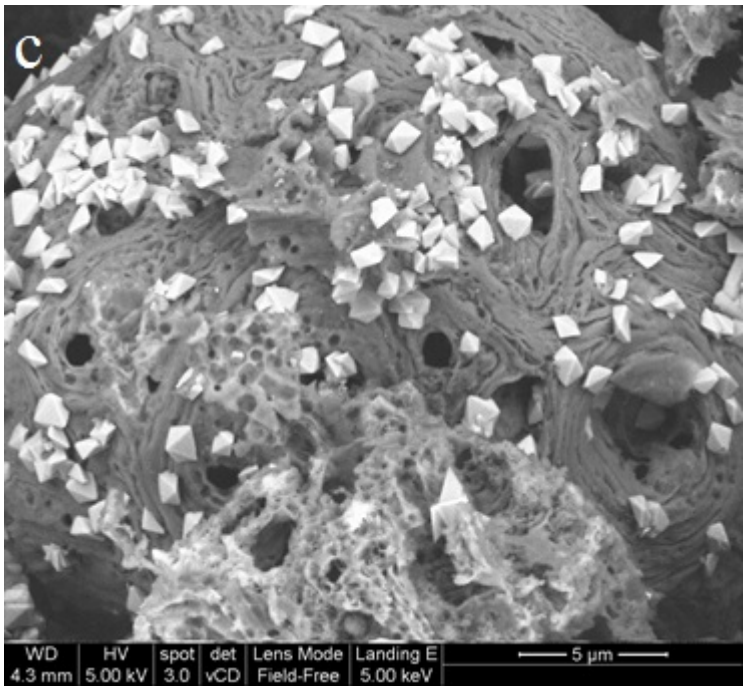

Figure 4.5: (c) SEM before chemical treatment.

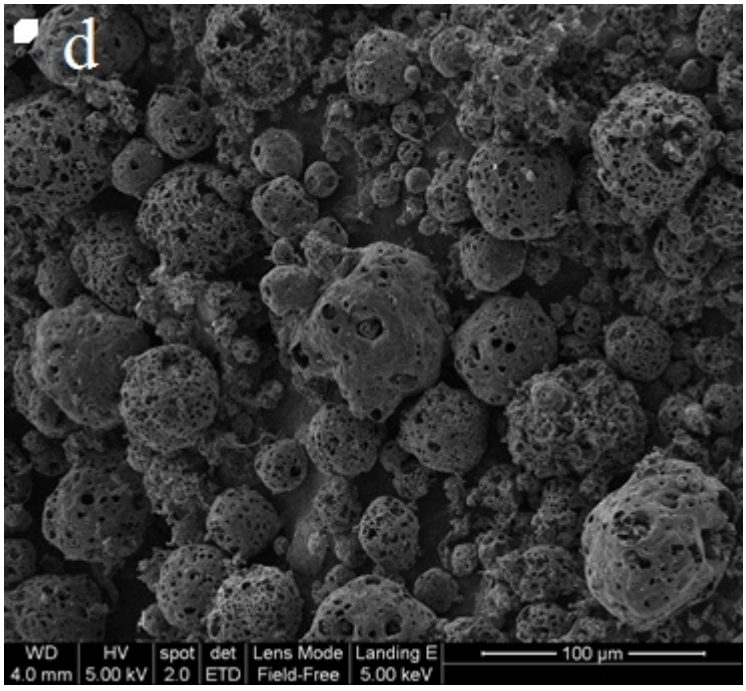

Figure 4.5: (d) SEM before chemical treatment.

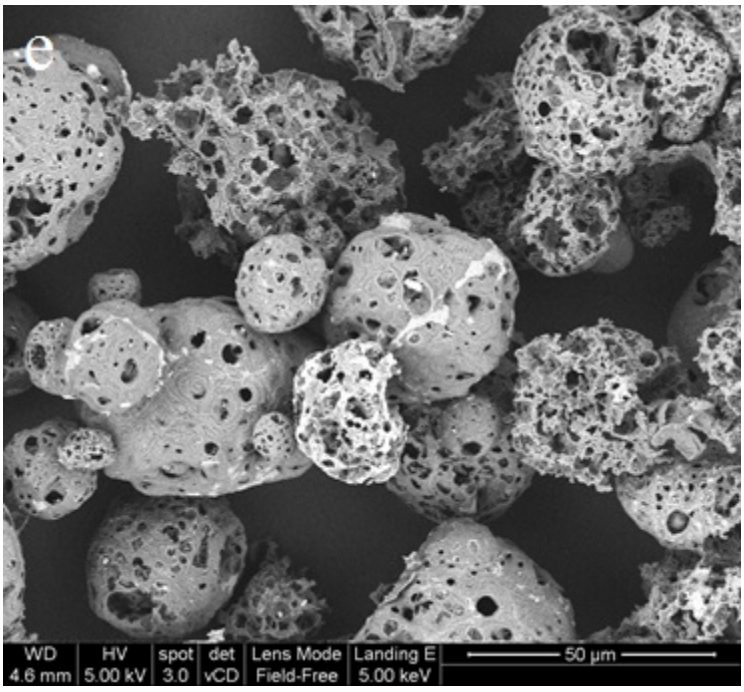

Figure 4.5: (e) SEM after chemical treatment.

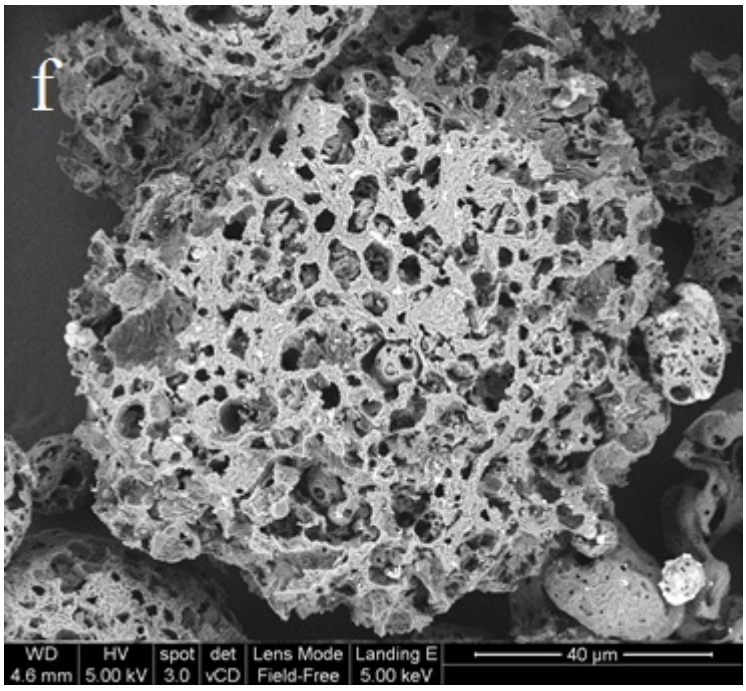

Figure 4.5: (f) SEM after chemical treatment.

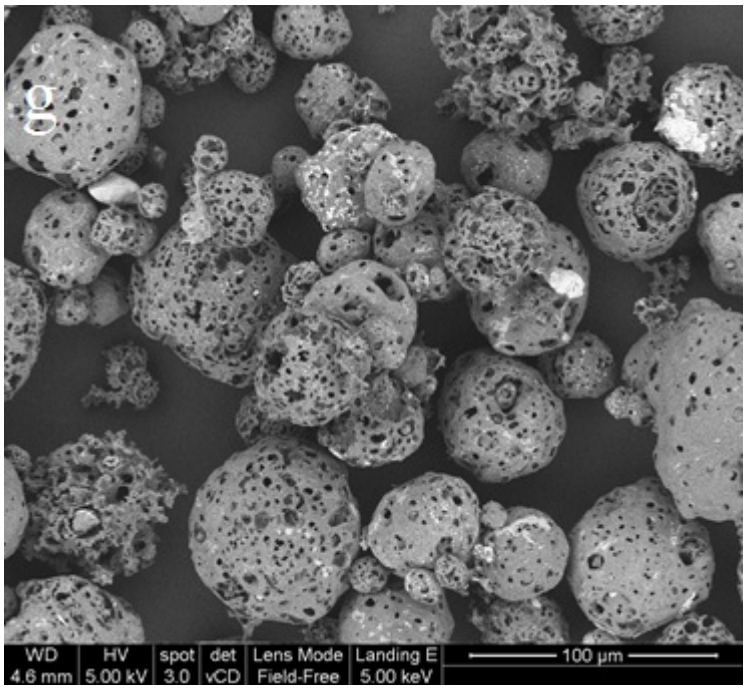

Figure 4.5: (g) SEM after chemical treatment.

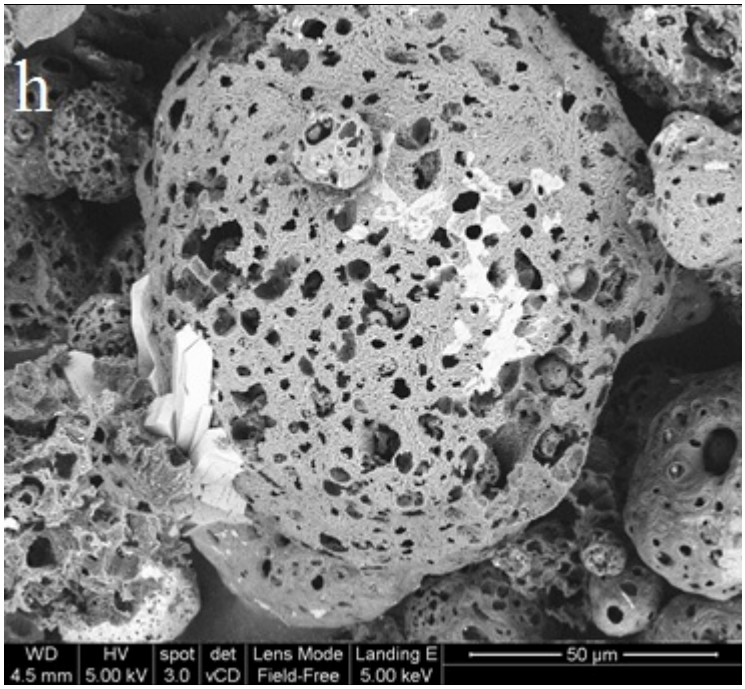

Figure 4.5: (h) SEM after chemical treatment

4.3 MECHANISM OF ADSORPTION

Adsorption is a process which a gas or liquid solute accumulates on the surface of a solid or a liquid called the adsorbent, forming a molecular or atomic film. It is operative in most natural, biological, physical, and chemical systems, and is widely used in industrial applications such as activated charcoal, synthetic resins and water purification. It is a consequence of surface energy similar to surface tension. In a real adsorption equilibrium system, the adsorbent is in contact with the bulk phase and the interfacial layer [7] part of the gas which resides in the force field of the surface area and the surface layer of the solid are the two main regions as of this layer. Therefore, the process by which molecules accumulate on the interfacial layer is termed adsorption and desorption is the converse process [85]. Adsorption isotherm is the fundamental concepts in adsorption science; it is the equilibrium relationship between the pressure and concentration in the bulk phase at constant temperature and the quantity of the adsorbed material. When the adsorption and desorption curve deviates from one another, they form the hysteresis loop which are mostly related to mesoporous solids.[86] and the shape of the hysteresis loop varies from one system to another. Adsorption isotherm is the primary source of information on the adsorption process. Adsorption of a gas by a porous material is described quantitatively by an adsorption isotherm, the amount of gas adsorbed by the material at a fixed temperature as a function of pressure [87].

As can be seen from this study, the adsorption- desorption curve was plotted for all the 24 runs as shown in appendix A and the accumulated adsorption capacity,

qe for each run was also calculated. A sample plot showing adsorption-desorption and amount chemisorbed is shown in figure 4.6 and 4.7 at l0% RH, Temperature of 40^{o}C, Concentration of 365 ppm and flow rate of 0.3 L/min.

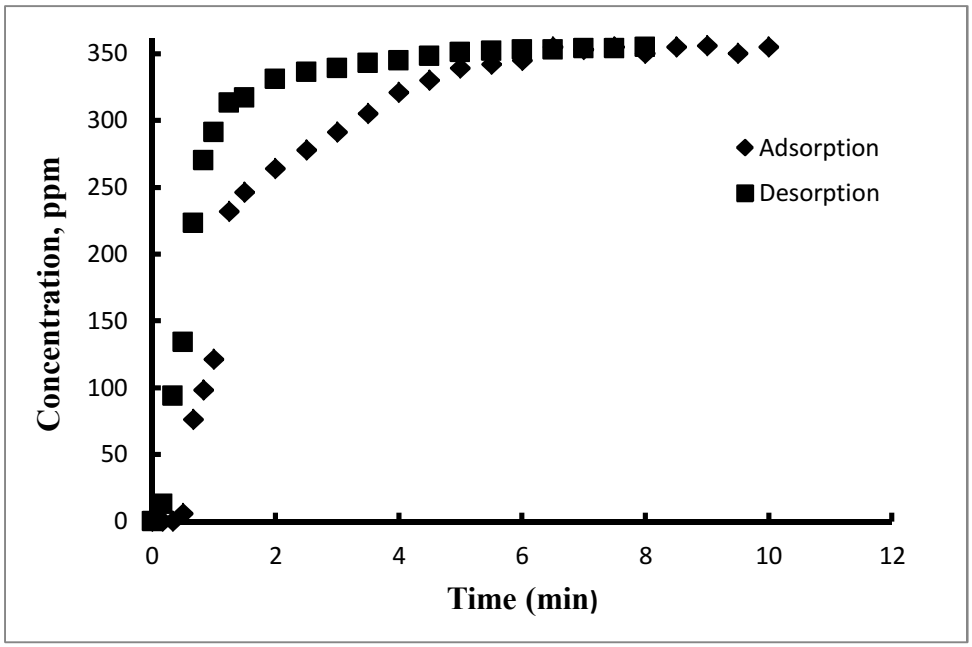

Figure 4.6: Adsorption- desorption curve for CO_2 adsorption

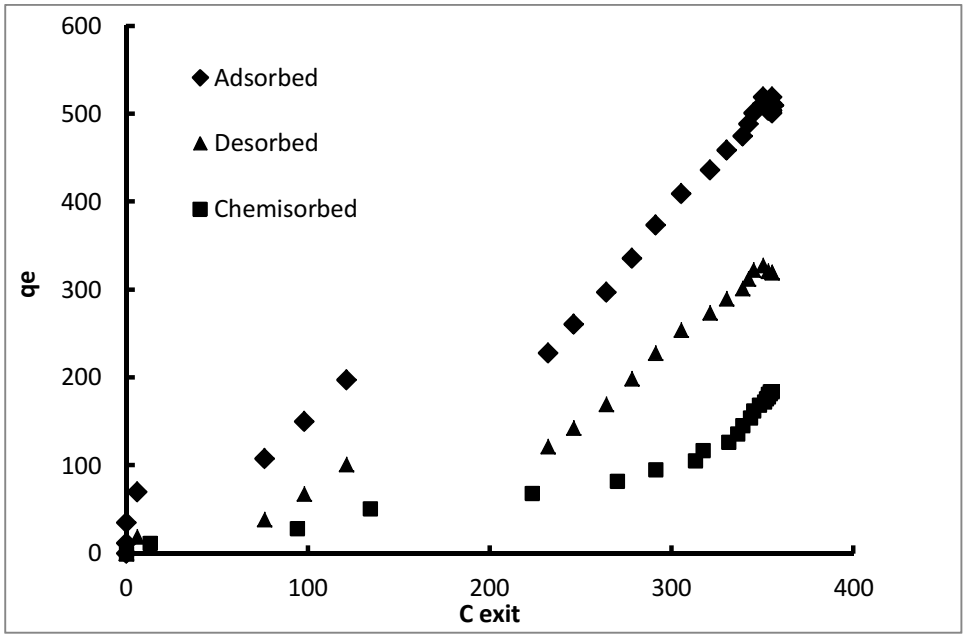

Figure 4.7: Plot showing the amount of CO_2 adsorbed, desorbed and chemisorbed

From figure 4.6, the area above the adsorption curve gives the amount adsorbed per unit mass while the area above desorption curve gives the amount desorbed and the area between them is the amount that reacted(chemisorbed). Based on favorable or unfavorable type, the effect of isotherm shape was studied. Treatment of the ash with ammonium hydroxide produced surface that adsorb CO_2 on to the ash surface. This is as a result of multiple layers on the surface of the ash. It is shown that the multilayer of adsorption takes place as a result of chemical reaction showing much more difference between the amount adsorbed and desorbed. It can be seen from figure 4.7, that the saturation adsorption capacity that covers monolayer of adsorption is about 240 mg/g, 90 mg/g for desorption and 50 mg/g was chemisorbed (reacted) respectively.

4.3.1 ADSORPTION ISOTHERM ANALYSIS

The adsorption isotherm shows the graphical representation showing the amount adsorbed by a unit weight of adsorbent to the amount of adsorbate. Langmuir, Freundlich and Brunauer–Emmett–Teller (BET) models were used model the experimental data.

Langmuir model describes the monolayer coverage on the surface of the solid as:

$$q = \frac{QbC_e}{(1 + bC_e)} \tag{5}$$

Where Q (mmol/g) is the maximum CO_2 adsorbed per unit mass for a complete monolayer and b (l/mmol) is the Langmuir constant related to the affinity of binding sites.

The Freundlich equation is given in equation (6)

$$q = kC_e^{\ b}. \tag{6}$$

Where both K and b are constants

On the other hand, Brunauer, Emmett and Teller (BET) model which assumes that multiple layers are formed on the surface of the adsorbent, which shows a multilayer coverage on the surface of the material, thus:

$$q = \frac{a_O a_1 C_e}{(a_2 - C_e)[1 + \frac{(a_o - 1)C_e}{a_2}]} \tag{7}$$

Where a_o, a_1 and a_2 represents the equilibrium constants for the first and subsequent layers respectively. The corresponding isotherm constants are presented in Table 4.4

The plot of all the models with the experimental results in figure 4.7 showed that BET model best fit the adsorption curves with regression coefficient of 0.984. This proves that the interaction between CO_2 and ash mixture has multilayer of adsorption which can be best fit by multilayer model such as the BET.

Table 4.4: Parameters for Langmuir, Freundlich and BET Model

Model	Adsorption	Desorption
Langmuir		
Q	430411	570263
b	3.11E-06	1.48E-06
R^2	0.954	0.876
x^2	28179	34061
Freundlich		
k	4.194	0.011
b	0.8	1.7546
R^2	0.938	0.965
x^2	38213	10362
BET		
ao	1.01981	1.18024
a_1	-137.635	93.0783
a_2	-9.42997	-85.0627
R^2	0.984	0.971
x^2	9547	8525

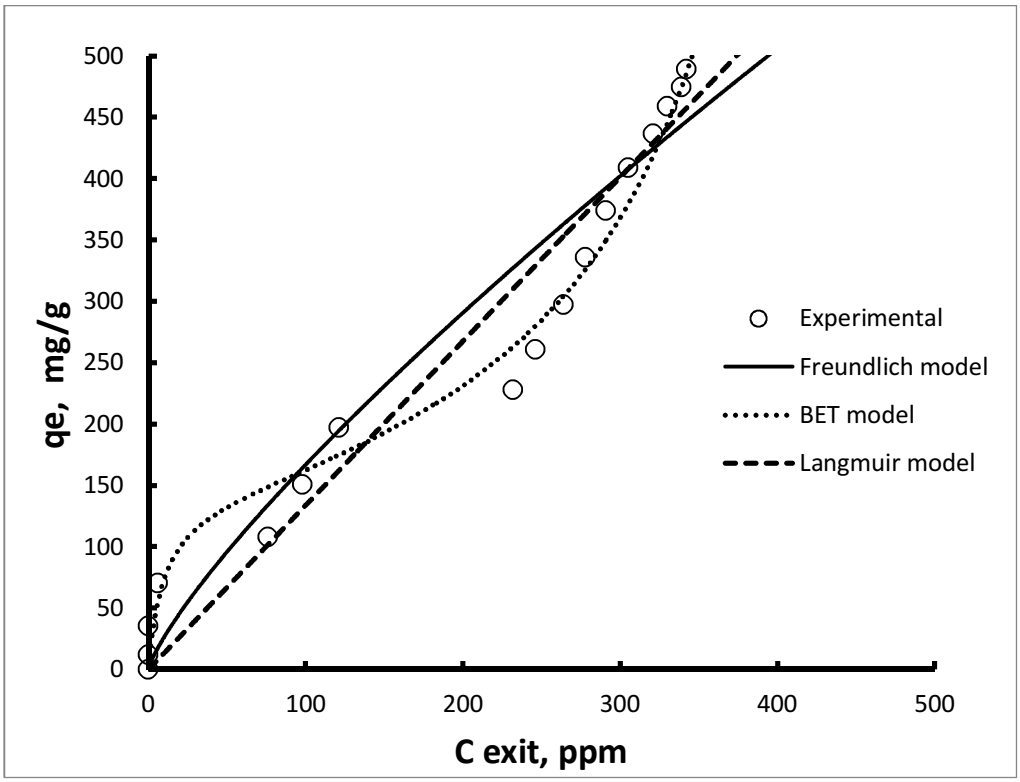

Figure 4.7: Plot showing the experimental data, Langmuir, Freunlich and BET model

Dispersion model: according to this model, the actual reactor can be represented by a tubular flow reactor in which axial dispersion takes place according to the effective diffusivity; D_{eff} is it is suppose that the axial velocity u and the concentrations are uniform across the diameter as in plug flow reactor. The PDE that describe the change in CO_2 concentration with respect to distance and time

$$\frac{\partial C_A}{\partial t} = D_{eff}\left(\frac{\partial^2 C_A}{\partial r^2} + \frac{1}{r}\frac{\partial C_A}{\partial r}\right) - u\frac{\partial C_A}{\partial x} - kC_A^n \qquad (8)$$

Where C_A is the concentration of carbon dioxide obtained at a distance r from the column entrance and D_{eff} and u are the axial diffusion and velocity of the gas of

the gas inside the column, respectively. The above equation was solved using MATHEMATICA V.8 and it was found that $D_{eff} = 0.35 \times 10^{-1}\ \frac{cm^2}{s}$, $k = 1.2 \times 10^{-7} s^{-1}$, L = 10cm, u = 35 cms^{-1} and the reaction order was 1.3.

However, the model proposes that in an actual reactor, the mixing state, consist of some segregated flow and some axial mixing which is represented by a particular value of D_{eff}/uL. The response curve for the dispersion model is shown in figure 4.8. The value of D_{eff}/uL was found to be 0.1×10^{-3} and the column fulfills the requirement of plug flow behavior. It can be seen from figure 4.8 that dispersion model fits the experimental data.

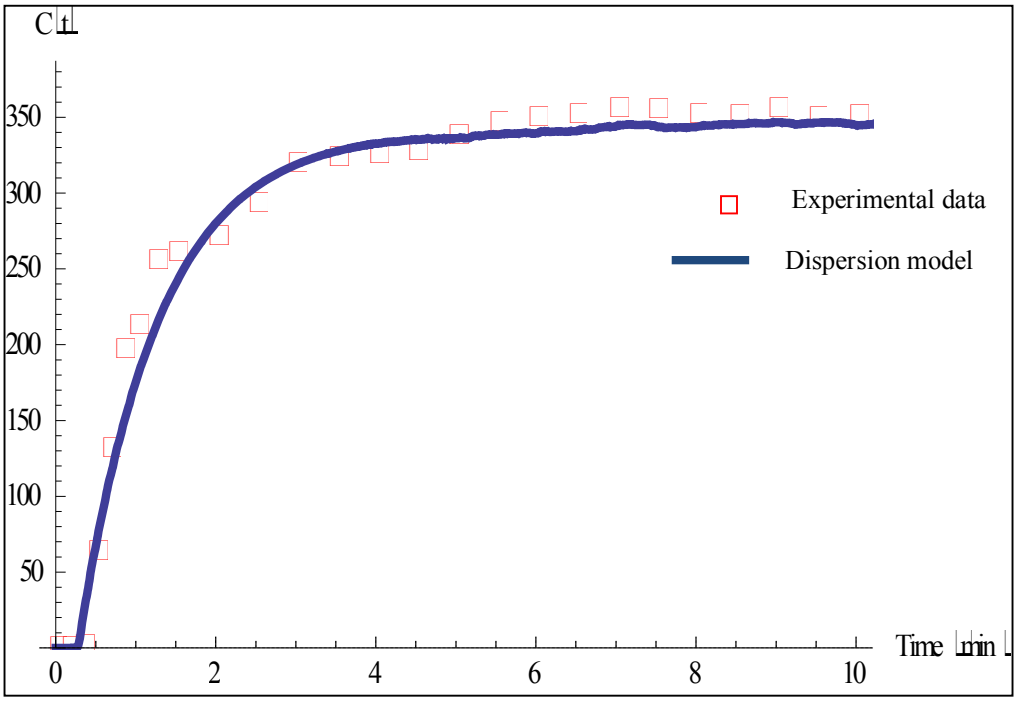

Figure 4.9: Experimental and dispersion model isotherm for CO_2 adsorption

4.4 ANALYSIS OF VARIANCE (ANOVA)

An ANOVA is an analysis of the variation present in an experiment. The ANOVA tests showed which of the kinetic parameters of the adsorption were significant statistically to a 95% confidence level and those that were not statistically significant.

Table 4.5: ANOVA variables and conditions

FACTORS	PAREMETER	LEVEL 1	LEVEL 2
A	Gas flow rate (L/min)	0.3	0.7
B	Temperature	0	40
C	Concentration	365	795
D	Humidity	Low	High

Interactions	Factor 1	Factor 2
A x B	Gas flow rate (L/min)	Temperature
A x C	Gas flow rate (L/min)	Concentration
A x D	Gas flow rate (L/min)	Humidity
B x C	Temperature	Concentration
B x D	Temperature	Humidity
C x D	Concentration	Humidity

4.4.1 LEVEL AVERAGE (MAIN EFFECTS)

I. Gas flow rate

Increasing the CO_2 flow rate means passing more pressure to the bed and the surface of the ash which increases the adsorption capacity as a result of increase in the diffusion of the molecules on to the surface of the particle. It was also reported [64, 87] that when high pressure of CO_2 is applied, there is more interaction between the amine and CO_2 molecules resulting in more chemical reaction and higher chemisorption.

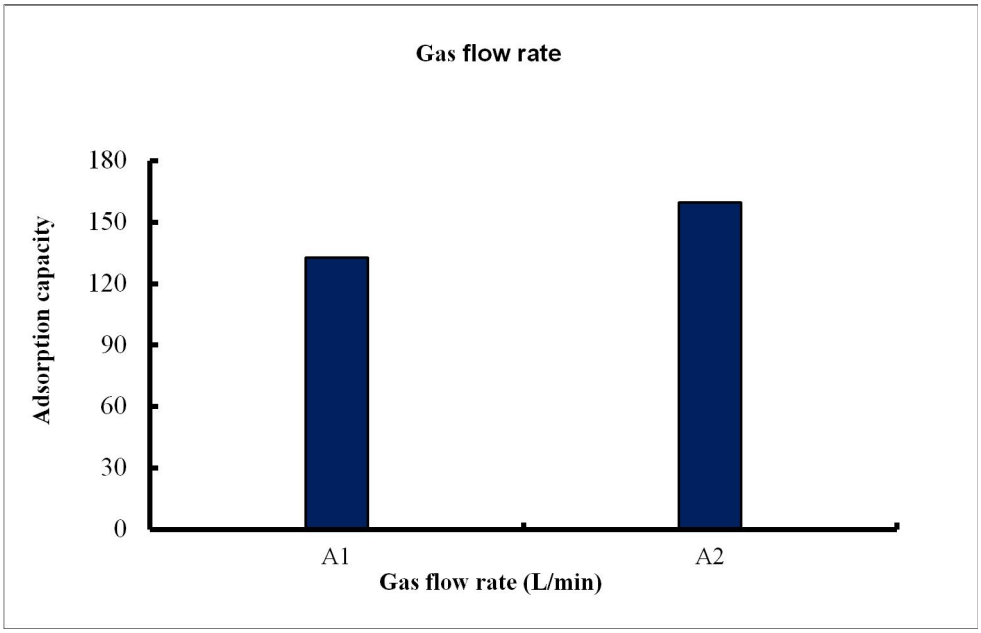

Figure 4.8: Gas flow rate main interactions

II. Temperature

Increasing the flow rate will increase the pressure to the bed which increases the temperature of the bed and hence increases the adsorption capacity per unit volume, At higher temperature the adsorbate CO_2 molecules tend to be in active energized form and are harder to adsorb compare to molecules at lower temperature which has lower activation energy to be adsorbed but increase in flow rate and a minor or negligible increase in pressure, temperature will not be affected. This was in accordance with the findings of [88] shows the CO_2 adsorption/desorption profile of the sample AC-MDEA ,the co2 uptake capacity and reaches maximum with increase in temperature indicating chemical adsorption process. As observed previously for the activated sorbents, no CO_2 remains after desorption cycle, implying the reversibility of the process, thus the sample can be regenerated and used in cyclical operation. It was also stated by [89] that the adsorption of CO_2 by porous materials or amines is an exothermic process. Accordingly, with the increase in temperature, the adsorption capacity decreases. However, He shows otherwise that the CO_2 adsorption capacity increases as the temperature increases. In the end, it is stated that if the adsorption time is long enough to ensure I reaches equilibrium, the adsorption capacity at low temperature will eventually be larger than in at high temperature.

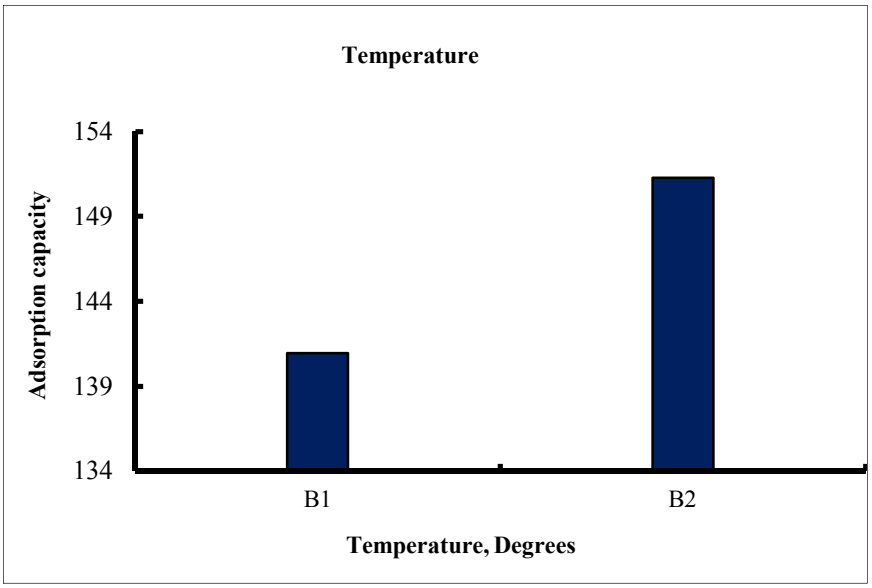

Figure 4.10: Temperature main interaction

III. Concentration

The adsorption capacity of CO_2 Increases as the concentration increases, this is because of the driving force between the bulk concentration and the concentration at the surface of the particle which enables diffusion as well as mass transfer and hence decreases their resistance.

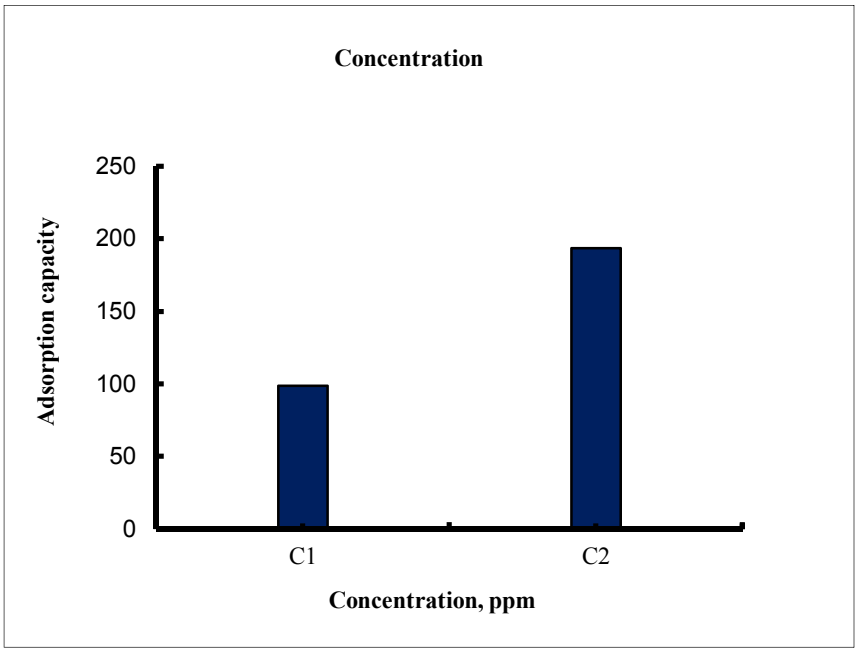

Figure 4.11: Concentration main interactions

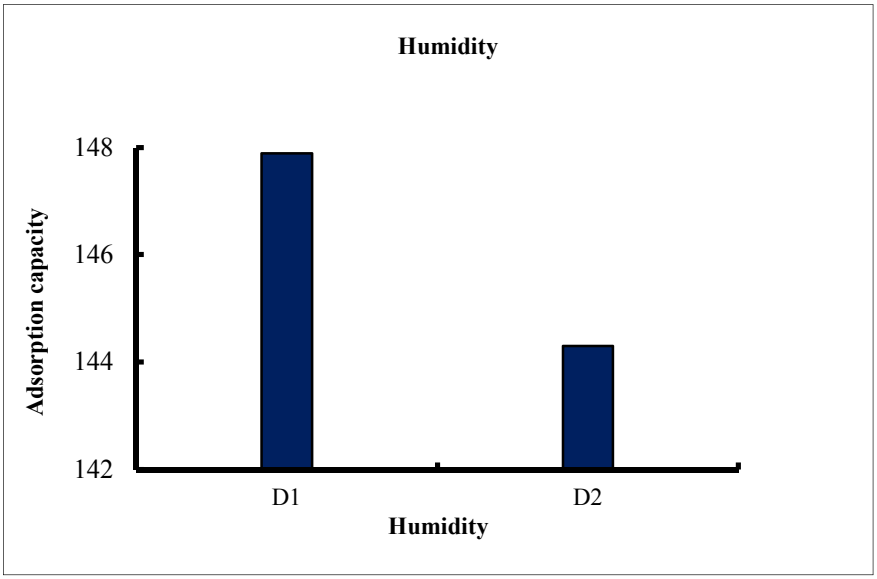

Figure 4.12: Humidity main interactions

IV. Humidity

Increasing the humidity will decrease the partial pressure of CO_2 in the gas phase which competes with the CO_2 adsorption onto the surface, which result in competitive adsorption and part of the pores will have water condensation instead of evaporation. However, at high humidity, humid air will cool down the bed and diffusion onto the surface of particle will be less and hence decreases the adsorption capacity [67]. When adsorption was performed with PEI-functionalized PAN from a humid feed with less CO_2 partial pressure, high adsorption capacity of CO_2 was observed.

4.4.2 LEVEL AVERAGE (INTERACTION)

I. Gas flow rate - Temperature Interaction

Increasing or decreasing both temperature and flow rate has negligible effect on the CO_2 adsorption capacity as shown in figure 4.13

II. Gas flow rate - Concentration Interaction

Increasing both flow rate and concentration doubles the adsorption capacity due to synergistic effect. However, increasing the concentration of CO_2 with decreasing the gas flow rate will have higher adsorption capacity then decreasing concentration and increasing gas the flow rate, as the resistance to flow rate is governed by convective mass transfer while concentration resistance is governed by diffusivity as shown by the dispersion model.

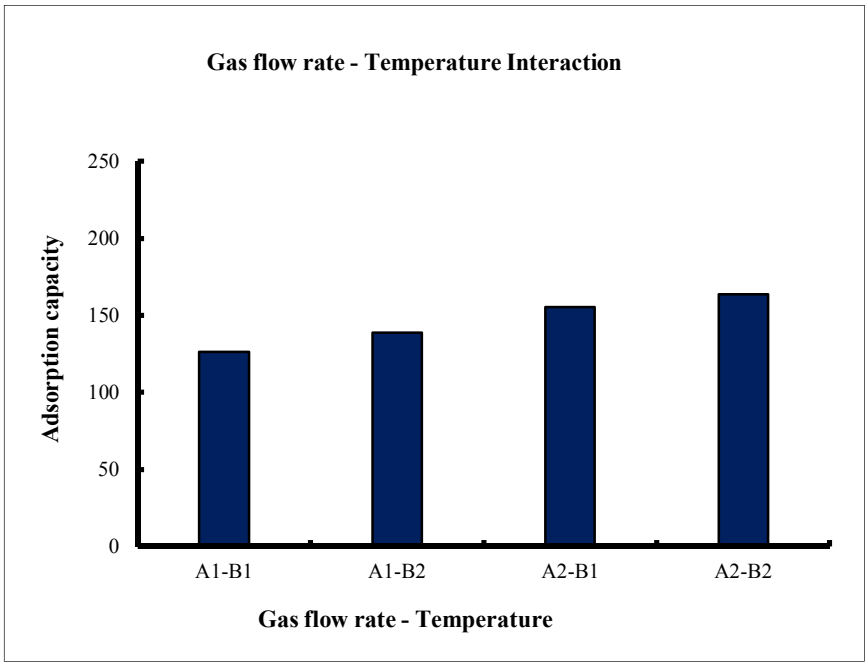

Figure 4.13: Gas flow rate – Temperature average level Interaction

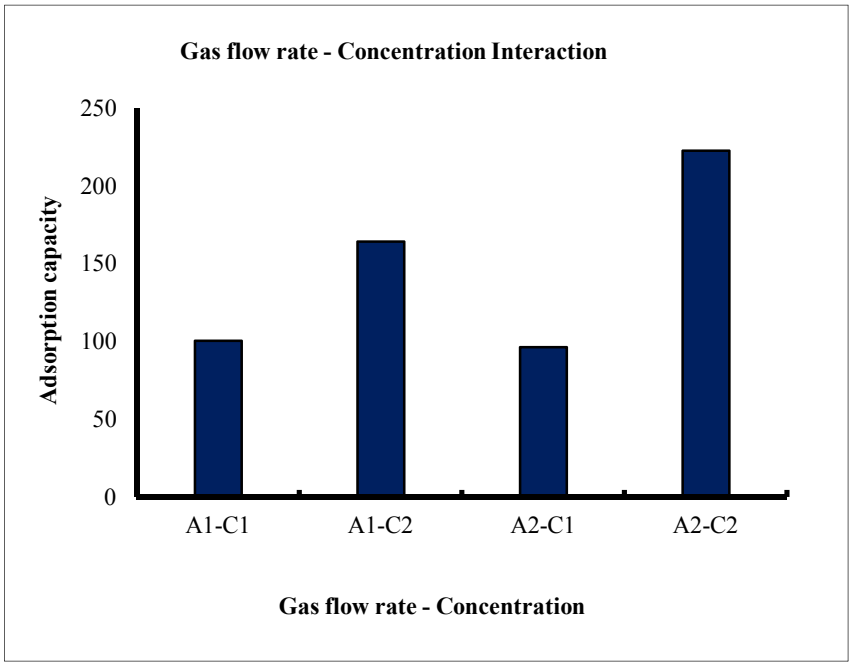

Figure 4.14: Gas flow rate – Concentration average level Interaction

III. Gas flow rate - Humidity Interaction

The effect of humidity is negligible by increasing or decreasing the gas flow rate; this is because the gas will carry out some water molecules which are absorbed along with the gas. The adsorption capacity increases at low humidity as the CO_2 gas is attracted to the surface with water molecules which forms hydrogen bond. At high gas flow rate, the convective external force will lead to higher force on the surface of the particle at high flow rate, thus increases the adsorption capacity much more than the hydrogen bond adsorption capacity increment.

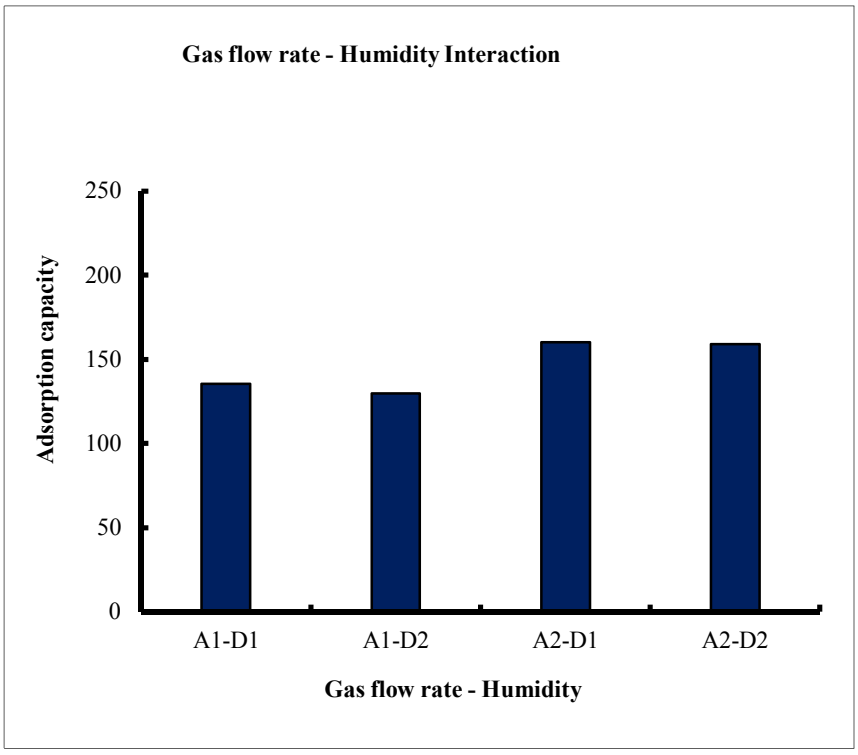

Figure 4.15: Gas flow rate – Humidity average level Interaction

IV. Temperature - Concentration Interaction

The adsorption capacity of CO_2 increases (double) when both temperature and concentration increases due to synergistic effect, but at low temperature and high concentration, the adsorption capacity is also doubled as the effect of temperature is negligible at low temperature range (0-40^{o}C) compared to concentration of the gas.

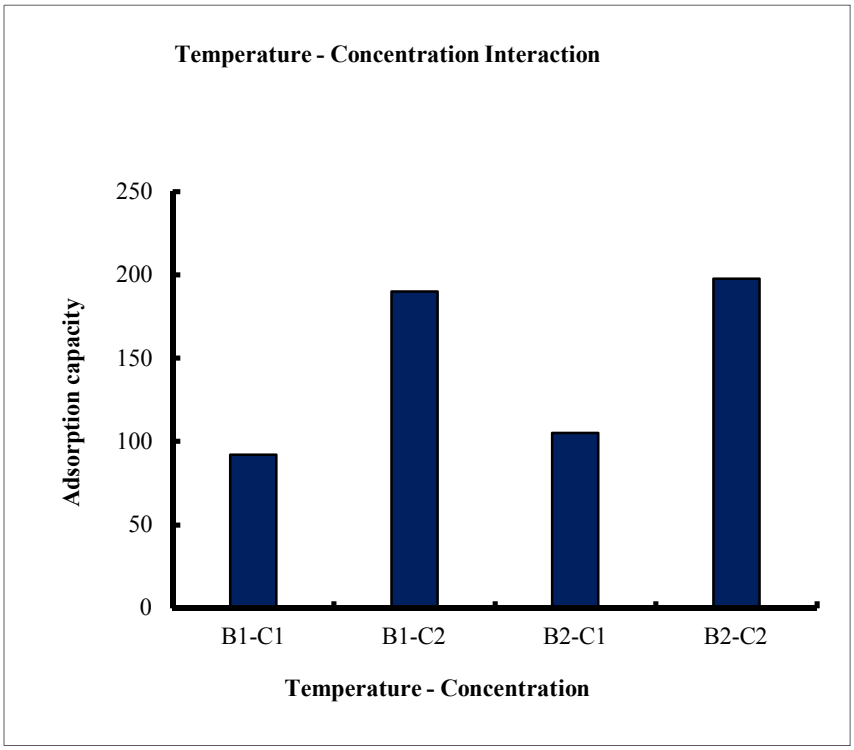

Figure 4.16: Temperature - Concentration average level Interaction

V. Temperature - Humidity Interaction

At low temperature and humidity, there is water vapor condensation into the mesopores which blocks the surface of the particle and hence blocks the adsorption process. It was also reported by [90] that the adsorption capacity of CO_2 on activated carbon are affected negatively by the presence of water due to its ability to adsorb competitively. Although this effect is reduced by the hydrophobic nature of most activated carbons compared to zeolites, storage under humid conditions still results in a decrease of adsorption capacity. Gradual oxidation of carbon surface is the reason for the detrimental effect on the adsorption capacity of activated carbons in the presence of moisture [91].

However, increasing the temperature and decreasing the humidity will open the mesopores which decreases the competitive effect of adsorption with water and hence increases the adsorption capacity making the process endothermic. At high humidity and low temperature there is high condensation of water molecules on to the surface of the fly ash particles and hence increases the adsorption capacity in to the absorbed water molecules which is better than low temperature and high humidity. Furthermore, at both high temperature and humidity the adsorption capacity is less compared to low temperature and high humidity, since the thickness of the film is less and part of the water is evaporated.

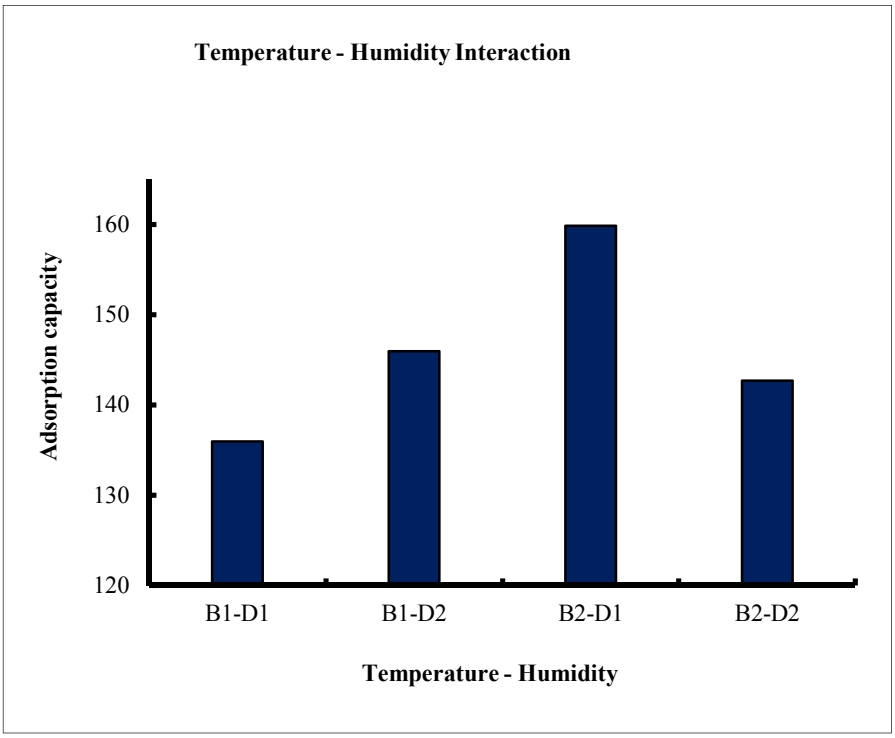

Figure 4.17: Temperature - Humidity average level Interaction

VI. Concentration - Humidity Interaction

At low concentration and low humidity, the adsorption capacity is less due to negligible diffusion effect at low concentration. However, regardless of the effect of humidity, increase in concentration increases the adsorption capacity, since the mole fraction of CO_2 compared to water is high which controls the adsorption as there are no water molecules to be adsorbed. Therefore, with either increase or decreases in concentration, humidity has no effect compared to the concentration on the adsorption capacity.

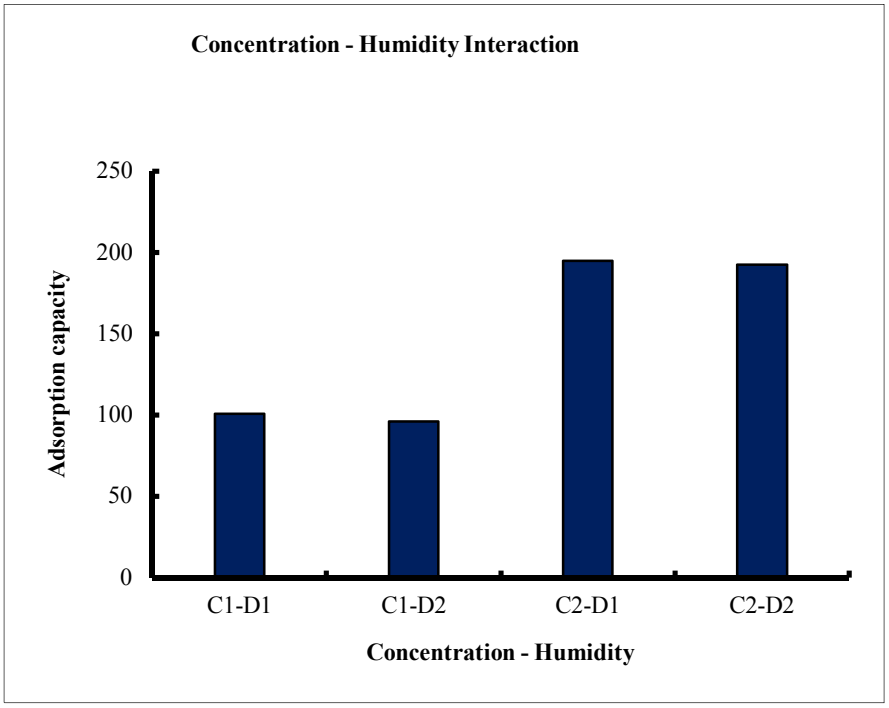

Figure 4.18: Concentration - Humidity average level Interaction

4.5 KINETIC PARAMETERS

Several kinetic parameters were studied which influence the adsorption of CO_2 onto fly ash; these parameters are concentration, gas flow rate, relative humidity and temperature.

4.5.1 Effect of concentration

Carbon dioxide adsorption is significantly influenced by the concentration of CO_2. The effect of concentration of CO_2 onto fly ash was investigated at 795ppm and 365ppm respectively at different flow rate and temperature as shown in figures 1-10 in appendix A. From the figures 4.19 and 4.20, it shows that adsorption capacity increases with increase in concentration of CO_2 [60, 61]. This is due to the driving force between the bulk concentration and the concentration at the surface of the particle which enables diffusion as well as mass transfer and hence decreases their resistance. However, when the ash surface is saturated, a further increase in concentration will not increase the adsorption capacity. The time for this ash to be saturated for the system of higher concentrations was observed to be shorter. This is due to the higher adsorbate concentration saturated the adsorbent more quickly. Therefore, the saturation time decreases by increasing the adsorbate concentration [62, 63]. This shows that the initial concentration plays an important role in the adsorption capacity of CO_2 on the fly ash.

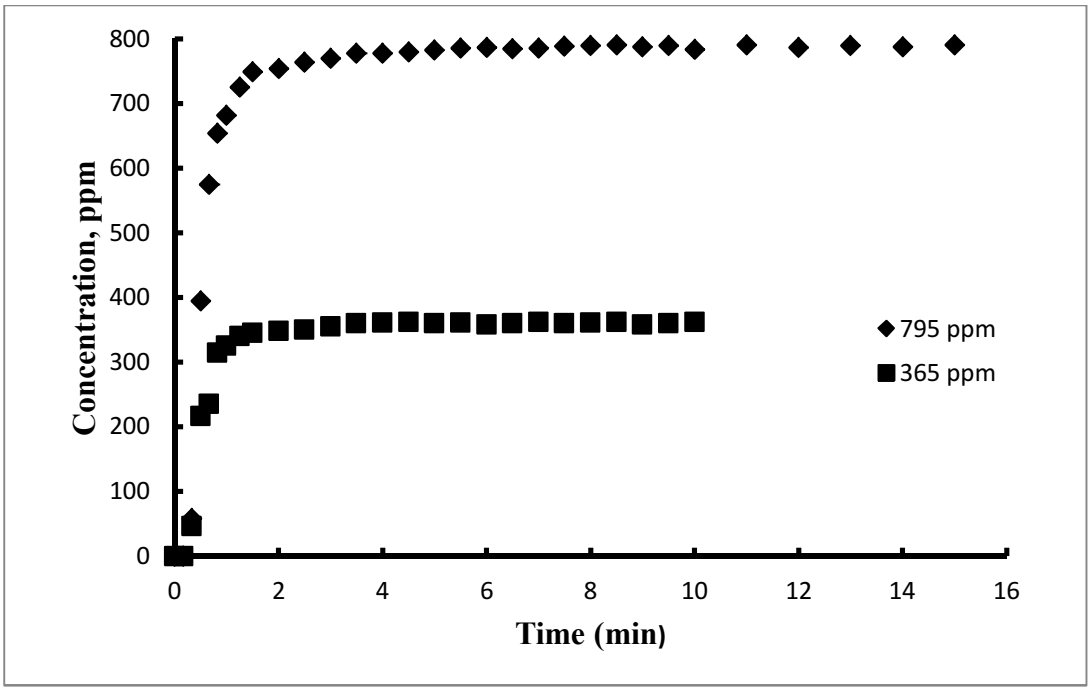

Fig 4.19: Effect of concentration at flow rate = 0.7L/min, Temp=40^{o}C and %RH= Low

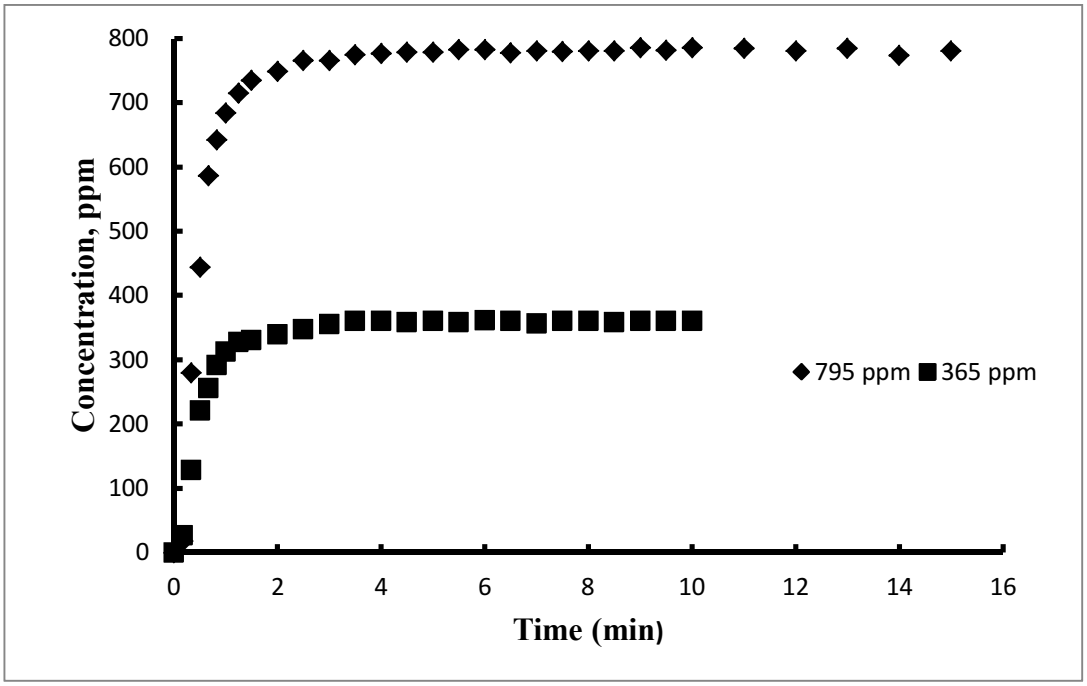

Fig 4.20: Effect of concentration at flow rate = 0.3L/min, Temp=40^{o}C and %RH= High

4.5.2 Effect of Flow Rate

The effect of gas flow rate was studied at concentrations of 795ppm and 365ppm for both low and high humidity by varying the CO_2 flow rate at 0.3, 0.7 and 1.0 L/min respectively with the corresponding curves shown in figures 19-26 in appendix B. Increasing the CO_2 flow rate means passing more pressure onto the bed and the surface of the fly ash particle which increases the adsorption capacity due to increase in the diffusion of the molecules on to the surface of the particle. It was also reported by [21, 64] that when high pressure of CO_2 is applied, there is a higher interaction between the amine and CO_2 molecules resulting in more chemical reaction and higher chemisorption. It was also observed that increasing the flow rate decreases both the breakthrough time and the total adsorption time showing a shorter life span of the column, at higher flow rates, the break through time occurred earlier. This is as a result of decrease in the residence time of gas and the contact time between the sorbent and the adsorbate as the flow rate increases [61]. When the gas flow rate increases, the mass transfer in the gas film may likely be enhanced since the thickness of the mass-transfer boundary layer around the ash is reduced by high floe rates resulting in reduced external mass-transfer resistance and saturation [35, 65].

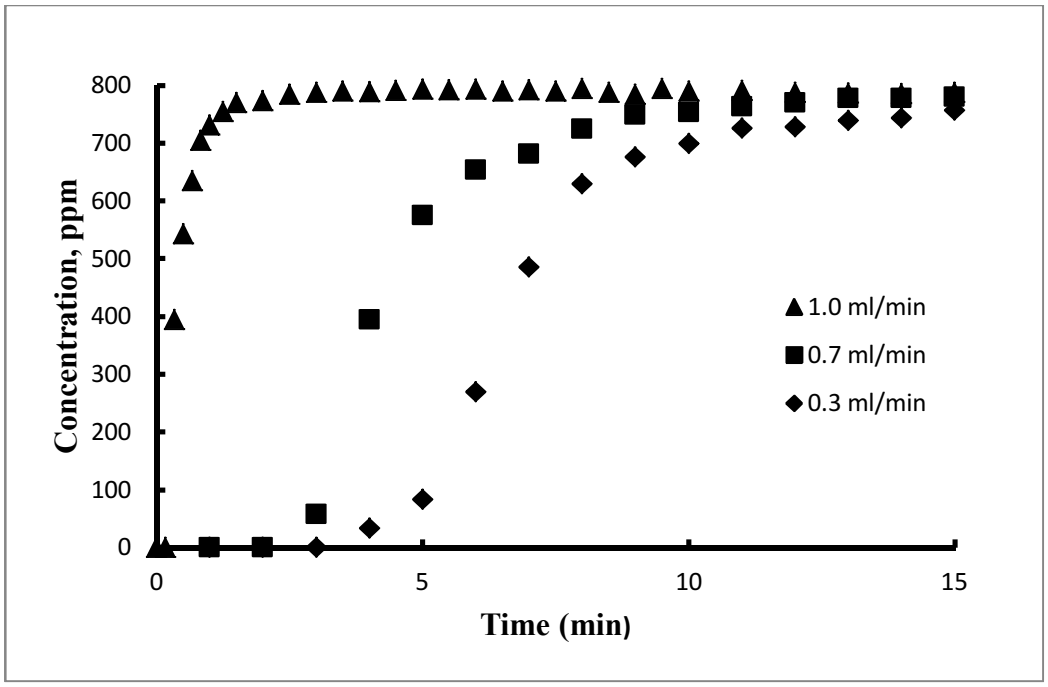

Fig 4.21: Effect of flow rate at C= 795ppm, T=40^{o}C and %RH= Low

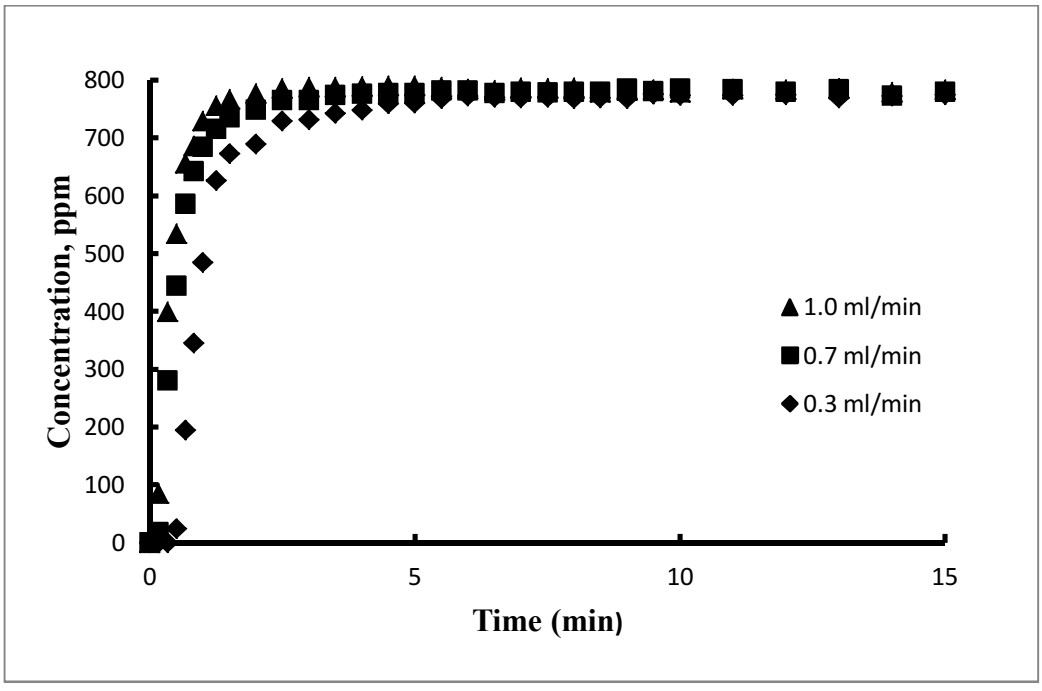

Fig 4.22: Effect of flow rate at C= 795ppm, T= 40^{o}C and %RH= High

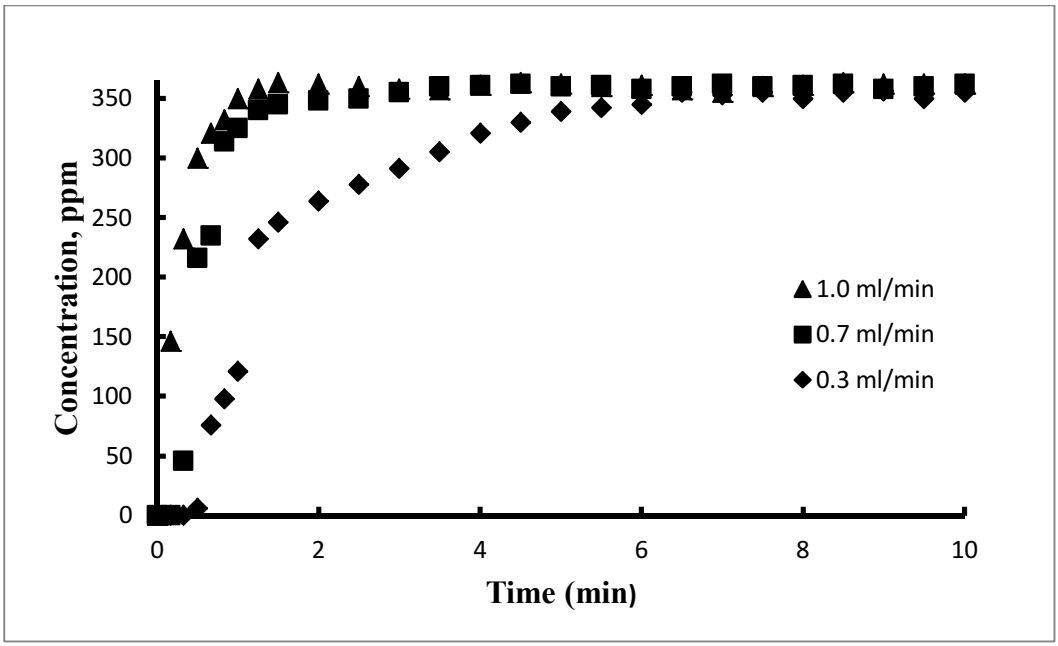

Fig 4.23: Effect of flow rate at C= 365ppm, T= 40^{o}C and %RH= Low

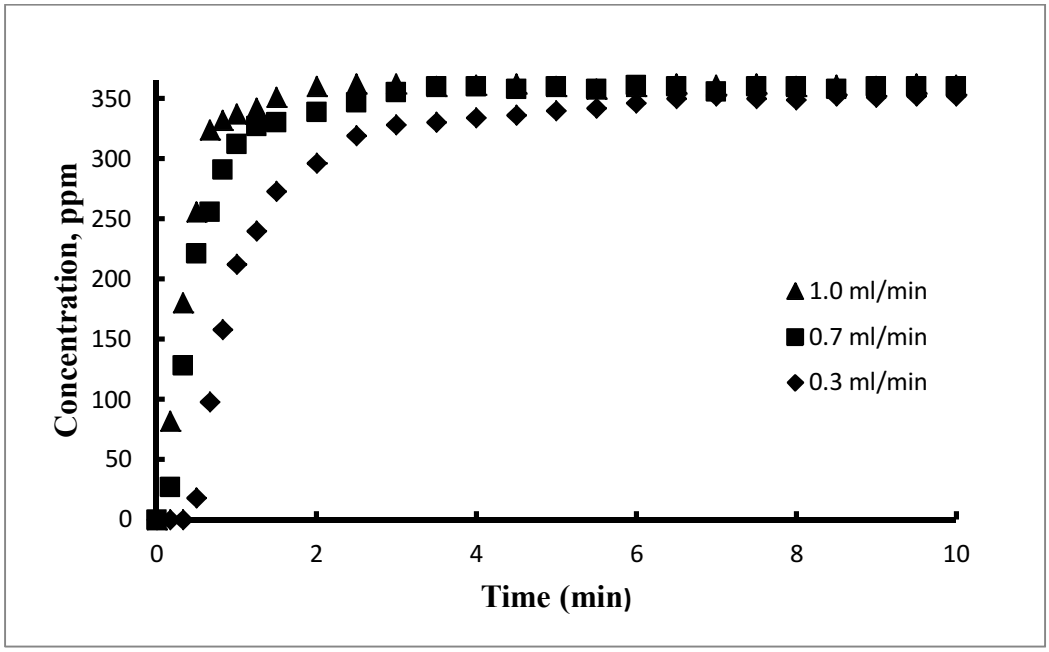

Fig 4.24: Effect of flow rate at C= 365ppm, T= 40^{o}C and %RH= High

4.5.3 Effect of Humidity

Figures 4.25 and 4.26 shows the effect of relative humidity on the adsorption of CO_2 onto fly ash at low and high humidity (10% and 80% RH) obtained in this study. There was a decrease in the adsorption capacity at high relative humidity as shown in figure 4.25 and 4.26 respectively. This can be explained by the effect of capillary condensation of water vapor in micropores were a large portion of active sites at the surface of the micropore would be blocked at 80% RH condition. Correspondingly, the adsorption capacity decreased dramatically at 80% RH [14, 23, and 66]. Increasing the humidity will decrease the partial pressure of CO_2 in the gas phase which competes with the CO_2 adsorption onto the surface, which result in competitive adsorption and part of the pores will have water condensation instead of evaporation. However, at high humidity, humid air will cool down the bed and diffusion onto the surface of particle will be less and hence decreases the adsorption capacity [67]. Furthermore, increasing the temperature and decreasing the humidity will open the mesopores which decreases the competitive effect of adsorption with water and hence increases the adsorption capacity making the process endothermic [68]. At high humidity and low temperature there is high condensation of water molecules on to the surface of the particles and hence increases the adsorption capacity in to the absorbed water molecules [66]. Furthermore, at high temperature and high humidity the adsorption capacity is less compared to low temperature and high humidity, since the thickness of the film is less and part of the water is evaporated.

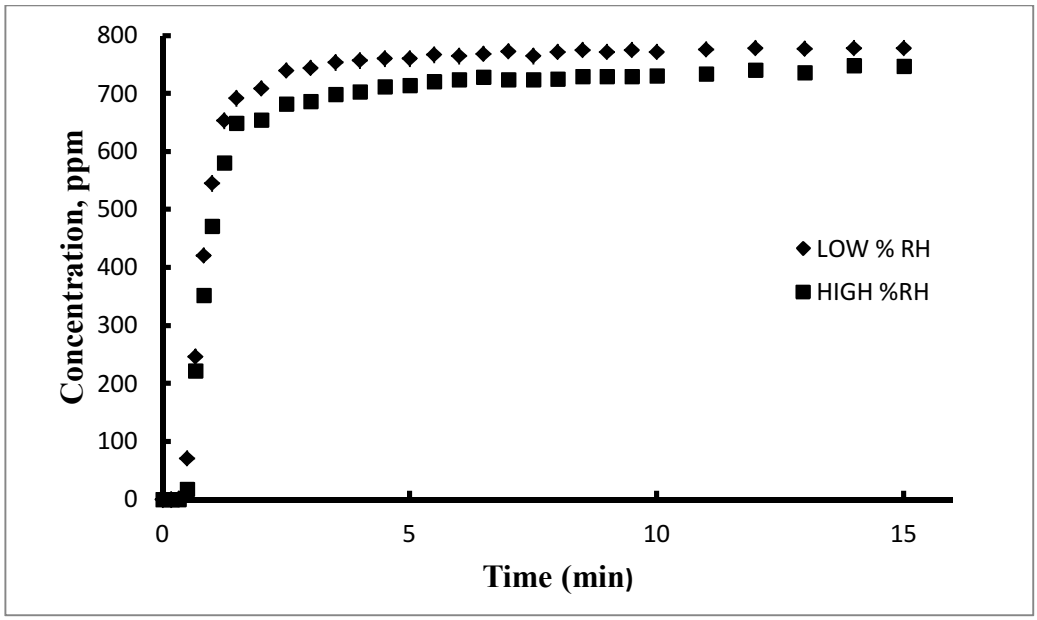

Fig 4.25: Effect of Humidity at Flow rate = 0.3L/min, Concentration = 795ppm and Temp = 0^{o}C

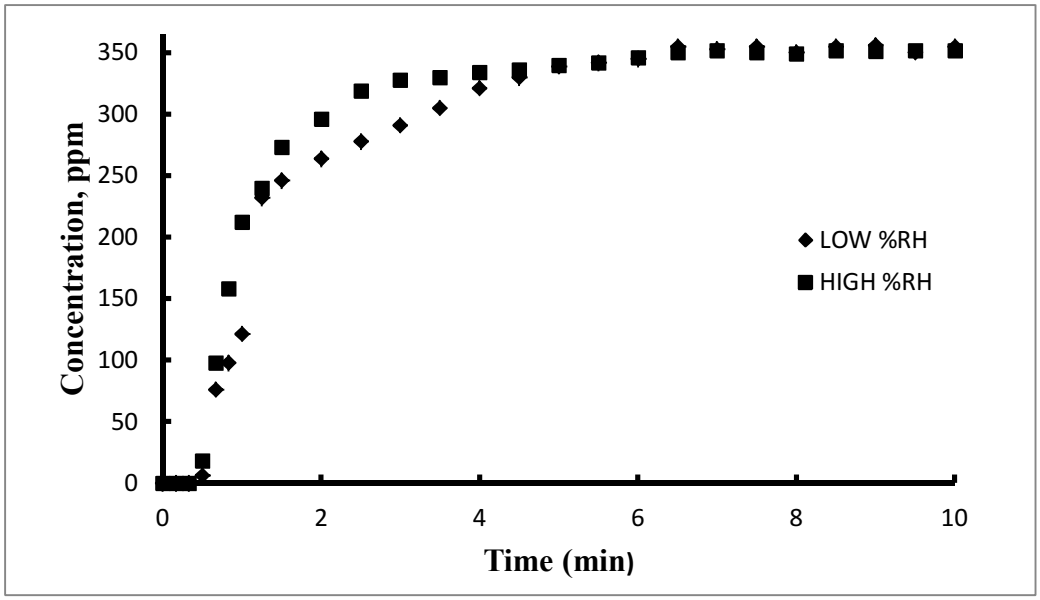

Fig 4.26: Effect of Humidity at Flow rate = 0.3L/min, Concentration = 365pp and Temp = 40^{o}C

4.5.4 Effect of Temperature

The effect of temperature was studied using seven different temperature values at -20, -10, 0, 10, 20, 30, and 40^{o}C respectively, while the flow rate, concentration and humidity were kept constant (flow rate = 0.3 L/min, concentration = 330 ppm). As shown in figures 4.27 and 4.28, increasing the bed and inlet gas temperature, there is increase in the adsorption of CO_2 per unit time. The breakeven point is increased as well; this suggests endothermic nature of the interaction between the gas molecules and the surface of the ash, where both physical and chemical adsorption takes place. Moreover, there is a direct link between increasing the temperature and the pressure drop across the bed [67, 69]. At higher temperature the adsorbate CO_2 molecules tend to be in active energized form and are harder to adsorb compare to molecules at lower temperature which has lower activation energy to be adsorbed but increase in flow rate and a minor or negligible increase in pressure, temperature will not be affected.

To determine the thermodynamic parameters such as the heat of adsorption, standard entropy and standard free energy of the process, equations 9 and 10 were used [70-74].

$$\Delta G^{0}_{ads} = -RTlnK_C \quad (9)$$

Where

$$lnK_c = \frac{\Delta S^{0}_{ads}}{R} - \frac{\Delta H^{0}_{ads}}{RT} \quad (10)$$

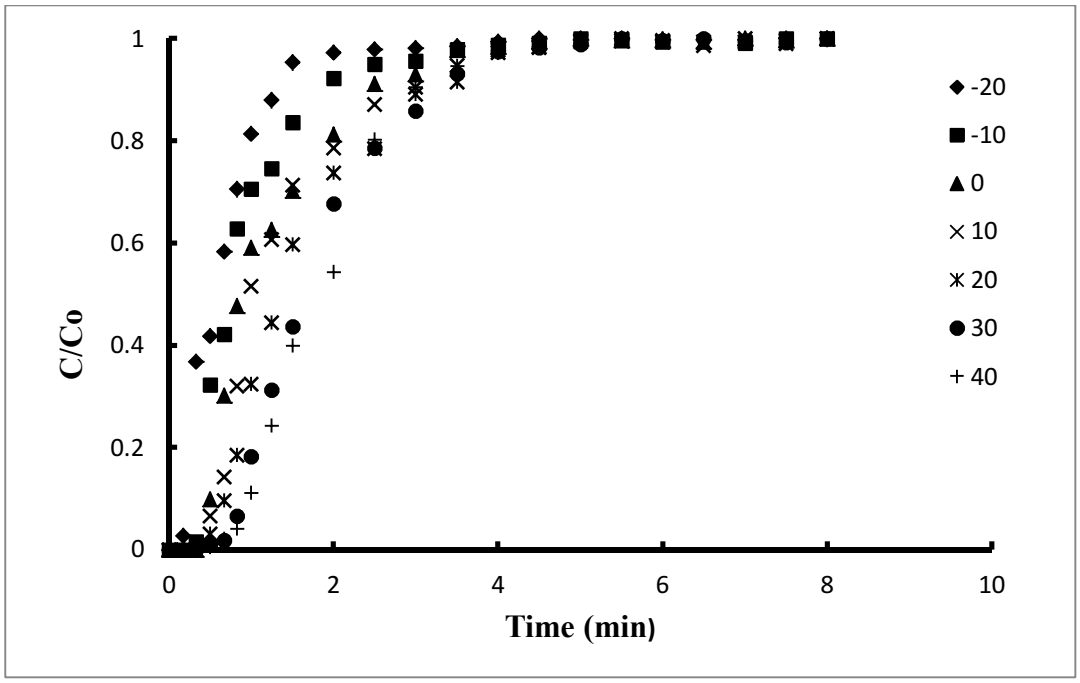

Fig 4.27: Effect of Temperature at Flow rate = 0.3L/min, concentration = 330ppm and %RH =Low

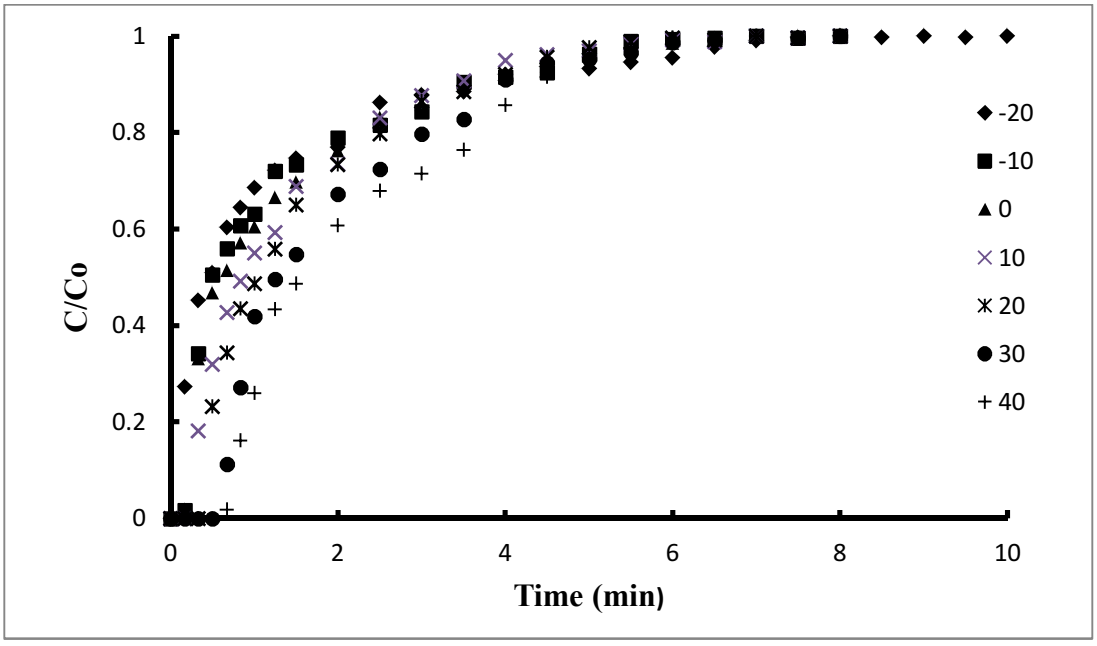

Fig 4.28: Effect of Temperature at Flow rate = 0.3L/min, concentration = 330ppm and %RH =High

Where $K_c = ae^{\frac{-\Delta H}{RT}}$

R = Gas constant

ΔH^0_{ads}= Heat of adsorption

ΔS^0_{ads}= Standard entropy

ΔG^0_{ads}= Standard free energy

The heat of adsorption and standard entropy can be evaluated by plotting the graph of lnKc against 1/T for both low and high humidity. The slope and the intercept from the resulting graph give the value of ΔH^0_{ads} and ΔS^0_{ads} respectively as shown in figures4.29 and 4.30 [70-74, 79].

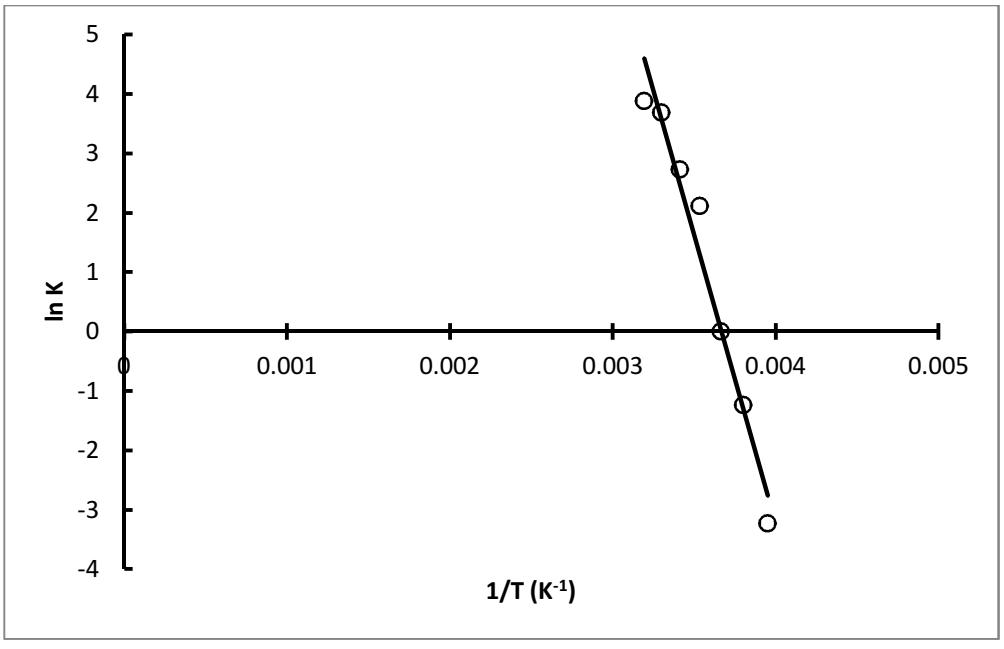

Figure 4.29: Determination of heat of adsorption at low RH

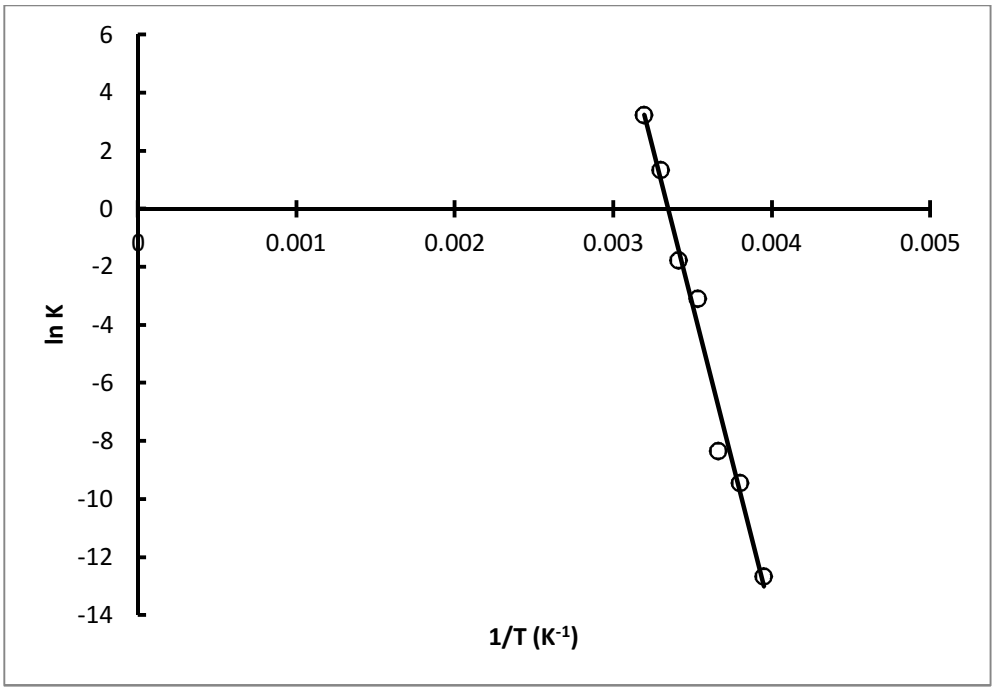

Figure 4.30: Determination of heat of adsorption at high RH

As the temperature increases, Kc increases and adsorption capacity increase, this is attributed to increase in the number of active surface sites available for adsorption and hence increasing the movement of CO_2 on to the ash surface [71]. The calculated values of $\Delta H_{ads,}$ S_{ads} and ΔG_{ads} are listed in Table 4.5. The positive value of ΔH_{ads} indicated the endothermic nature of the adsorption interaction [72, 73, and 74]. The positive value of ΔS_{ads} showed the affinity of the chemically treated fly ash for CO_2 adsorption and the increasing randomness during the adsorption process [73, 74 and 75]. The negative value of ΔG_{ads} at -10 and -20^oC indicates spontaneous nature of adsorption of CO_2 on to fly ash [79]. Positive ΔG_{ads} values were observed at 0, 10, 20 30 and 40^oC, indicating that spontaneity is not favored at high temperatures.

A similar trend has been observed from activated carbon prepared from coir pith for the removal of Congo red from water by adsorption [72].

In addition, ΔG_{ads} also increases as the temperature increases which shows the endergonic nature of the reaction [76]. To certain extend, Physiosorption and chemisorption can be classified based on the magnitude of enthalpy change. It is accepted that physiosorption has a bond strength of <84 kJ/mol while Chemisorption bond strength ranging 84 to 420 KJ/mol [77, 78]. It found that CO_2 adsorption onto fly ash appears to be a chemisorption process.

Table 4.5: Thermodynamic parameters for the adsorption of CO2 using treated fly ash.

	LRH		HRH	
T (^{0}C)	**K_c**	**ΔG_{ads} (KJ/mol)**	**K_c**	**ΔG_{ads}(KJ/mol)**
-10	3.95×10^{-2}	-6.82×10^{2}	3.08×10^{-6}	-26.69×10^{2}
-20	2.89×10^{-1}	-2.72×10^{2}	7.82×10^{-5}	-20.68×10^{2}
0	1.00×10^{2}	4.55×10^{-3}	2.36×10^{-4}	-18.95×10^{2}
10	8.26×10^{2}	4.98×10^{2}	4.46×10^{-2}	-7.32×10^{2}
20	15.32×10^{2}	6.07×10^{2}	1.66×10^{-1}	-4.37×10^{2}
30	39.92×10^{2}	9.32×10^{2}	3.74×10^{1}	3.34×10^{2}
40	48.09×10^{2}	10.11×10^{2}	25.10×10^{2}	8.39×10^{2}
ΔH_{ads} (kJ/mol)	**80**		**178**	
ΔS_{ads} (J/mol.K)	**296**		**597**	

CHAPTER FIVE

5.0 CONCLUSION AND RECOMMENDATIONS

5.1 CONCLUSION

The development of cost effective technique for the separation of CO_2 is the main aim of reducing CO_2 emission. Considering its low energy requirement, cost effectiveness and ease of applicability over a relatively wide range of temperatures and pressures, adsorption is considered as one of the potential options for CO_2 capture from flue gas streams. However, the development of easily regenerable and durable adsorbent with high CO_2 selectivity and adsorption capacity is relative to the success of this approach. Fly ash which is mainly composed of aluminosilicate and unburned carbon can be regarded as a low cost adsorbent for such as EDXA, FTIR, XRD, SEM and BET adsorption. Fly ash is the by product of fossil fuel combustion from power generating plants. Landfill of fly ash is current the dominant management strategy, however, it has serious environmental problem. Using ammonium hydroxide, chemical modification of fly ash was performed so as to improve its adsorption capacity and removal efficiency.

Several techniques such as such as EDXA, FTIR, XRD, SEM and BET were used to characterize the amine functionalized so as to know the physical properties and chemical composition of the ash. The chemically treated fly was then used for the adsorption of CO_2. Several kinetic parameters for adsorption of CO_2 were studied to obtain the best rate of adsorption.

The results revealed that the surface morphology was quite different as a result of the chemical treatment of the fly ash surface. A high surface area of 318 m^2/g was achieved using the BET after the chemical treatment. The maximum adsorption capacity of the amine functionalized ash was found to be 240 mg/g. The kinetic studies showed that adsorption capacity increases with increase in flow rate, concentration, low humidity and temperature. Thermodynamic studies showed that the heat of adsorption was 80 and 178 KJ/mol at low and high relative humidity's suggesting that the process is endothermic. In addition, the Gibb's free energy, ΔG_{ads} also increases as the temperature increases which shows the endergonic nature of the reaction. The experimental data was modeled using Langmuir, Freunlich, BET and dispersion model. It was found that BET and dispersion models best fits the experimental data with regression coefficients of 0.984.

5.2 RECOMMENDATIONS

The following recommendations were made based on the findings of this study:

1. Similar experiment can be carried out for the adsorption of other flue gases using the amine functionalized fly ash.
2. More chemical treatment with other compounds containing amine functional groups can be done in order to increase its specific surface area and to promote the development of micropores within the fly ash, as these treatments are known to change adsorption capacity.
3. Thorough pilot scale experiment using the same operating conditions should be conducted with the same prior to design scale up.

APPENDIX

APPENDIX A: ADSORPTION – DESORPTION GRAPH

RUN 1

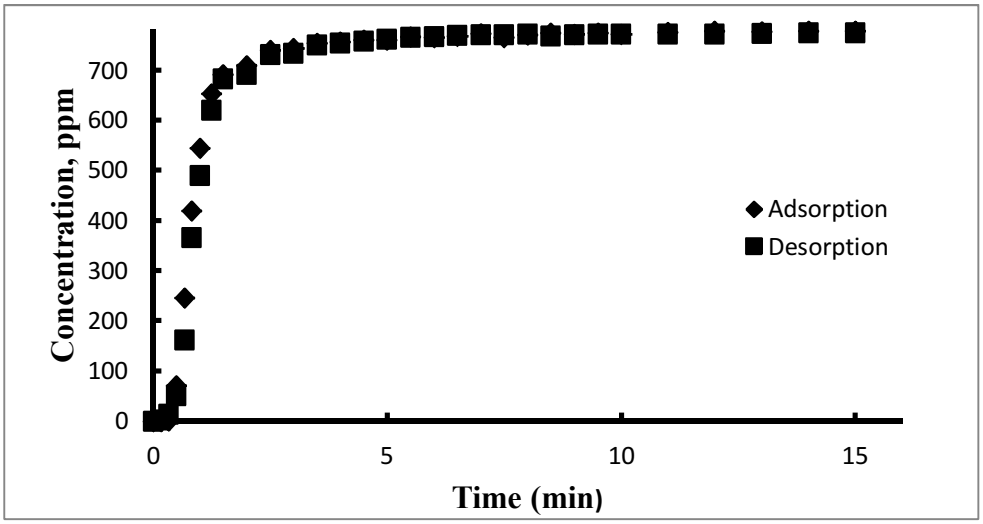

Figure 4.3.1: Adsorption-desorption curve at %RH = Low, Conc= 795ppm, flowrate= 0.3L/min and Temp=0^0C

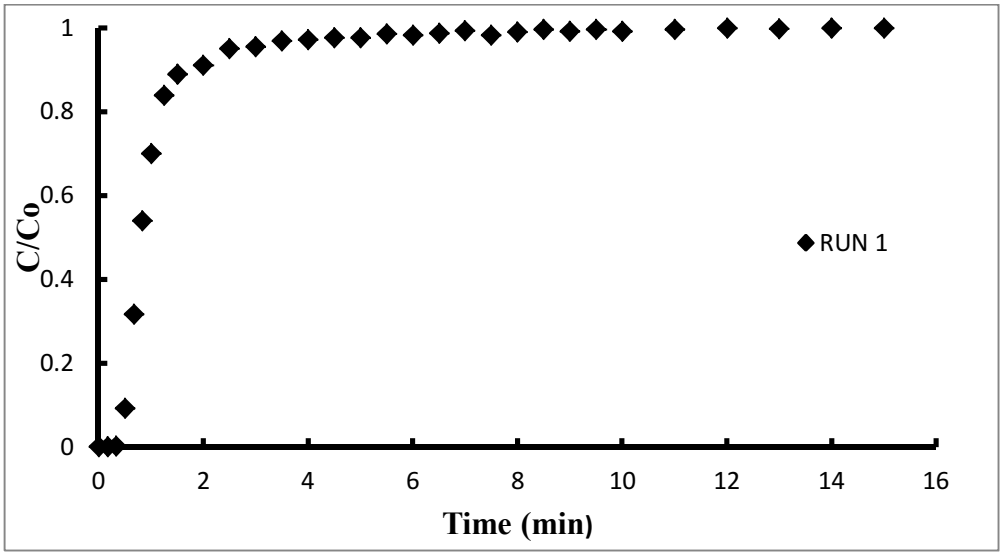

Figure 4.3.2: Exit concentration curve at %RH = Low, Conc= 795ppm, flowrate= 0.3L/min and Temp=0^0C

RUN 2

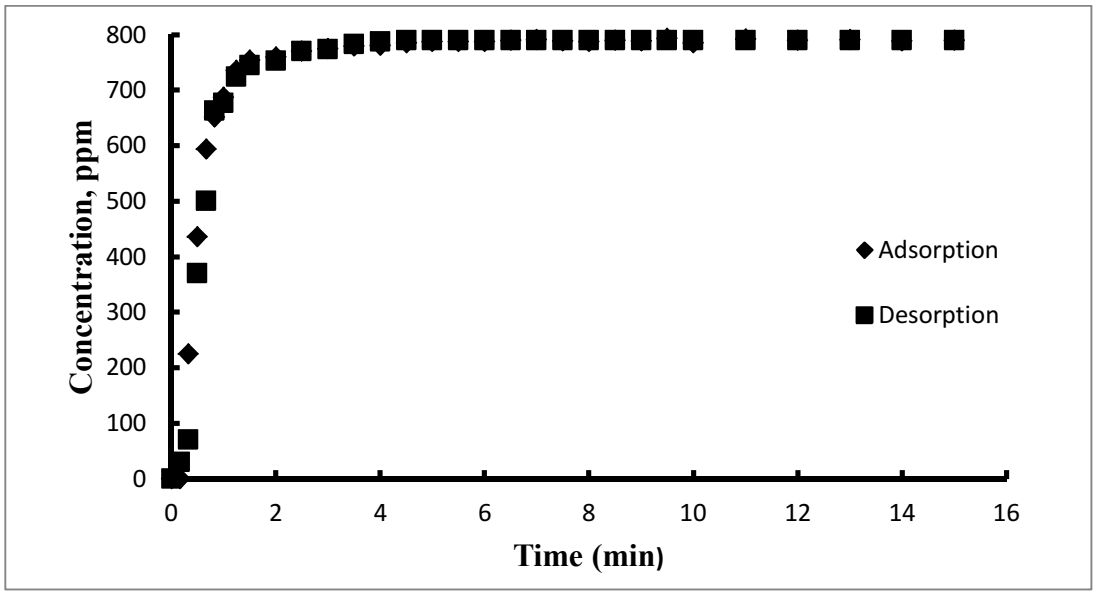

Figure 4.3.3: Adsorption-desorption curve at %RH = Low, Conc= 795ppm, flowrate= 0.7L/min and Temp=0^0C

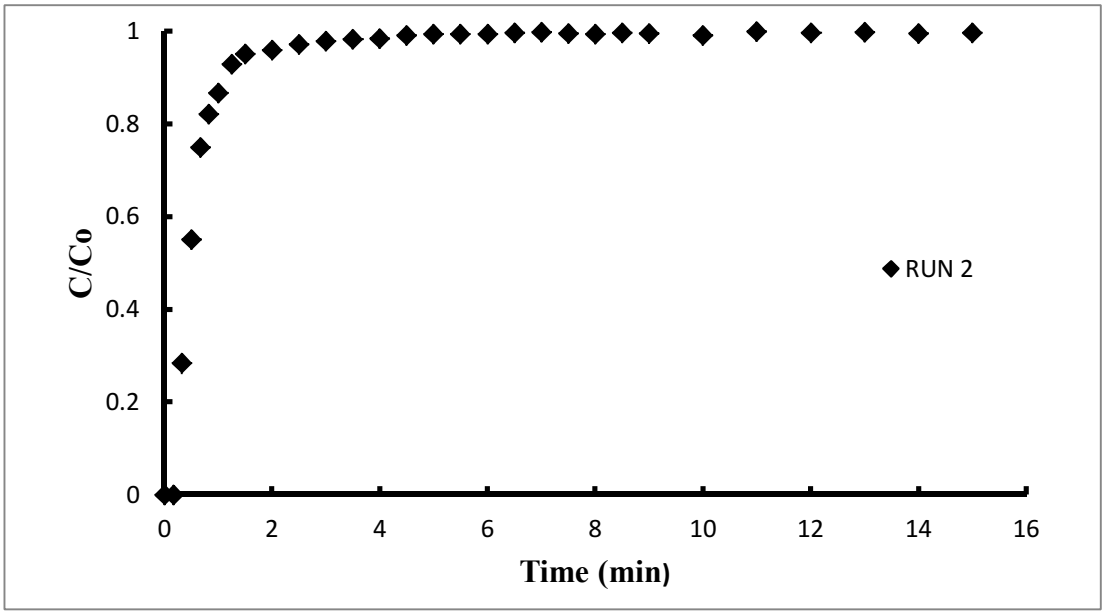

Figure 4.3.4: Exit concentration curve at %RH = Low, Conc= 795ppm, flowrate= 0.7L/min and Temp=0^0C

RUN 3

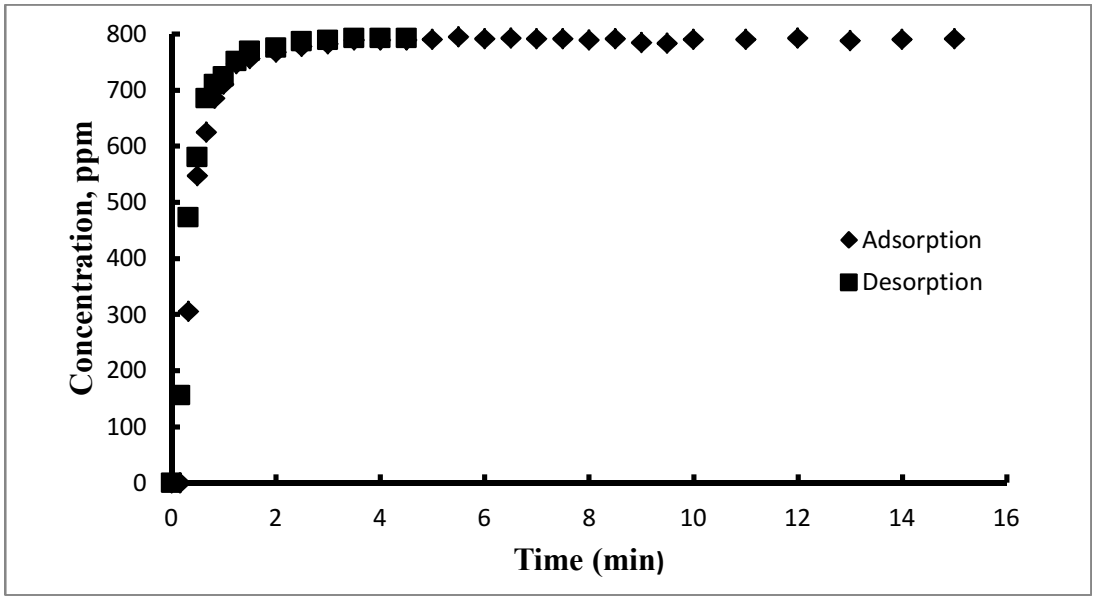

Figure 4.3.5: Adsorption-desorption curve at %RH = Low, Conc= 795ppm, flowrate= 1.0L/min and Temp=0^0C

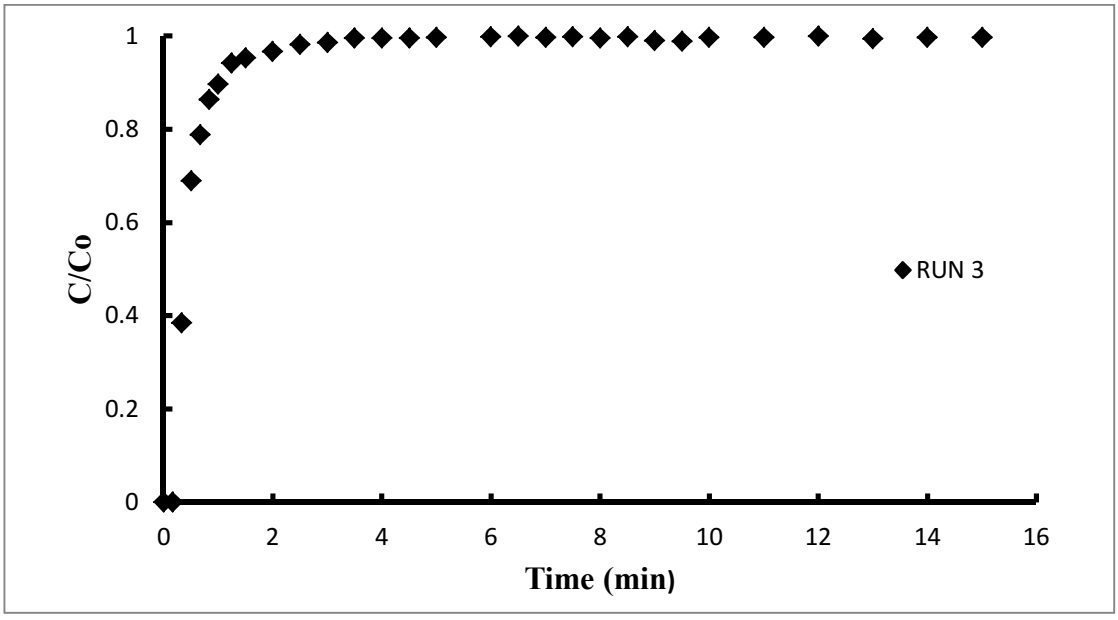

Figure 4.3.6: Exit concentration curve at %RH = Low, Conc= 795ppm, flowrate = 1.0L/min and Temp=0^0C

RUN 4

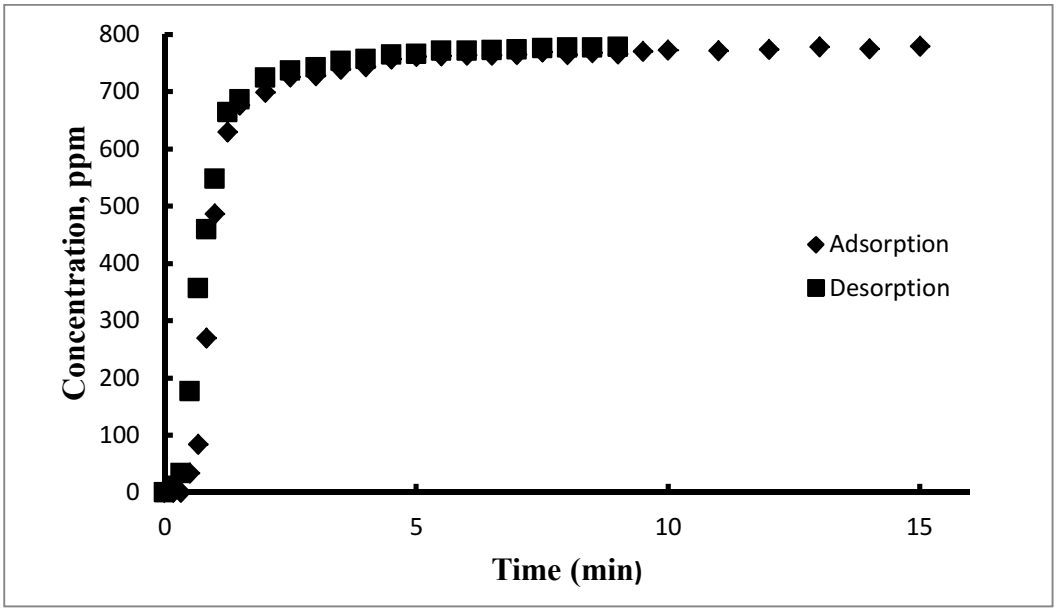

Figure 4.3.7: Adsorption-desorption curve at %RH = Low, Conc= 795ppm, flowrate= 0.3L/min and Temp=40^0C

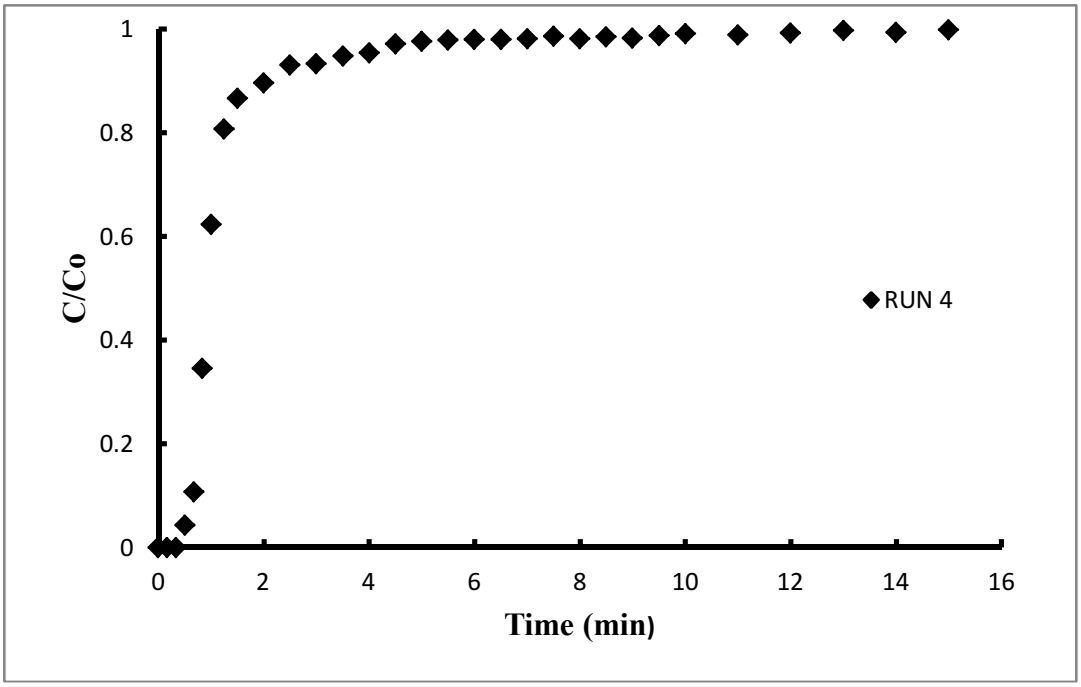

Figure 4.3.8: Exit concentration curve at %RH = Low, Conc= 795ppm, flowrate= 0.7L/min and Temp=40^0C

RUN 5

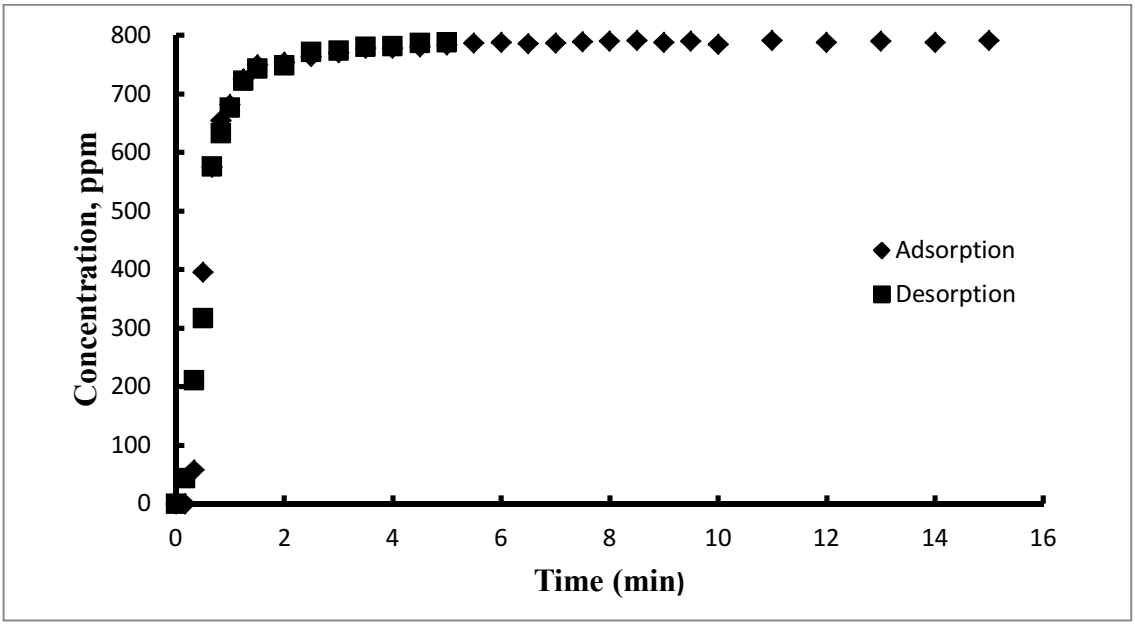

Fig 4.3.9: Adsorption-desorption curve at %RH = Low, Conc= 795ppm, flowrate= 0.7L/min and Temp=40^{0}C

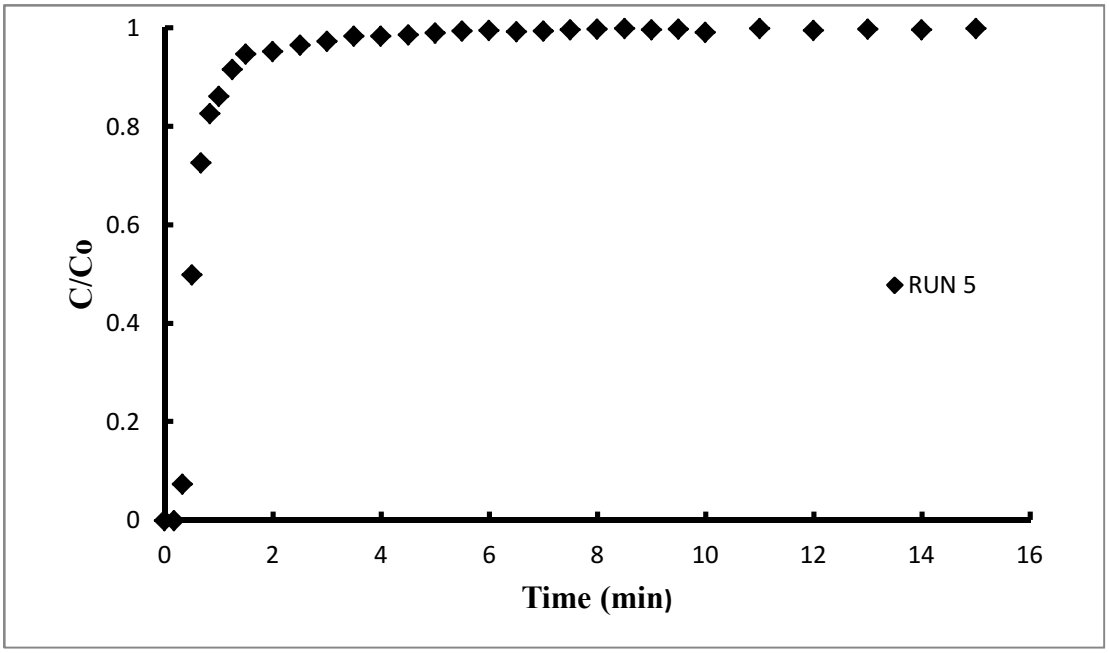

Fig 4.3.10: Exit concentration curve at %RH = Low, Conc= 795ppm, flowrate= 0.7L/min and Temp=40^{0}C

RUN 6

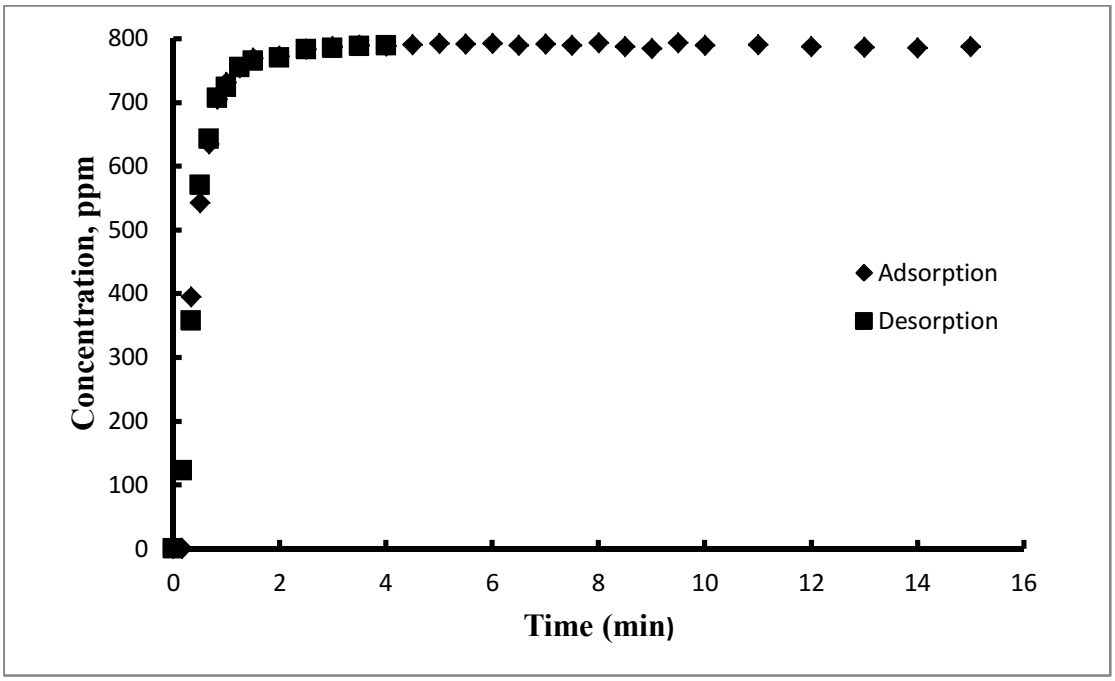

Fig 4.3.11: Adsorption-desorption curve at %RH = Low, Conc= 795ppm, flowrate= 1.0L/min and Temp=40^0C

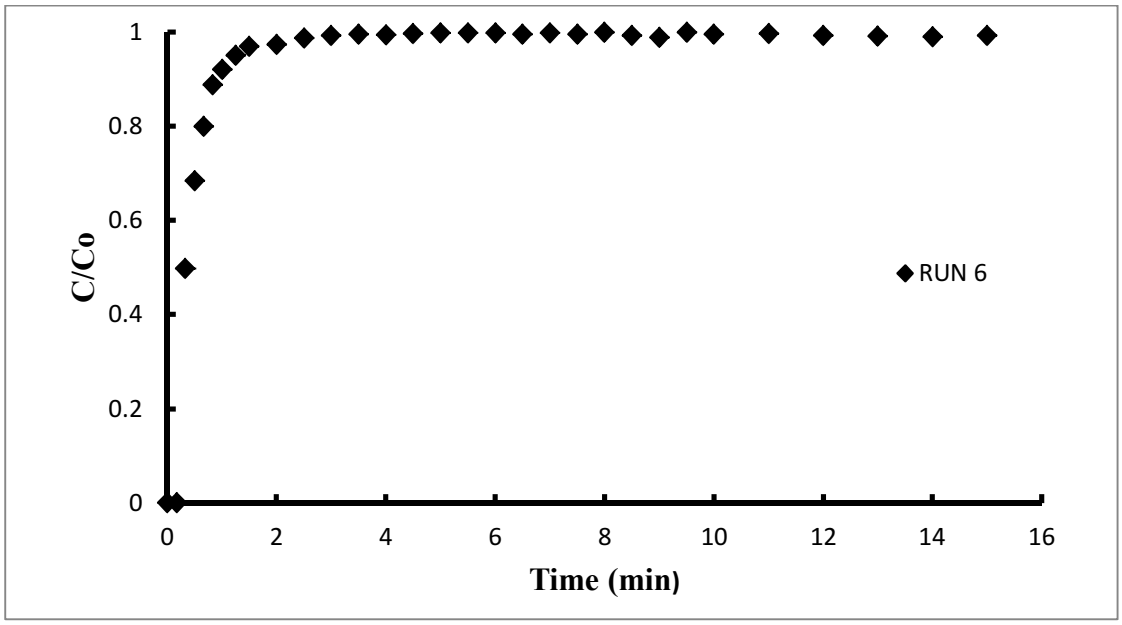

Fig 4.3.12: Exit concentration curve at %RH = Low, Conc= 795ppm, flowrate= 1.0L/min and Temp=40^0C

RUN 7

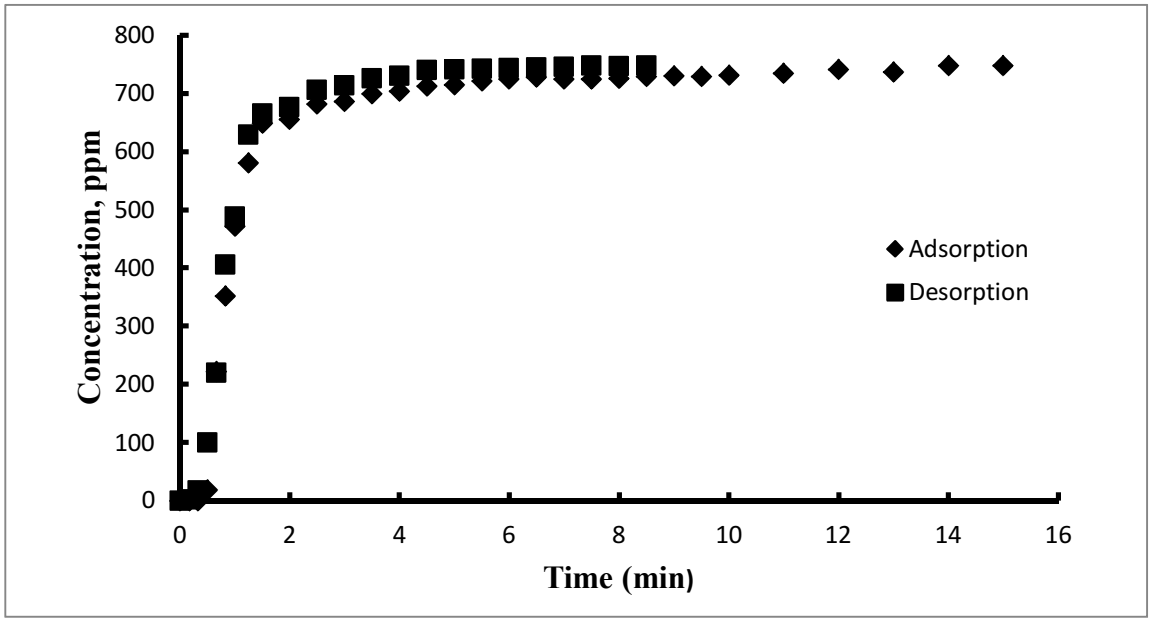

Fig 4.3.13: Adsorption-desorption curve at %RH = High, Conc= 795ppm, flowrate= 0.3L/min and Temp=0^0C

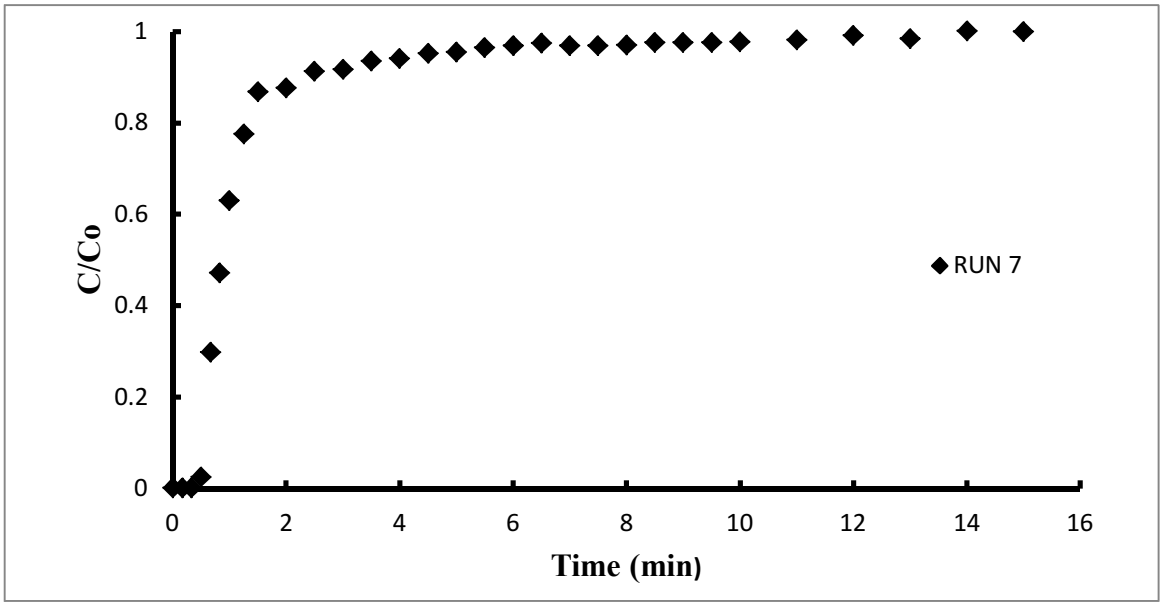

Fig 4.3.14: Exit concentration curve atb%RH = High, Conc= 795ppm, flowrate= 0.3L/min and Temp=0^0C

RUN 8

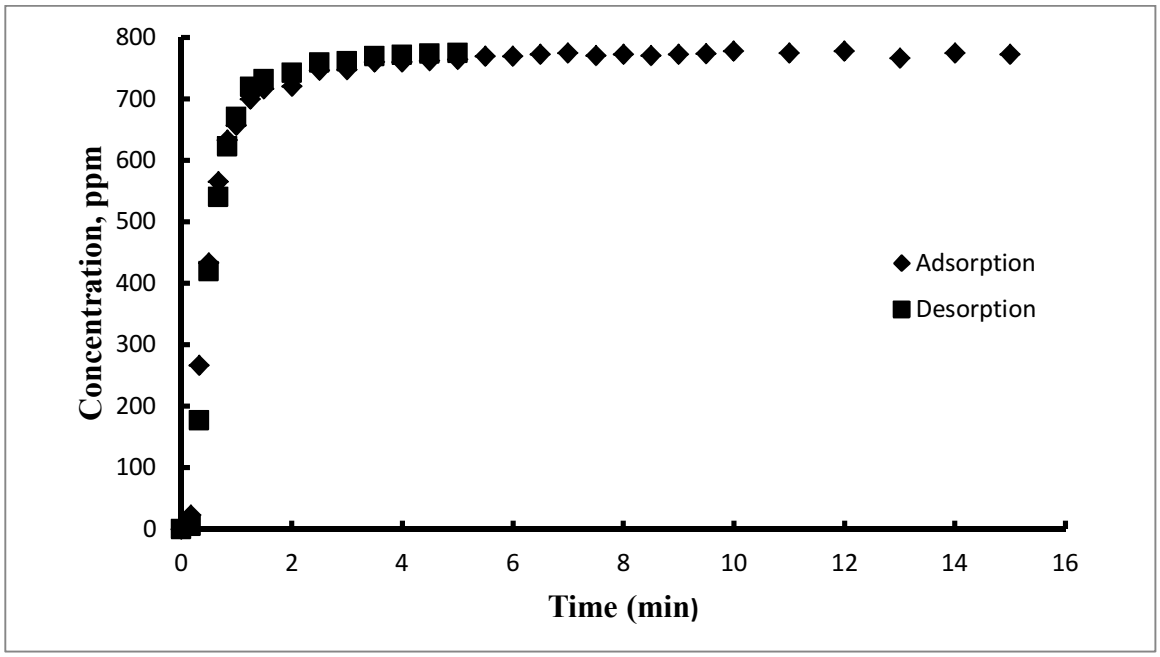

Fig 4.3.15: Adsorption-desorption curve at %RH = High, Conc= 795ppm, flowrate= 0.7L/min and Temp=0^0C

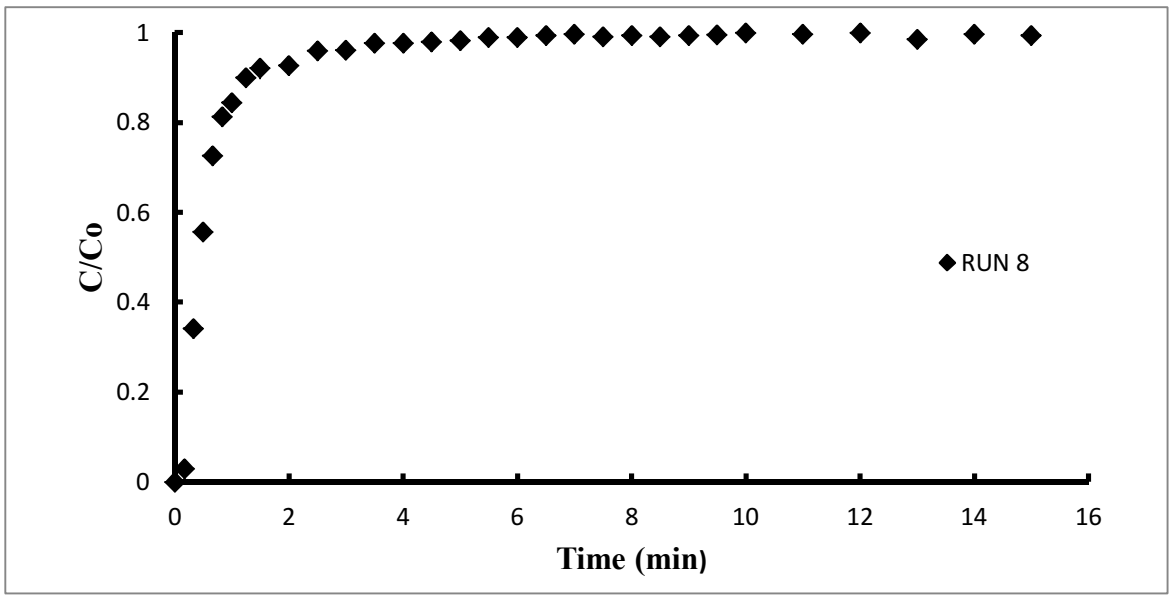

Fig 4.3.16: Exit concentration curve at %RH = High, Conc= 795ppm, flowrate= 0.7L/min and Temp=0^0C

RUN 9

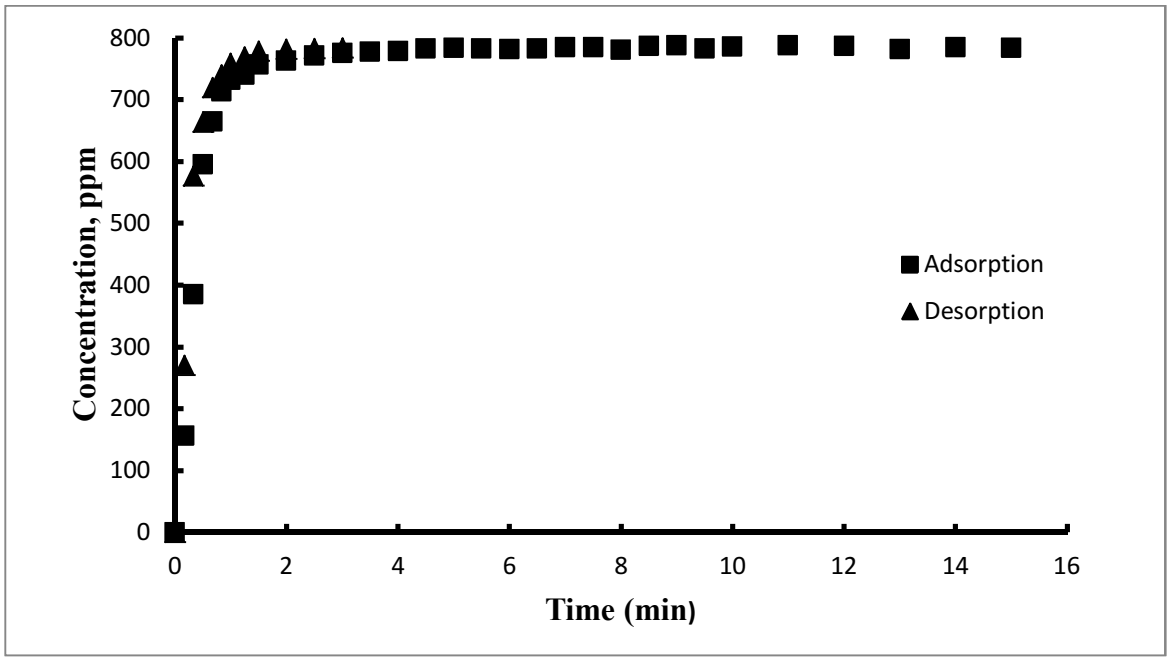

Fig 4.3.17: Adsorption-desorption curve at %RH = High, Conc= 795ppm, flowrate= 1.0L/min and Temp=0^0C

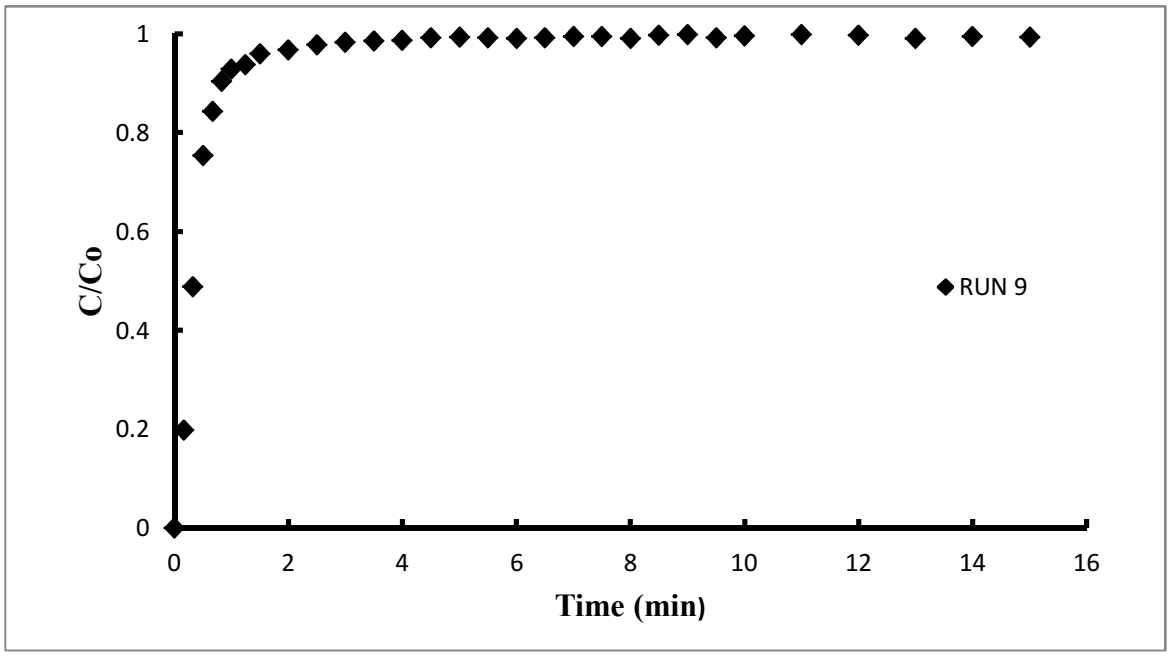

Fig 4.3.18: Exit concentration curve at %RH = High, Conc= 795ppm, flowrate= 1.0L/min and Temp=0^0C

RUN 10

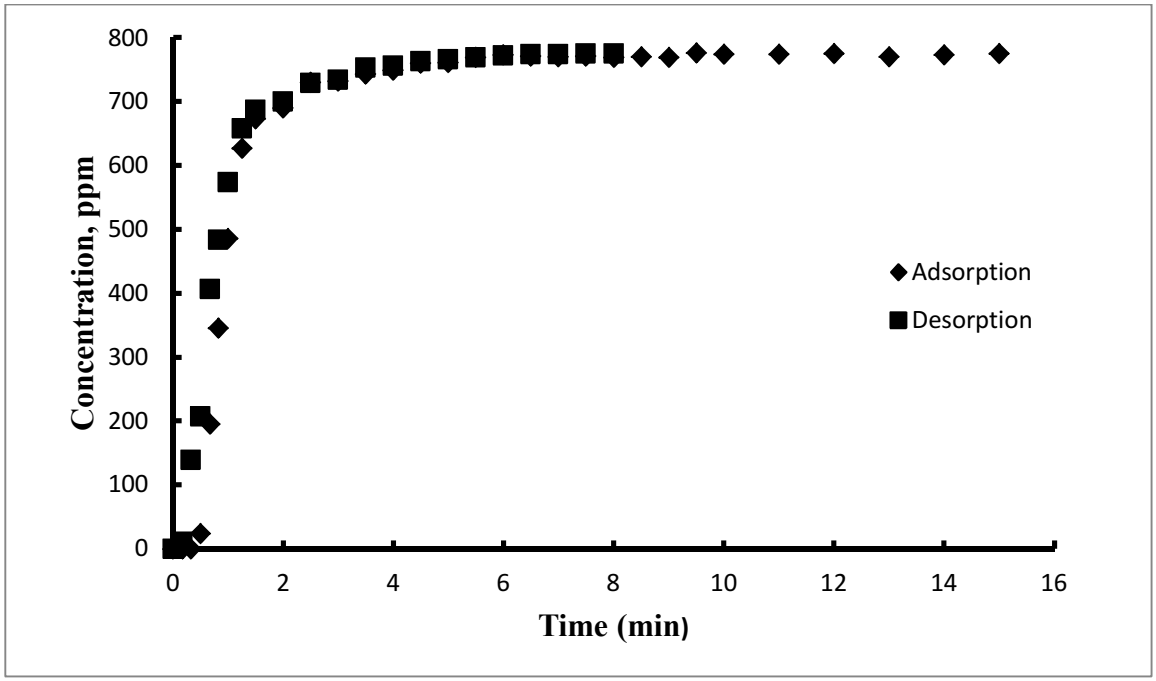

Fig 4.3.19: Adsorption-desorption curve at %RH = High, Conc= 795ppm, flowrate= 0.3L/min and Temp=40^0C

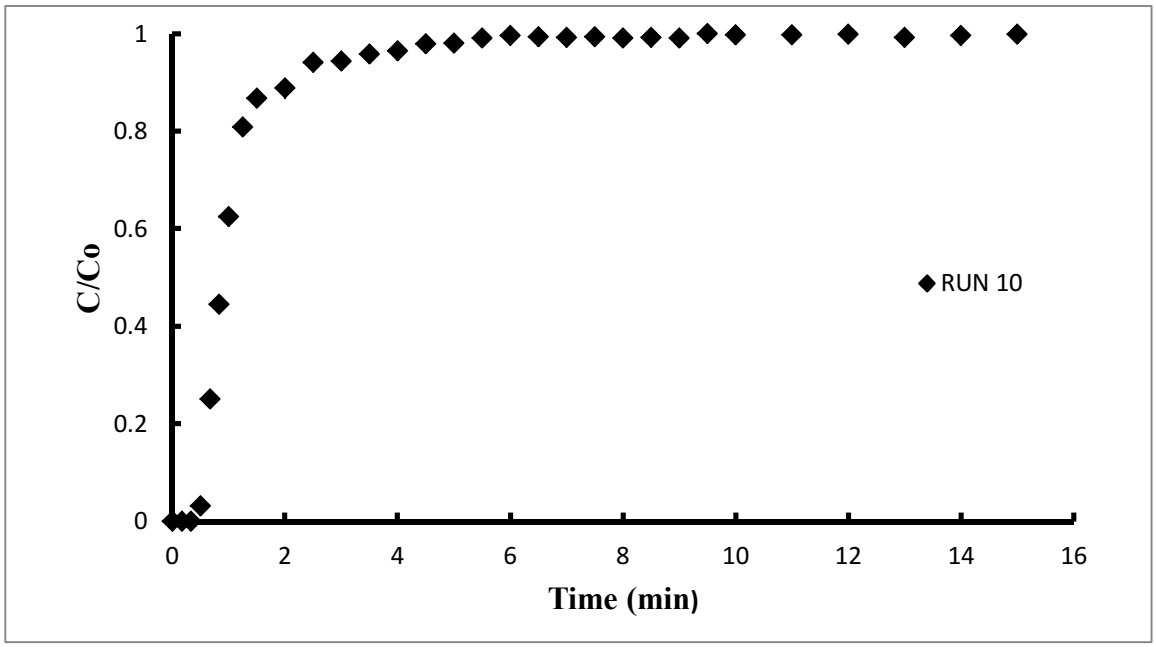

Fig 4.3.20: Exit concentration curve at %RH = High, Conc= 795ppm, flowrate= 0.3L/min and Temp=40^0C

RUN 11

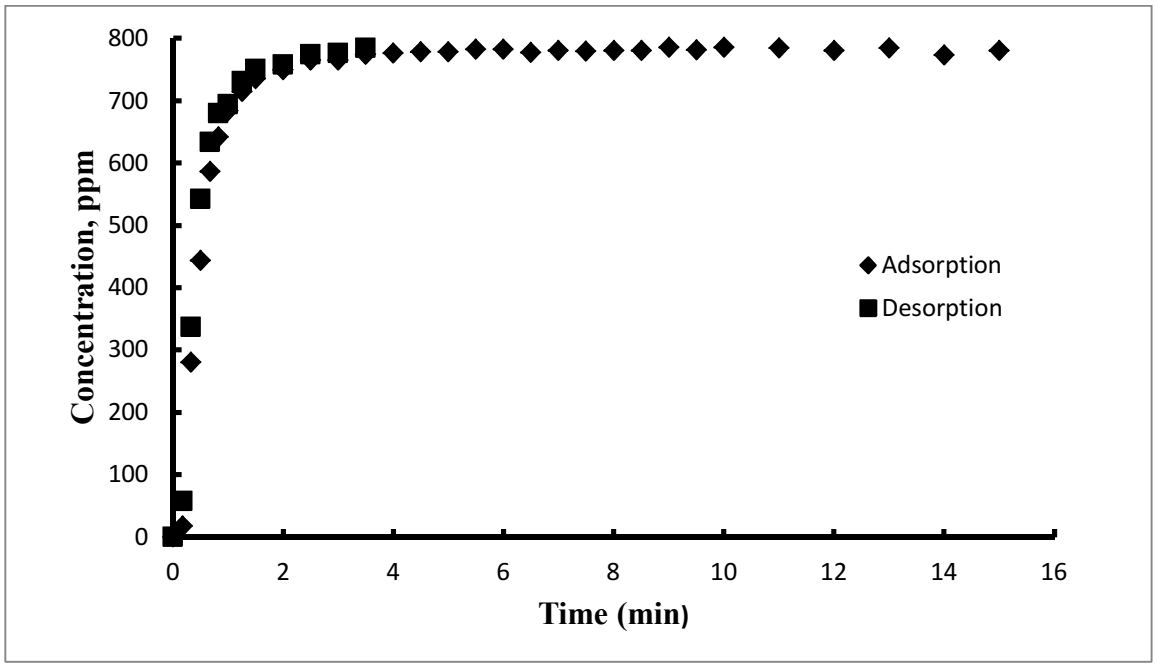

Fig 4.3.21: Adsorption-desorption curve at %RH = High, Conc= 795ppm, flowrate= 0.7L/min and Temp=40^0C

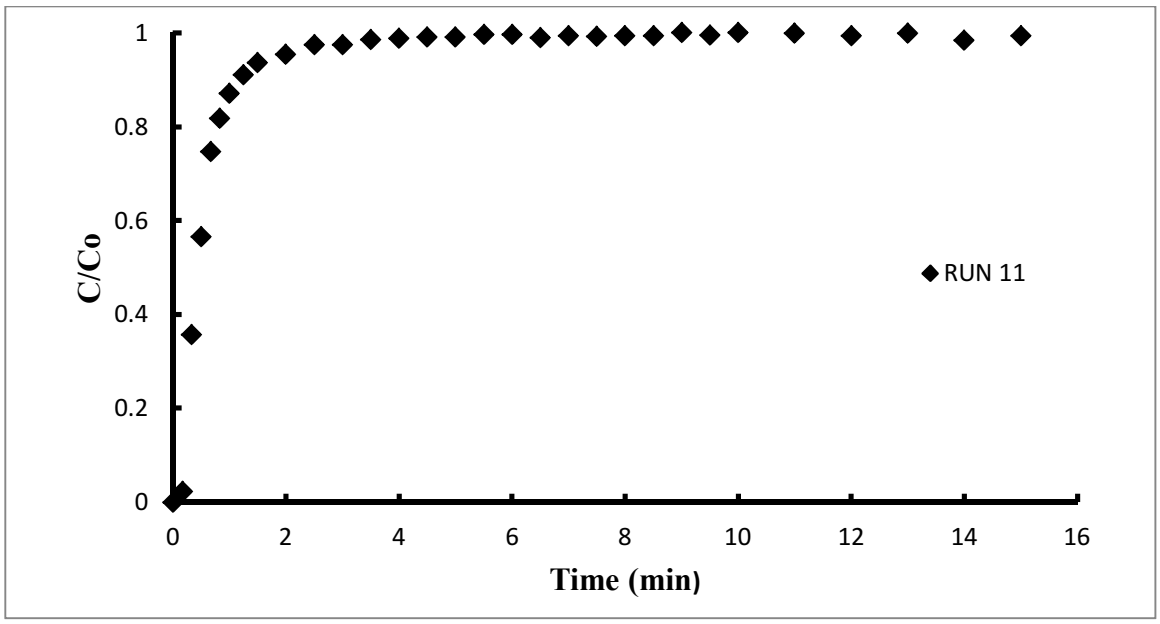

Fig 4.3.22: Exit concentration curve at %RH = High, Conc= 795ppm, flowrate= 0.7L/min and Temp=40^0C

RUN 12

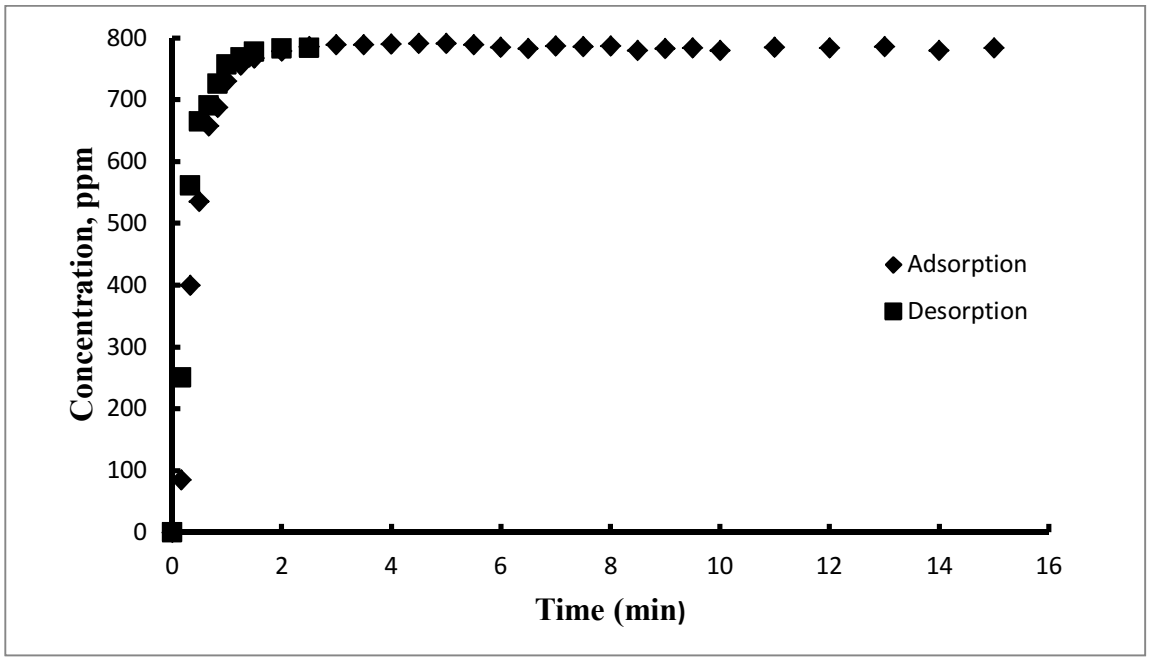

Fig 4.3.23: Adsorption-desorption curve at %RH = High, Conc= 795ppm, flowrate= 1.0L/min and Temp=40^0C

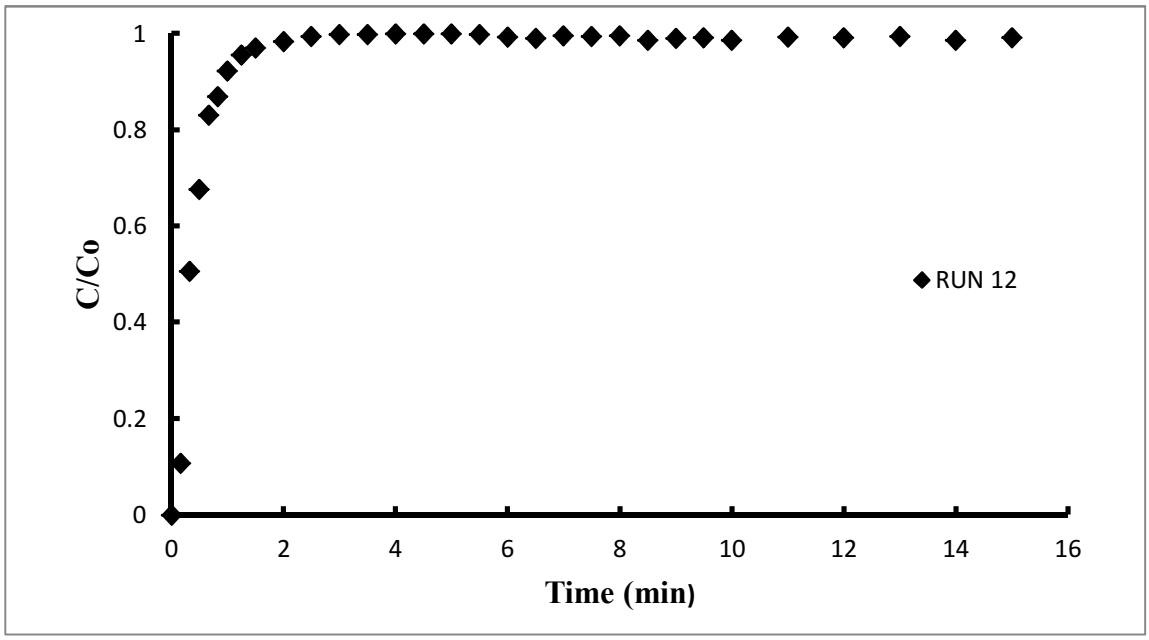

Fig 4.3.24: Exit concentration curve at %RH = High, Conc= 795ppm, flowrate= 1.0L/min and Temp=40^0C

RUN 13

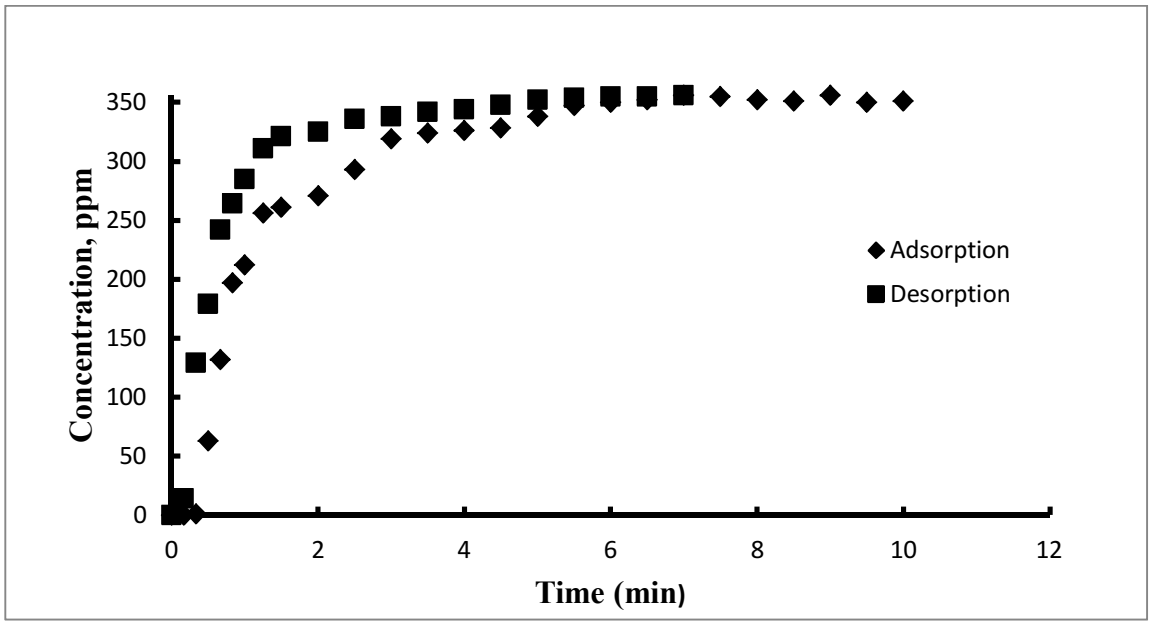

Fig 4.3.25: Adsorption-desorption curve at %RH = Low, Conc=365ppm, flowrate= 0.3L/min and Temp=0^0C

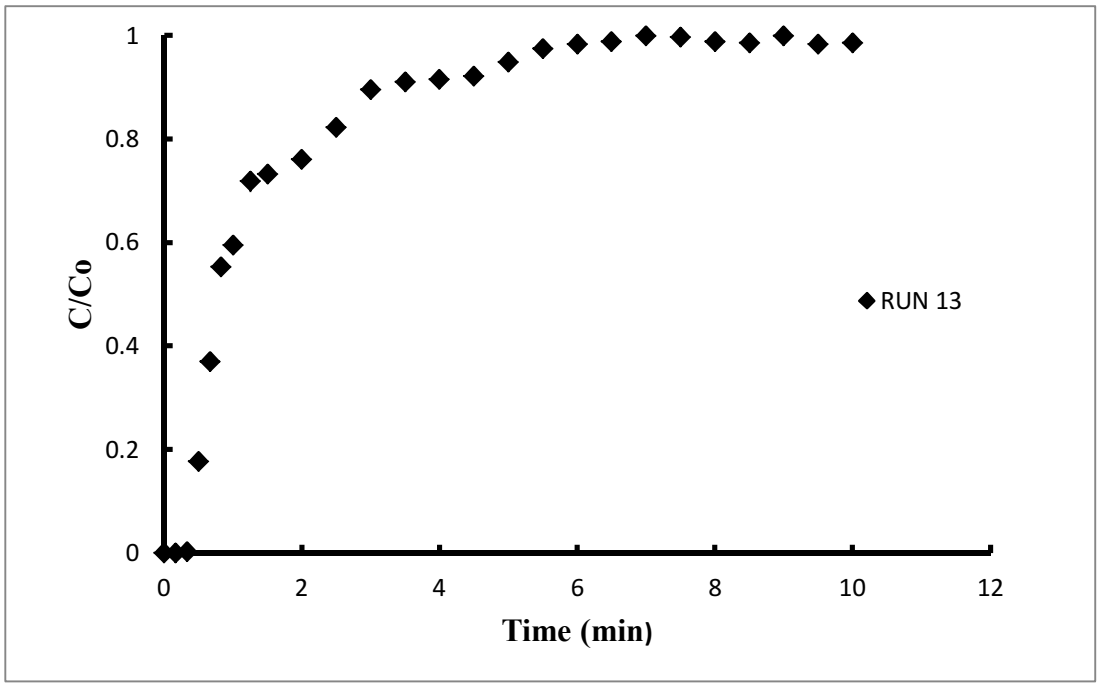

Fig 4.3.26: Exit concentration curve at %RH = Low, Conc= 365ppm, flowrate= 0.3L/min and Temp=0^0C

RUN 14

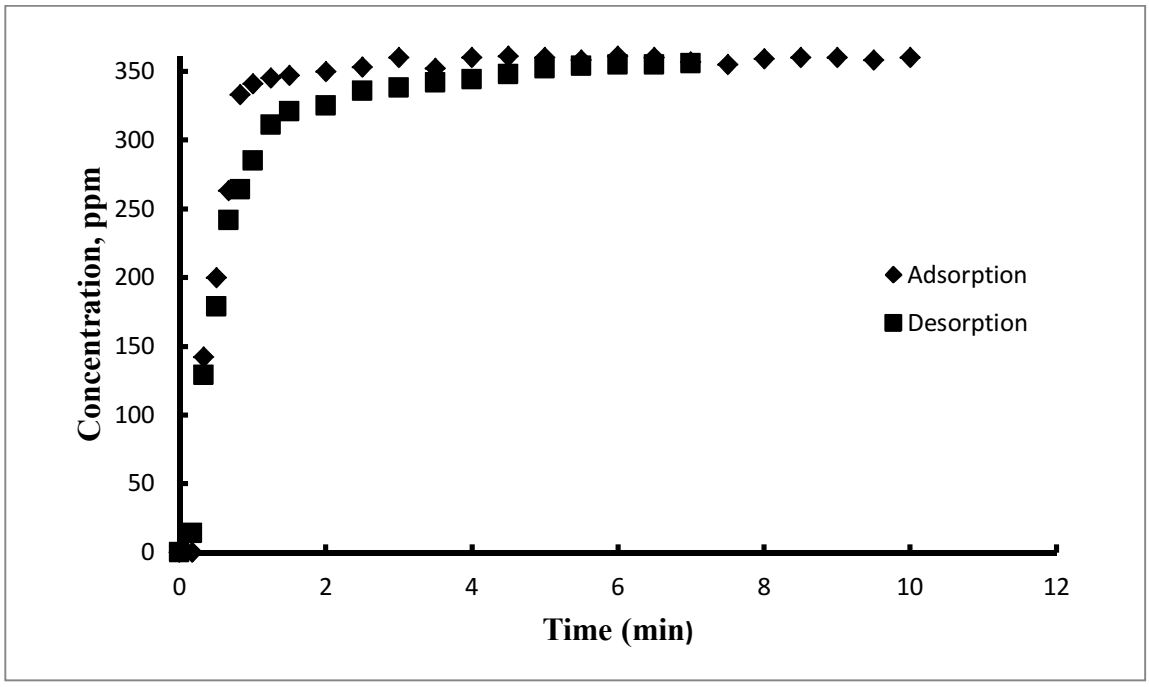

Fig 4.3.27: Adsorption-desorption curve at %RH = Low, Conc= 365ppm, flowrate= 0.7L/min and Temp=0^0C

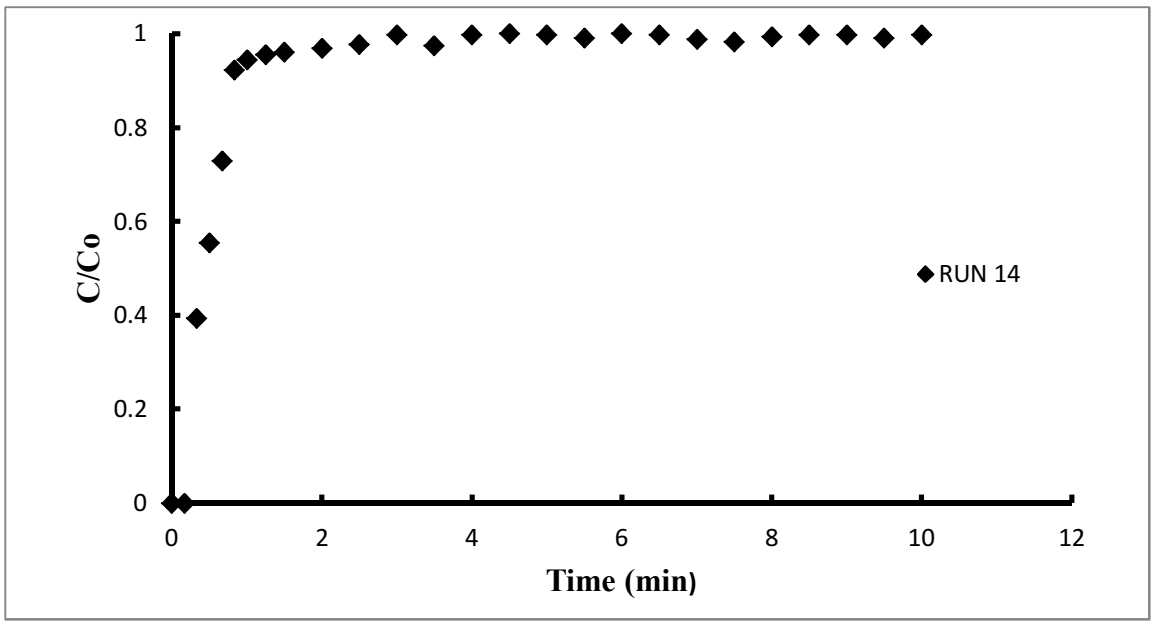

Fig 4.3.28: Exit concentration curve at %RH = Low, Conc= 365ppm, flowrate= 0.7L/min and Temp=0^0C

RUN 15

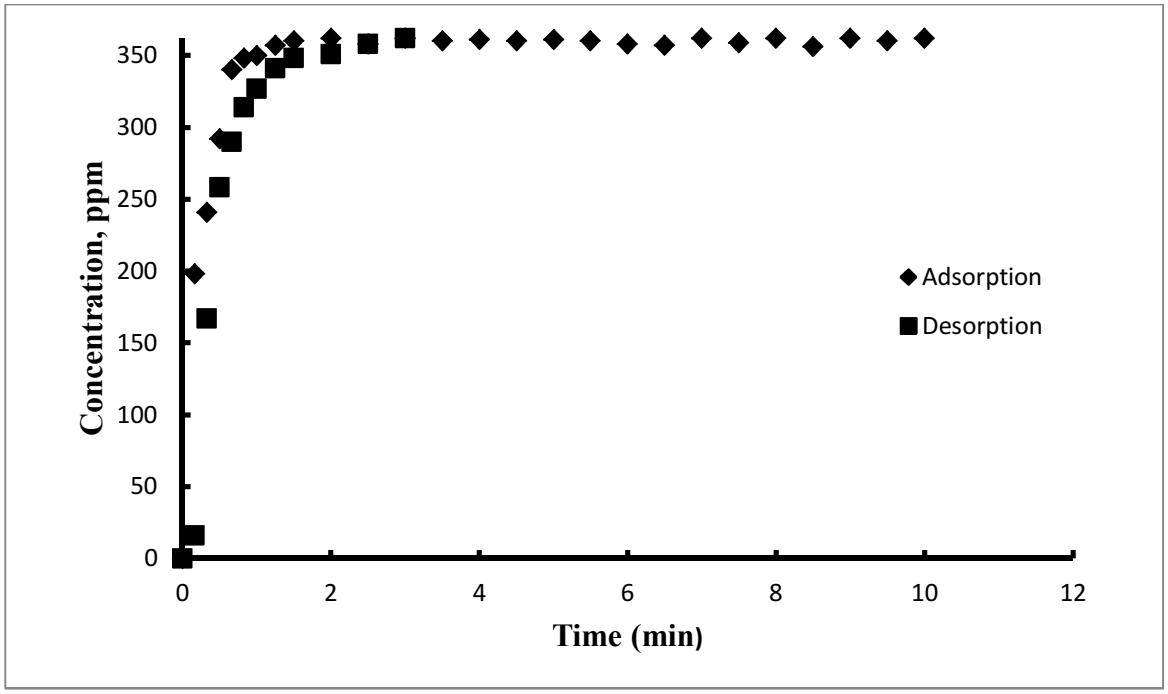

Fig 4.3.29: Adsorption-desorption curve at %RH = Low, Conc= 365ppm, flowrate= 1.0L/min and Temp=0^0C

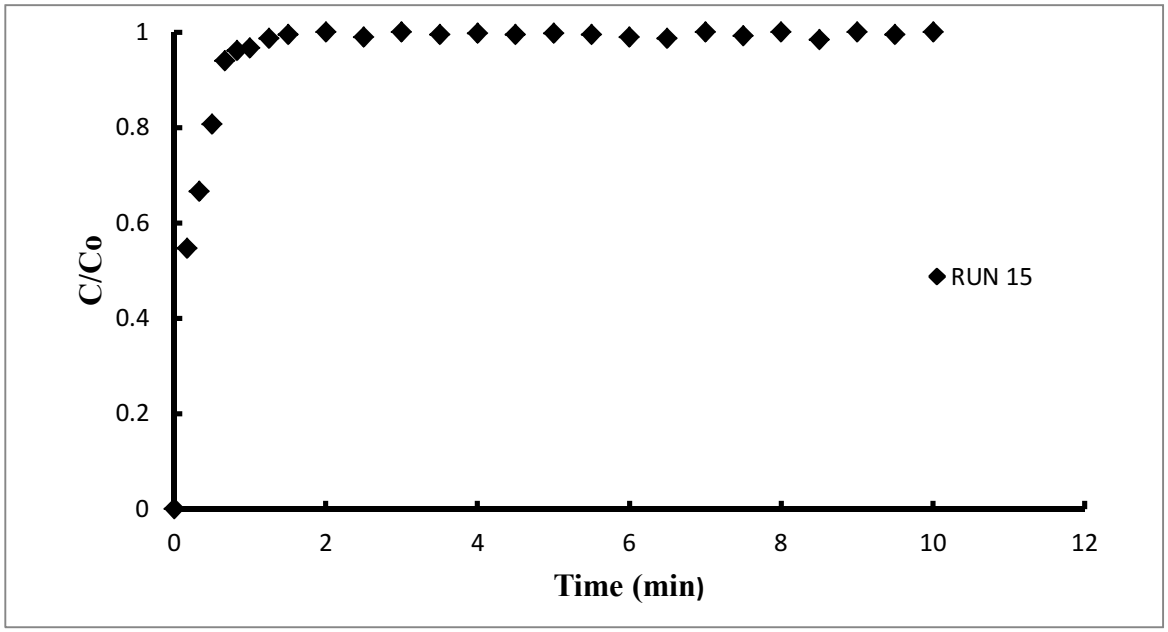

Fig 4.3.30: Exit concentration curve at %RH = Low, Conc= 365ppm, flowrate= 1.0L/min and Temp=0^0C

RUN 16

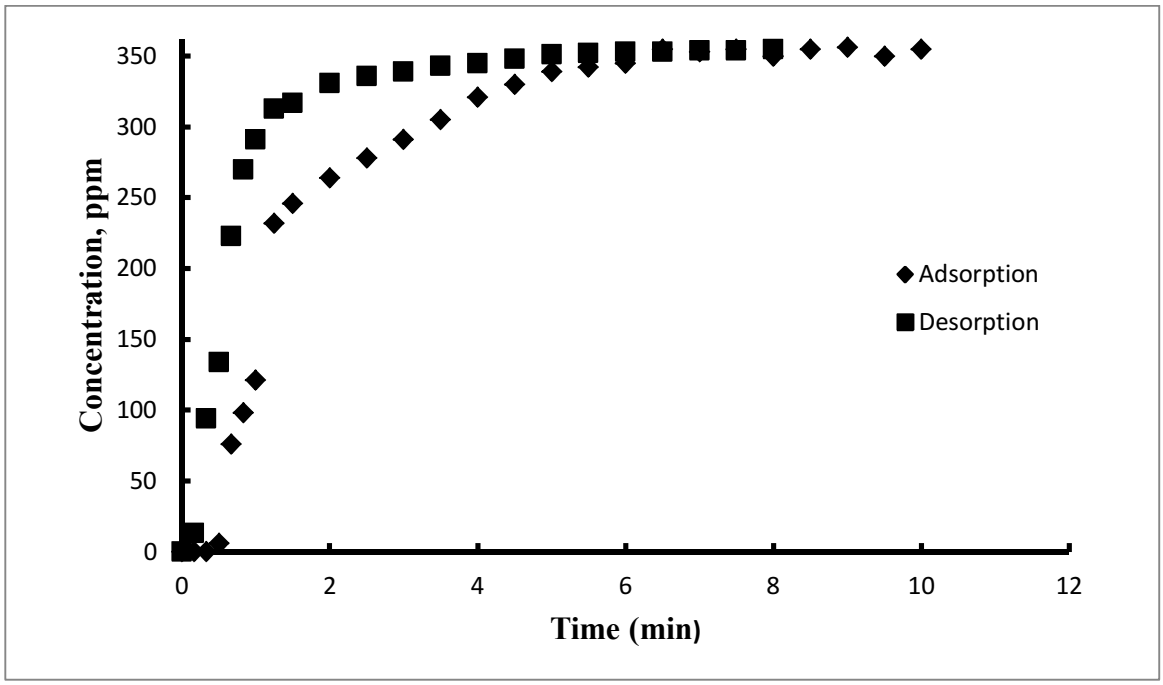

Fig 4.3.31: Adsorption-desorption curve at %RH = Low, Conc= 365ppm, flowrate= 0.3L/min and Temp=40^0C

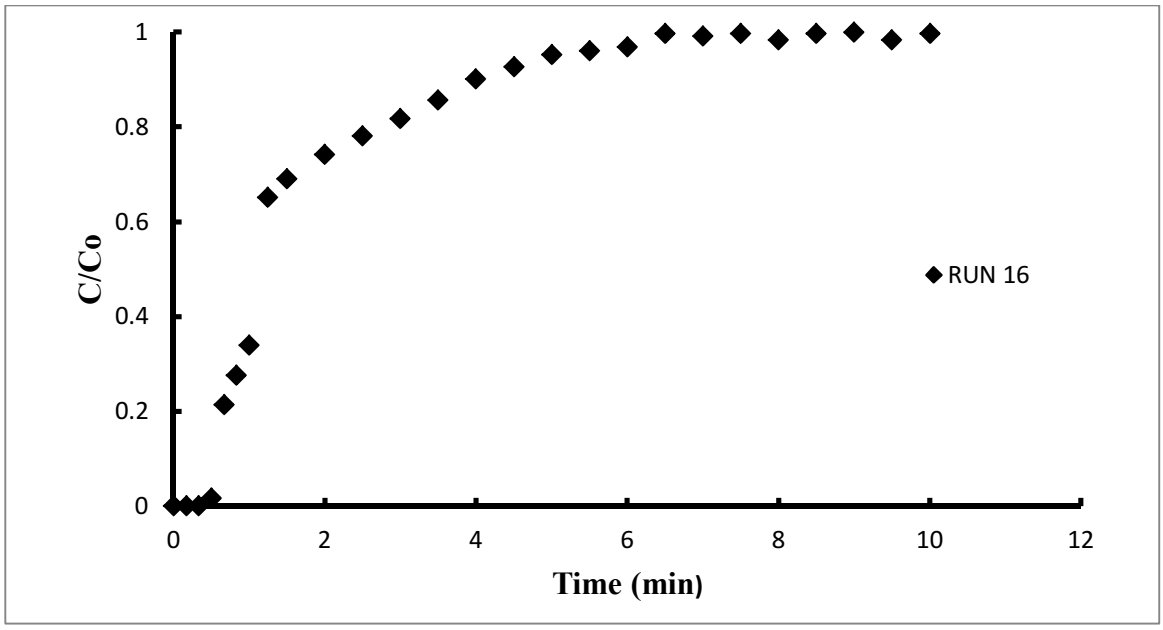

Fig 4.3.32: Exit concentration curve at %RH = Low, Conc= 365ppm, flowrate= 0.3L/min and Temp=40^0C

RUN 17

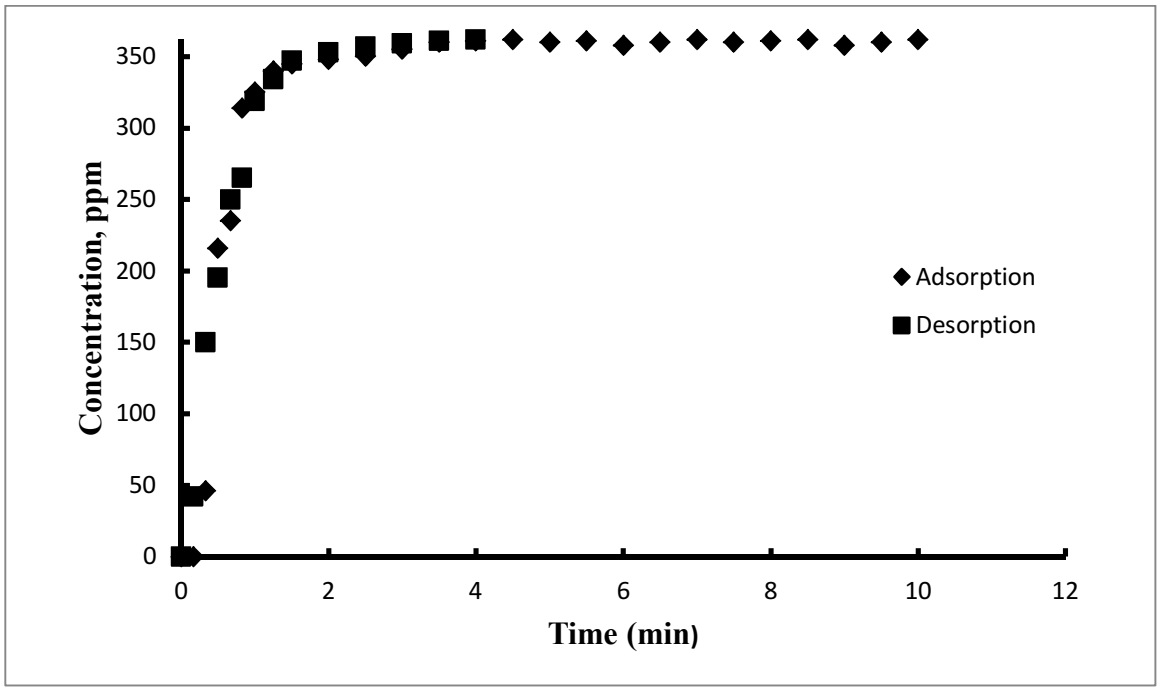

Fig 4.3.33: Adsorption-desorption curve at %RH = Low, Conc= 365ppm, flowrate= 0.7L/min and Temp=40^0C

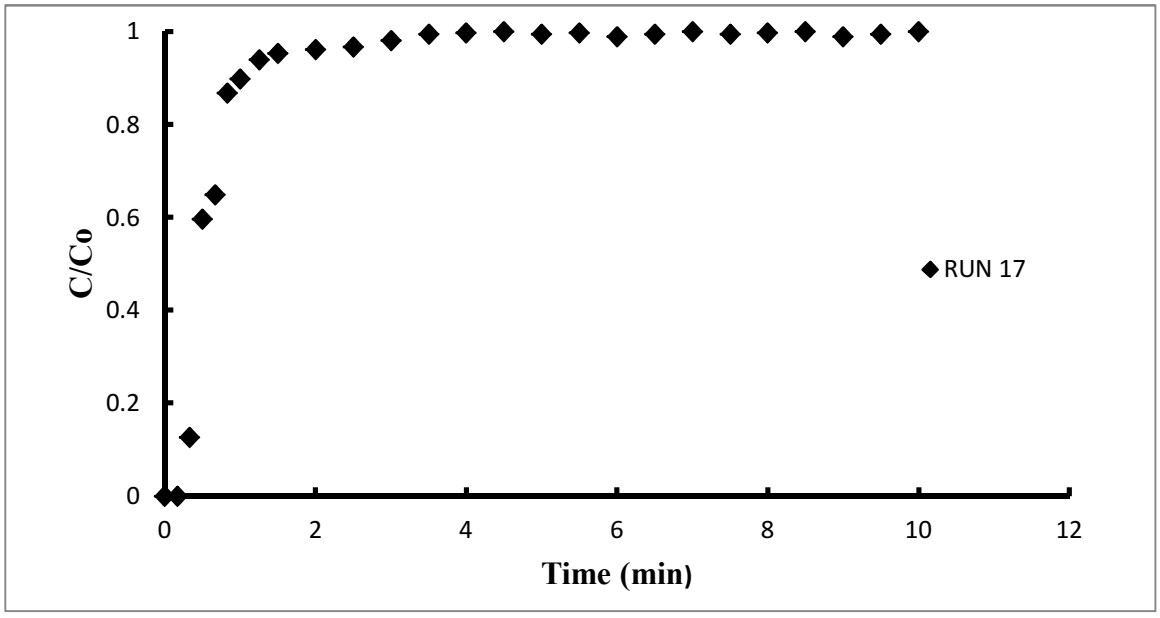

Fig 4.3.34: Exit concentration curve at %RH = Low, Conc= 365ppm, flowrate= 0.7L/min and Temp=40^0

RUN 18

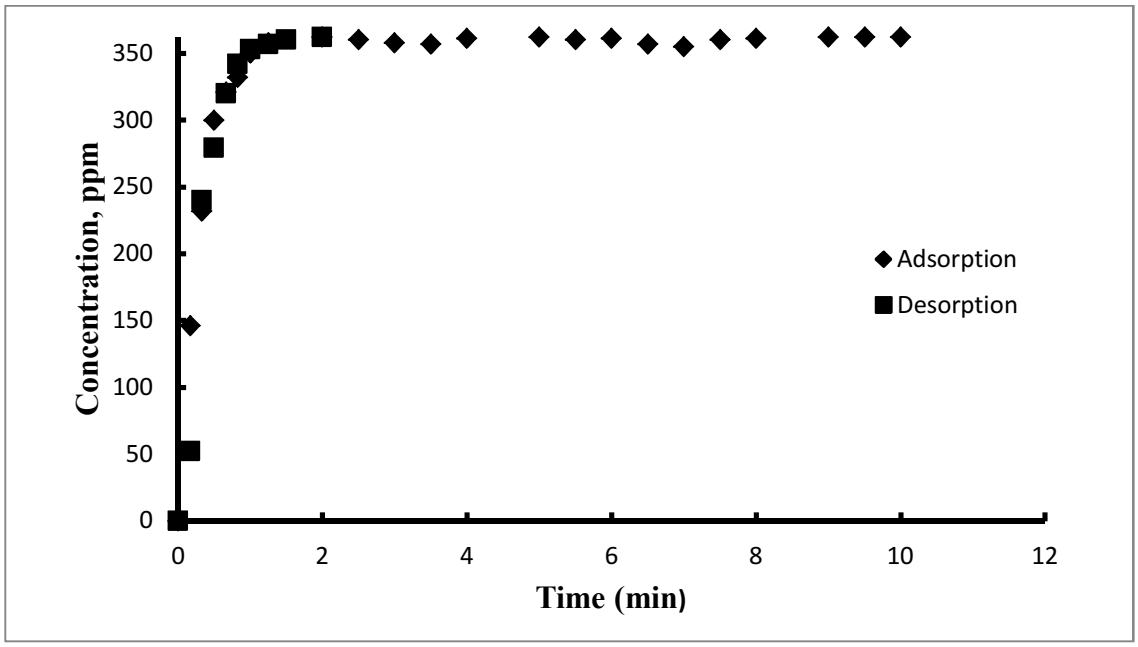

Fig 4.3.35: Adsorption-desorption curve at %RH = Low, Conc= 365ppm, flowrate= 1.0L/min and Temp=40^{0}C

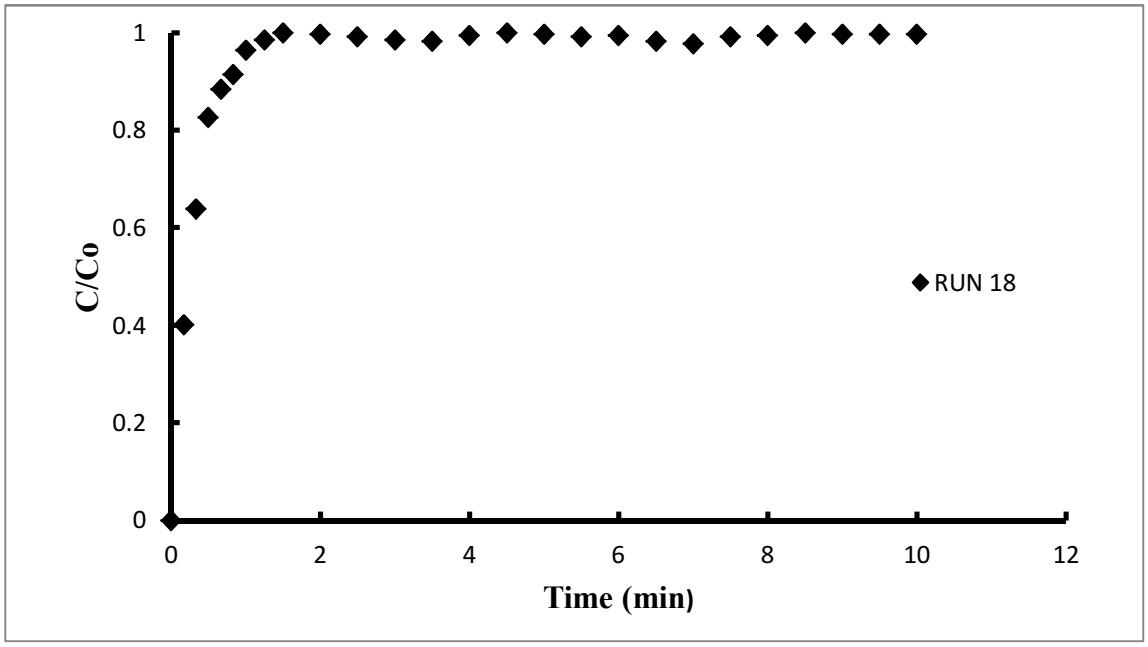

Fig 4.3.36: Exit concentration curve at %RH = Low, Conc= 365ppm, flowrate= 1.0L/min and Temp=40^{0}C

RUN 19

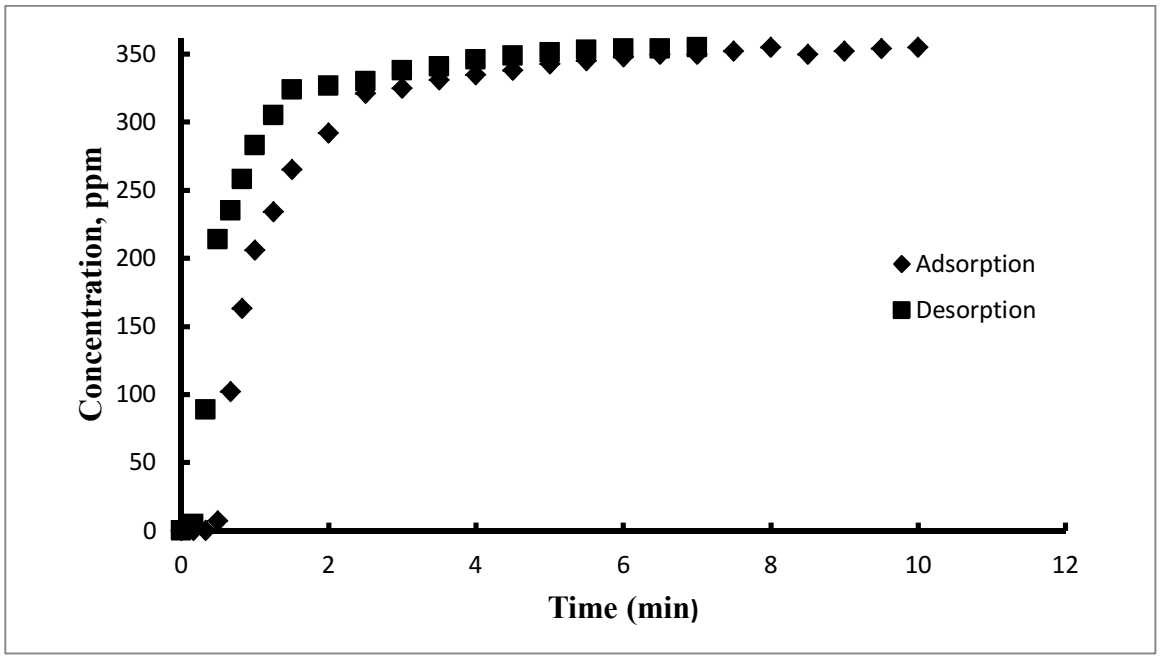

Fig 4.3.37: Adsorption-desorption curve at %RH = High, Conc= 365ppm, flowrate= 0.3L/min and Temp=0^0C

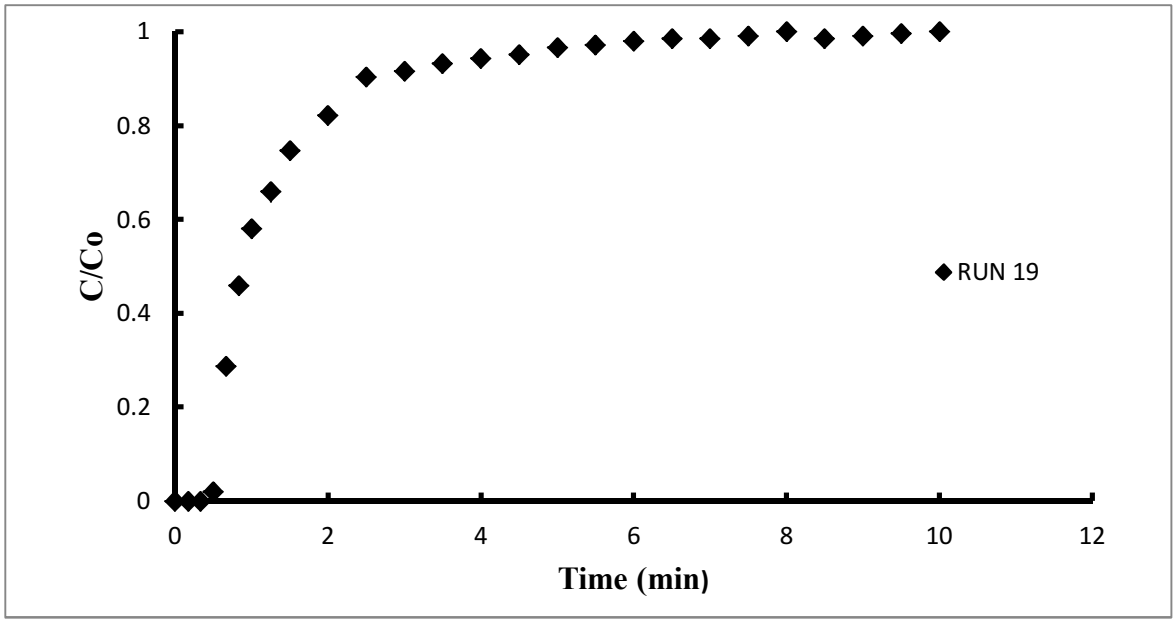

Fig 4.3.38: Exit concentration curve at %RH = High, Conc= 365ppm, flowrate= 0.3L/min and Temp=0^0C

RUN 20

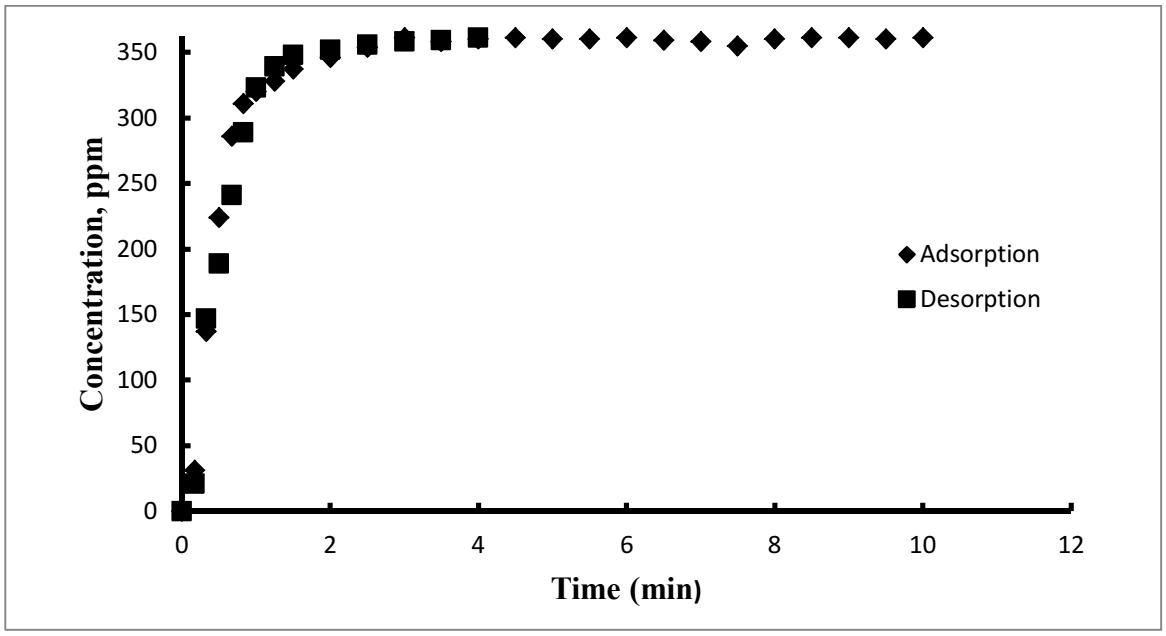

Fig 4.3.39: Adsorption-desorption curve at %RH = High, Conc= 365ppm, flowrate= 0.7L/min and Temp=0^0C

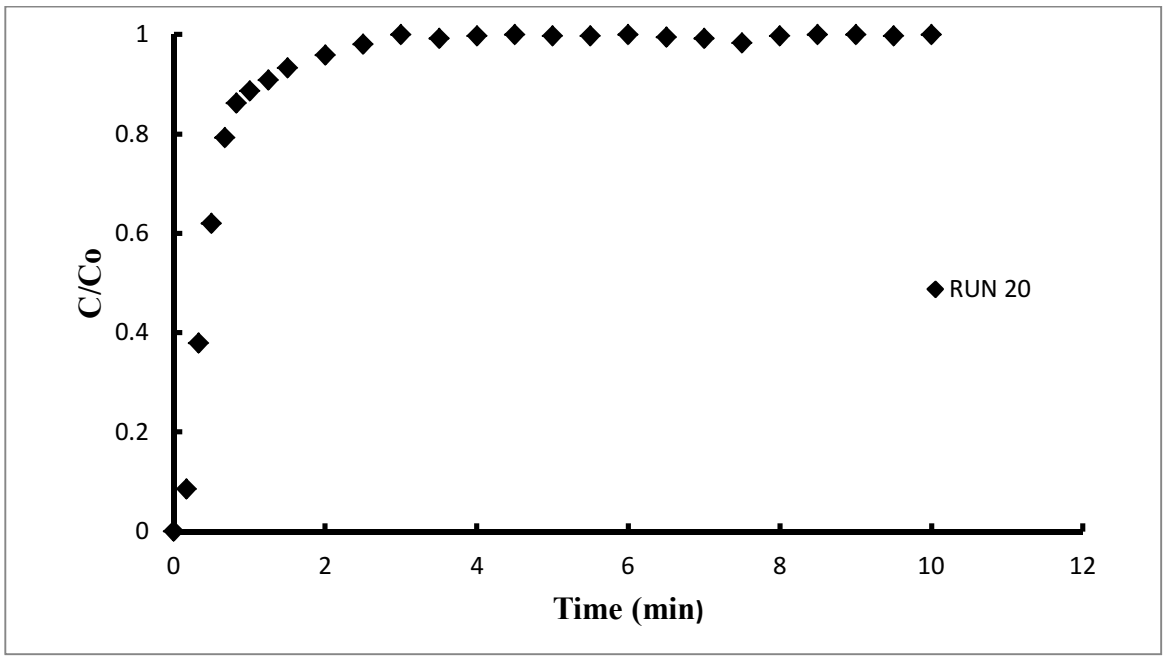

Fig 4.3.40: Exit concentration curve at %RH = High, Conc= 365ppm, flowrate= 0.7L/min and Temp=0^0C

RUN 21

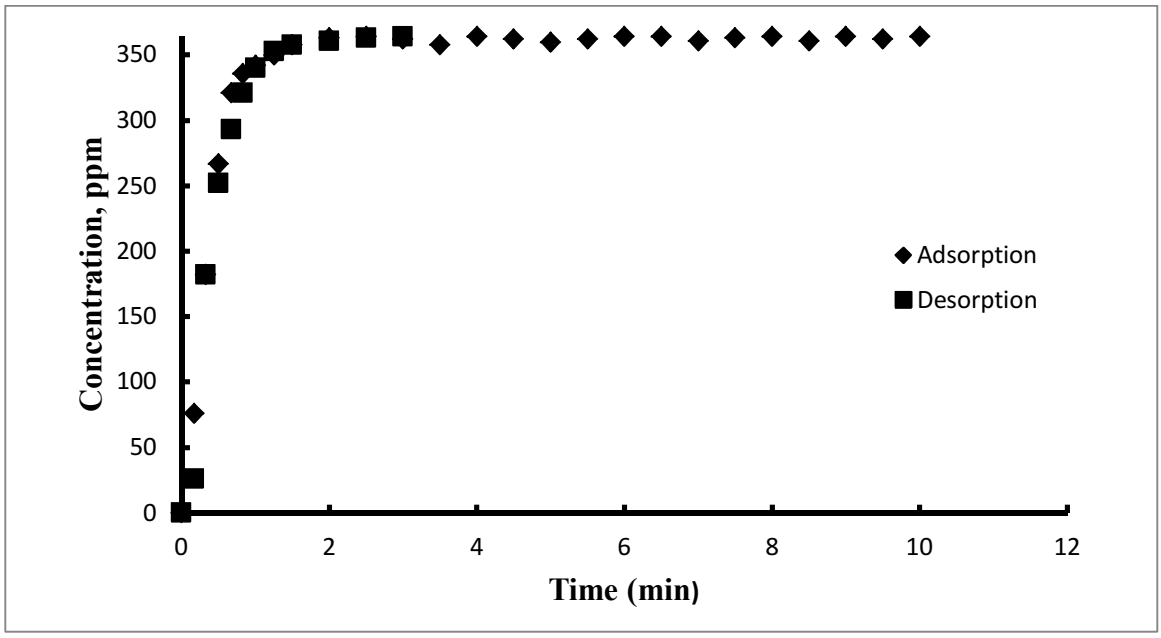

Fig 4.3.41: Adsorption-desorption curve at %RH = High, Conc= 3655ppm, flowrate= 1.0L/min and Temp=0^0C

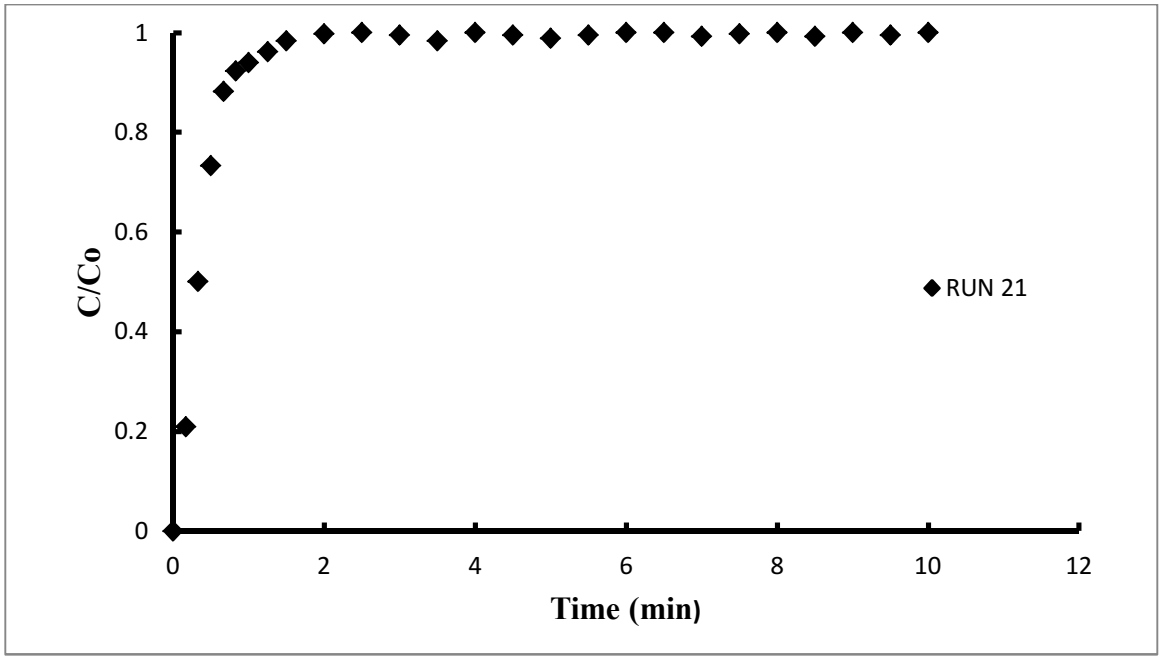

Fig 4.3.42: Exit concentration curve at %RH = High, Conc= 365ppm, flowrate= 1.0L/min and Temp=0^0C

RUN 22

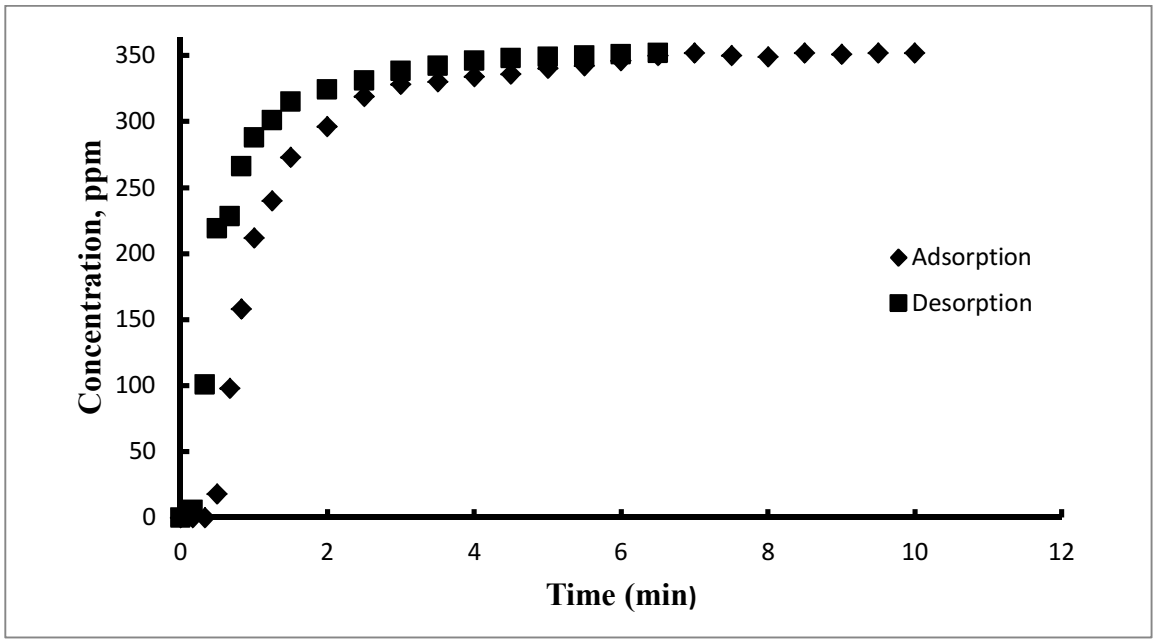

Fig 4.3.43: Adsorption-desorption curve at %RH = High, Conc= 365ppm, flowrate= 0.3L/min and Temp=40^0C

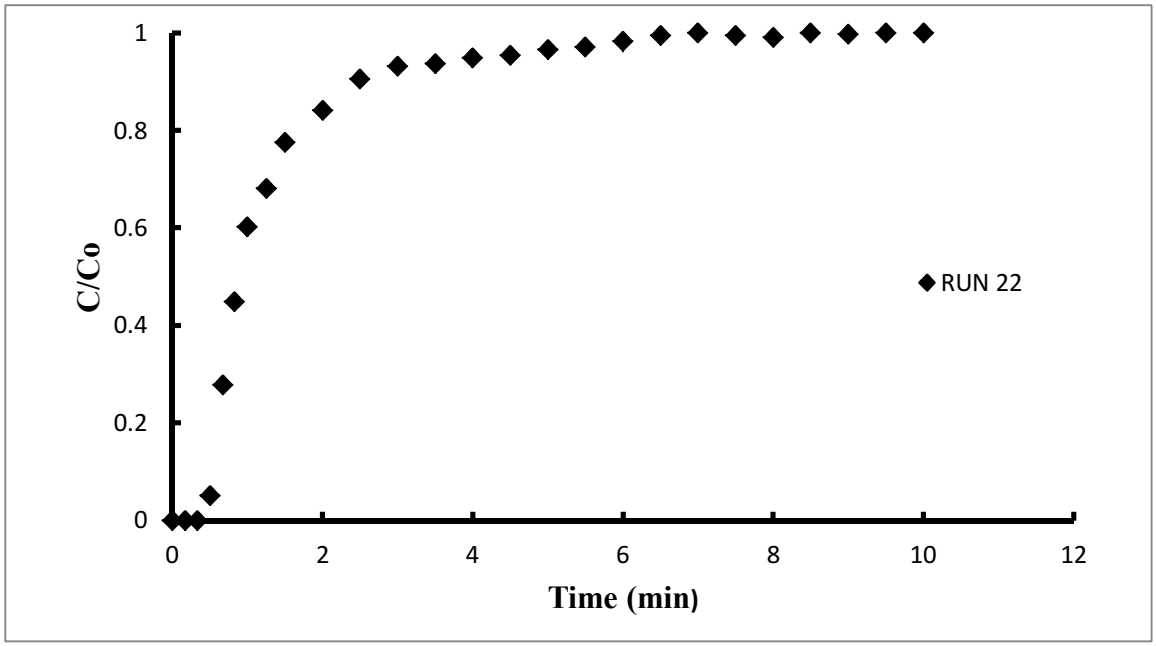

Fig 4.3.44: Exit concentration curve at %RH = High, Conc= 365ppm, flowrate= 0.3L/min and Temp=40^0C

RUN 23

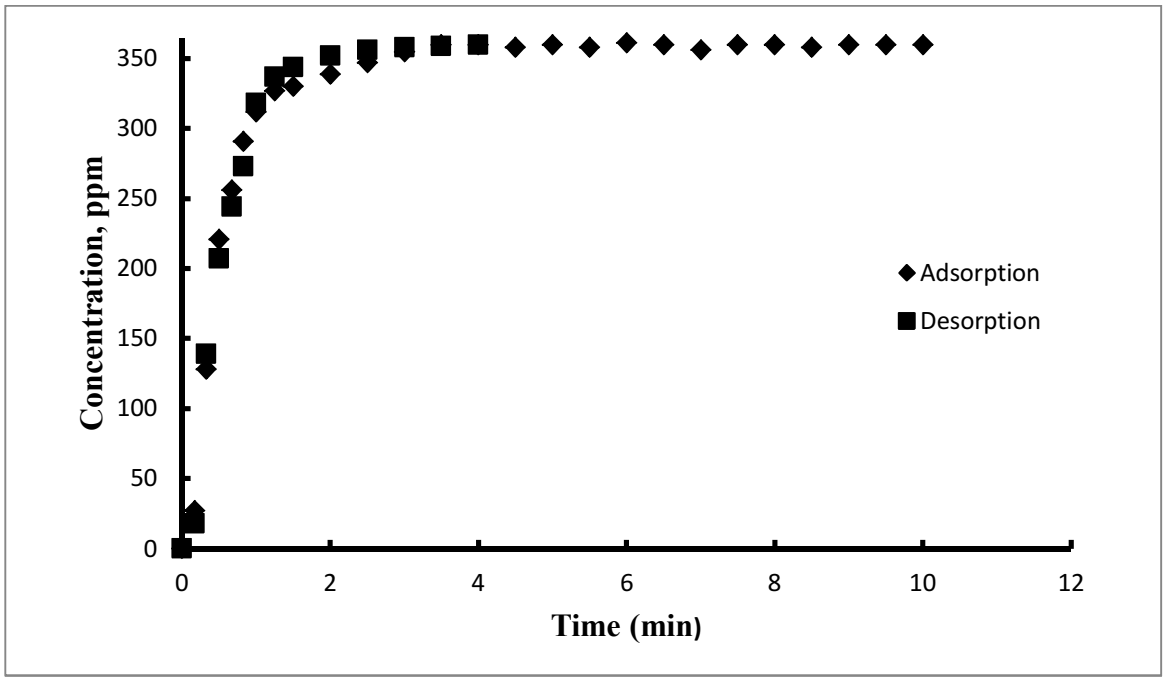

Fig 4.3.45: Adsorption-desorption curve at %RH = High, Conc= 365ppm, flowrate= 0.7L/min and Temp=40^0C

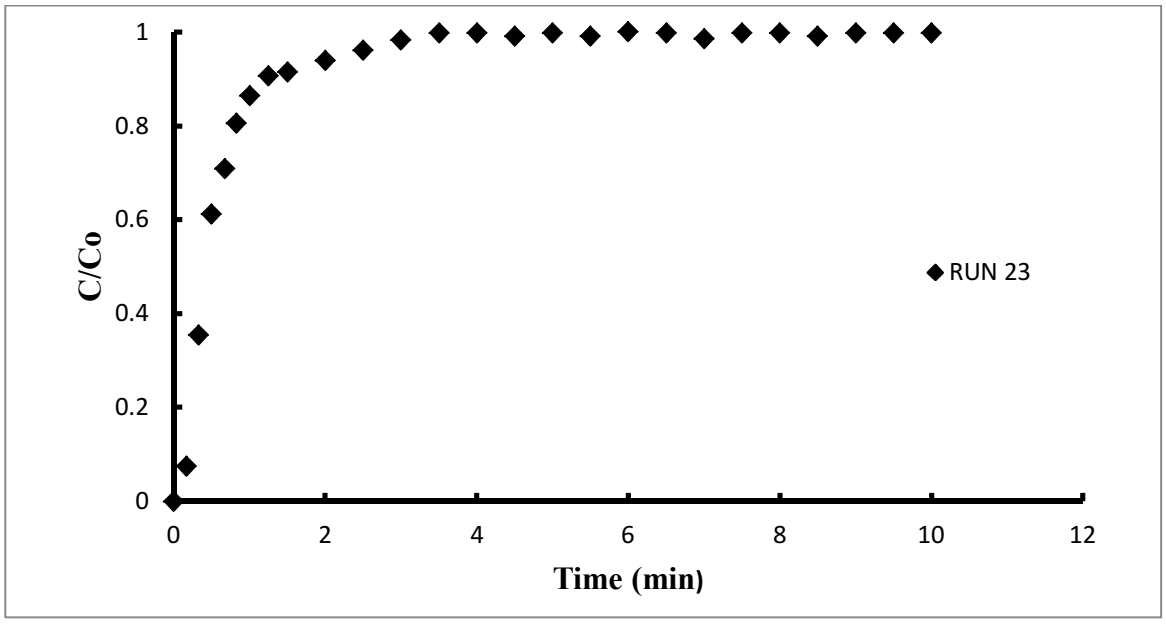

Fig 4.3.46: Exit concentration curve at %RH = High, Conc= 365ppm, flowrate= 0.7L/min and Temp=40^0C

RUN 24

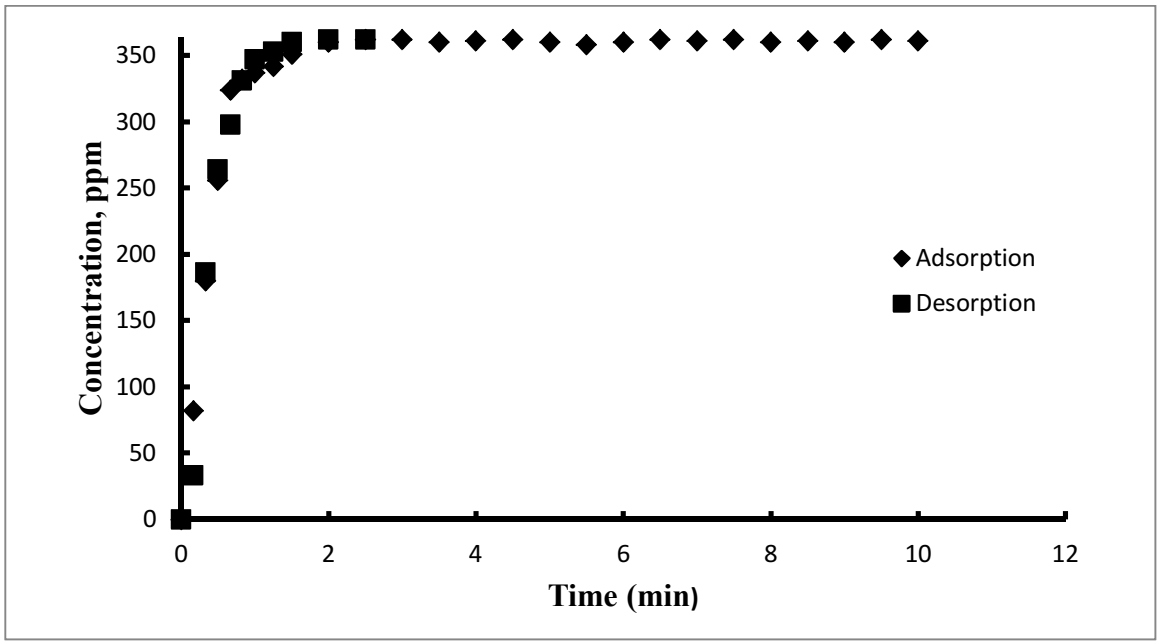

Fig 4.3.47: Adsorption-desorption curve at %RH = High, Conc= 365ppm, flowrate= 1.0L/min and Temp=40^{0}C

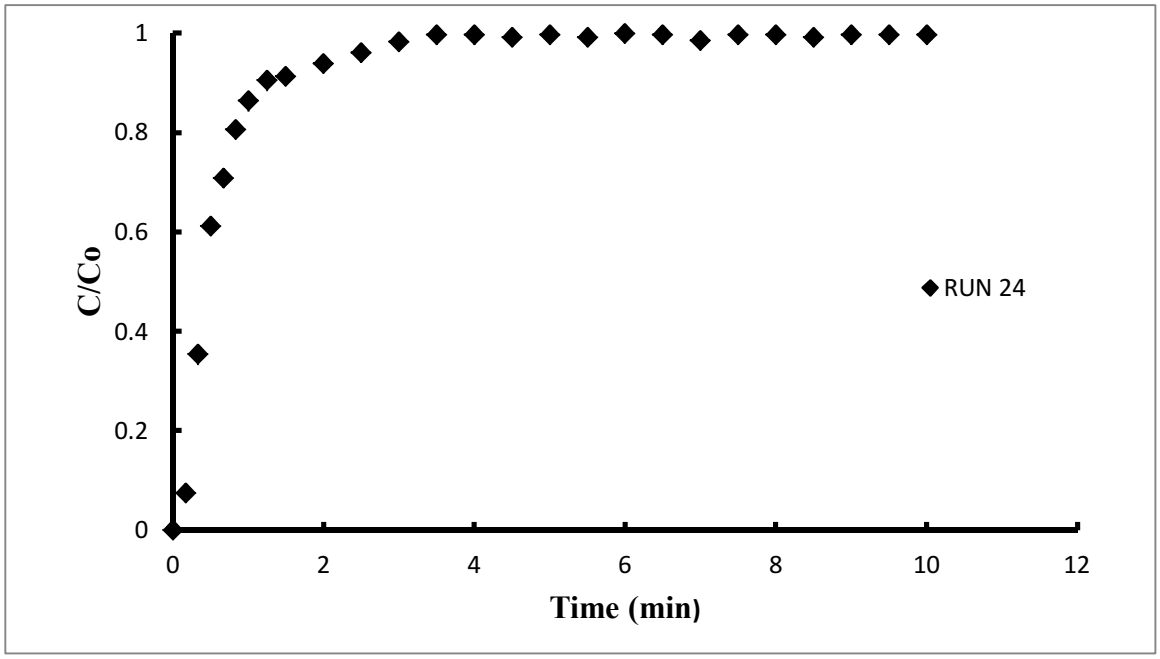

Fig 4.3.48: Exit concentration curve at %RH = High, Conc= 365ppm, flowrate= 1.0L/min and Temp=40^{0}C

APPENDIX B: EFFECT OF CONCENTRATION

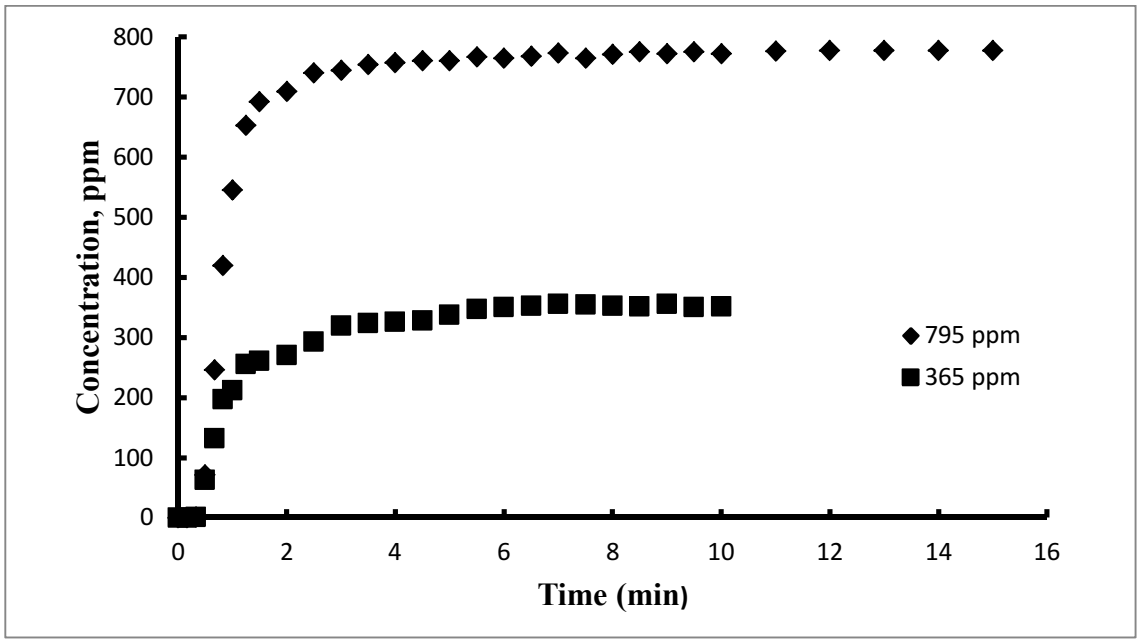

Fig 4.5.1: Effect of concentration at flow rate = 0.3L/min, Temp=0^0C and %RH= Low

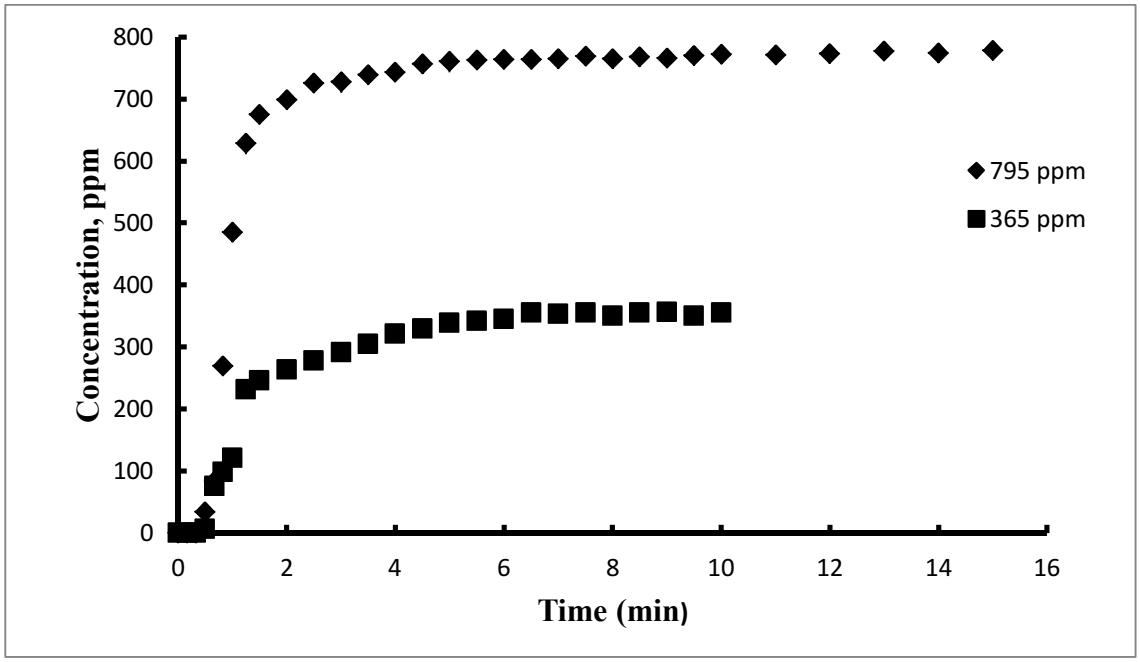

Fig 4.5.2: Effect of concentration at flow rate = 0.3L/min, Temp=40^0C and %RH= Low

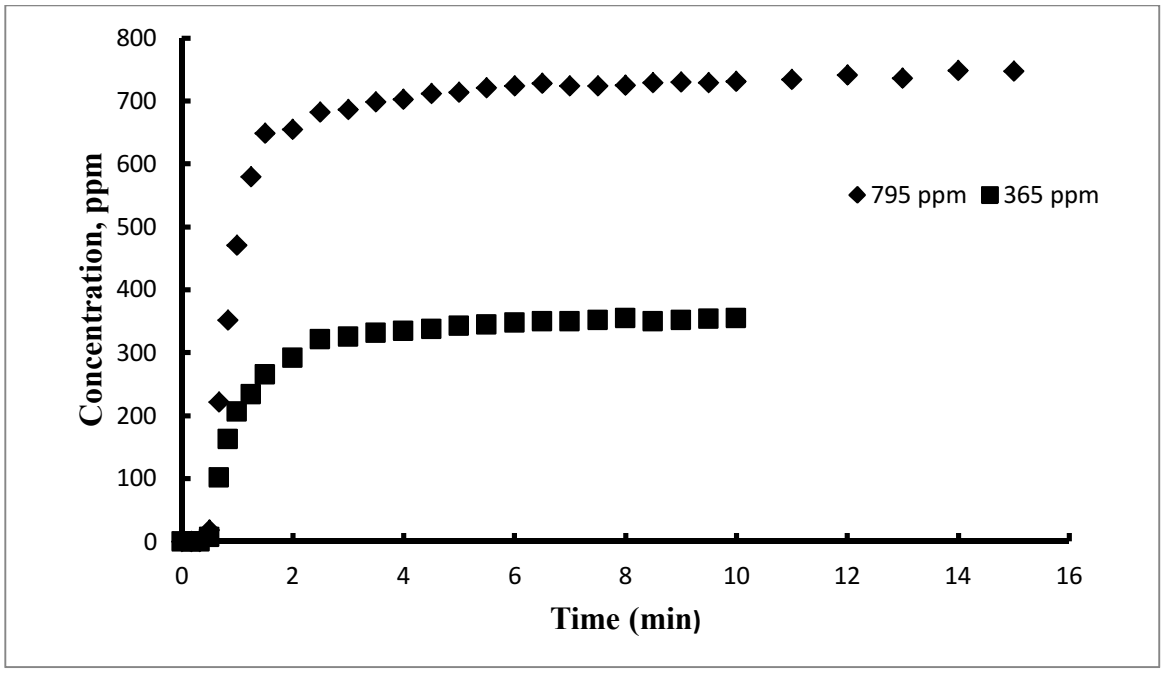

Fig 4.5.3: Effect of concentration at flow rate = 0.3L/min, Temp=0^0C and %RH= High

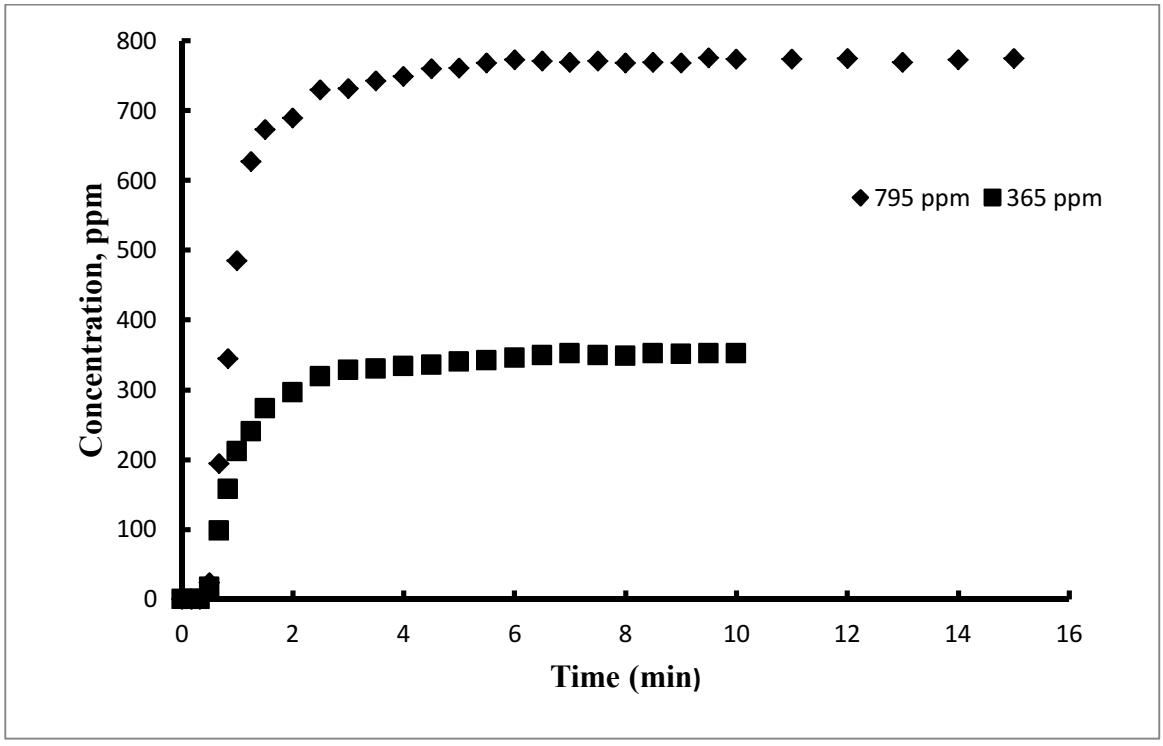

Fig 4.5.4: Effect of concentration at flow rate = 0.3L/min, Temp=40^0C and %RH= High

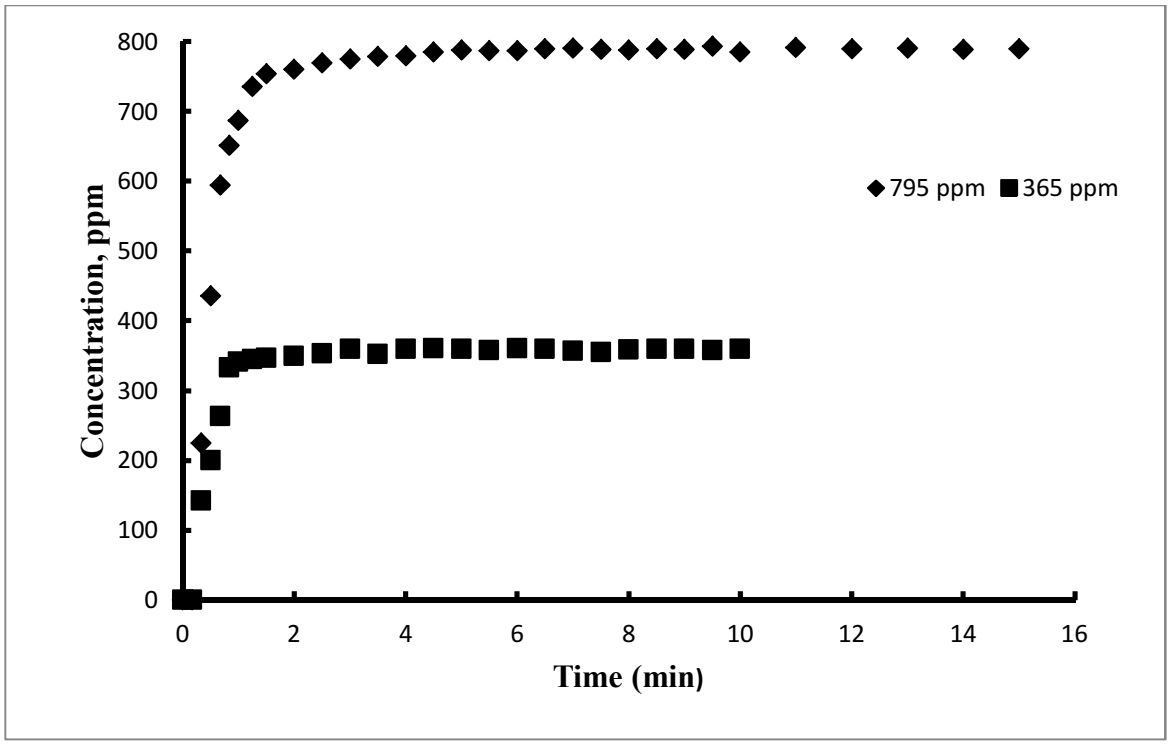

Fig 4.5.5: Effect of concentration at flow rate = 0.7L/min, Temp=0^0C and %RH= Low

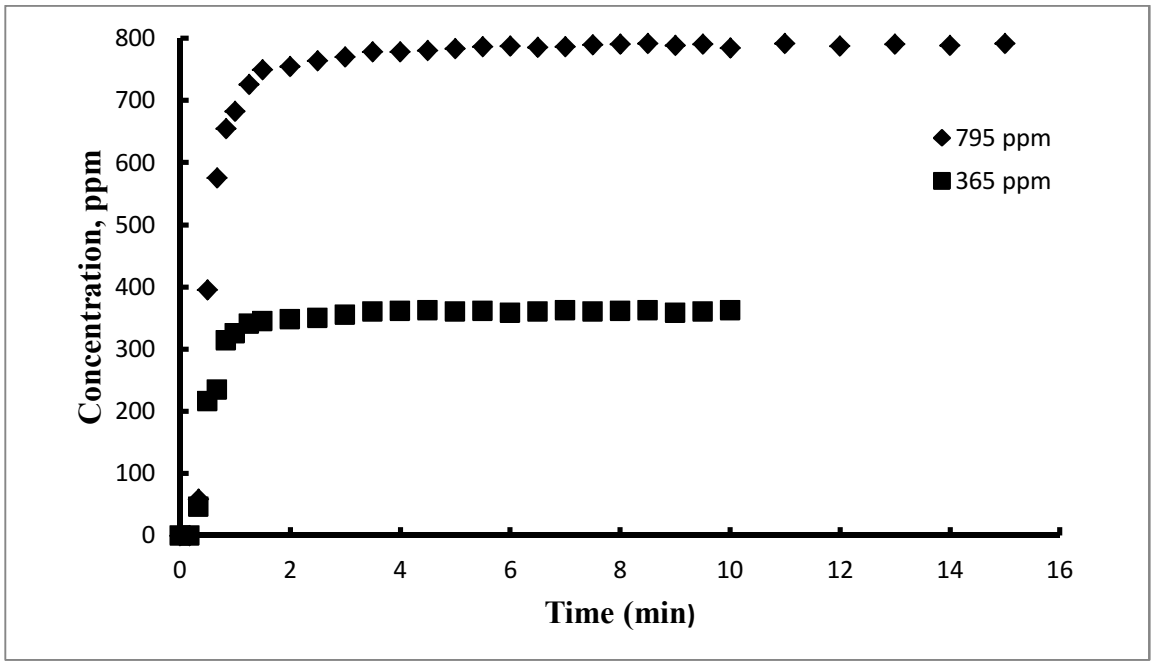

Fig 4.5.6: Effect of concentration at flow rate = 0.7L/min, Temp=40^0C and %RH= Low

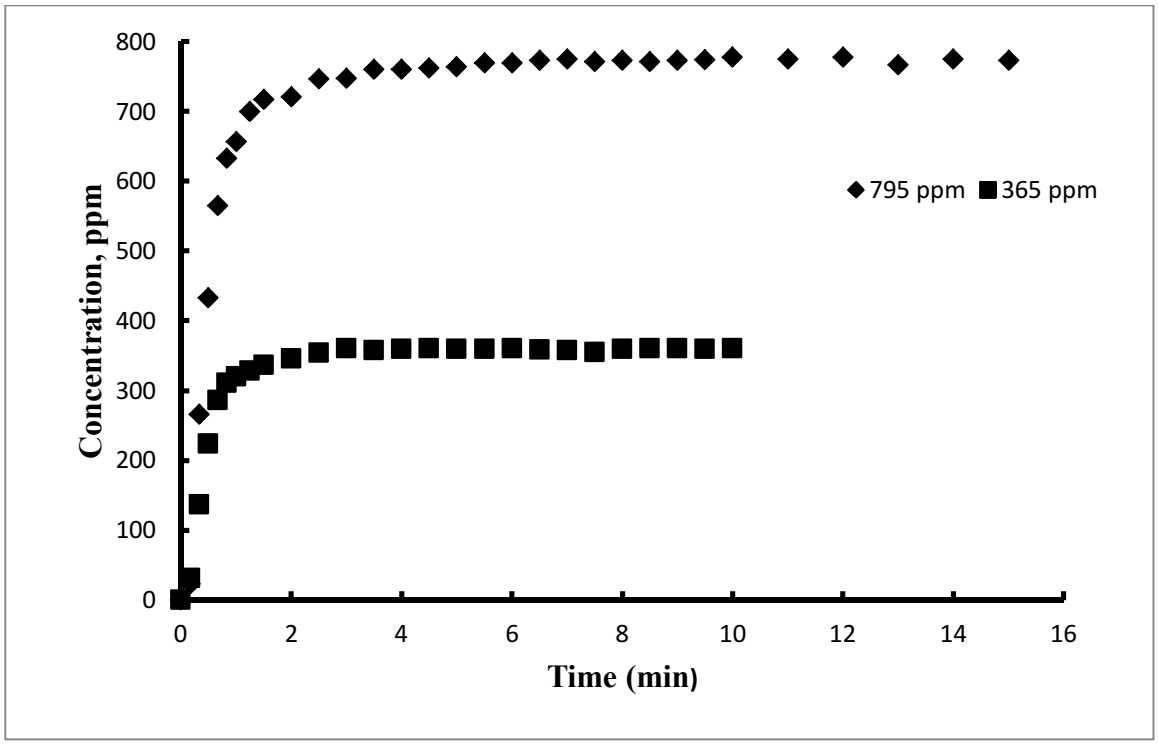

Fig 4.5.7: Effect of concentration at flow rate = 0.7L/min, Temp=0^0C and %RH= High

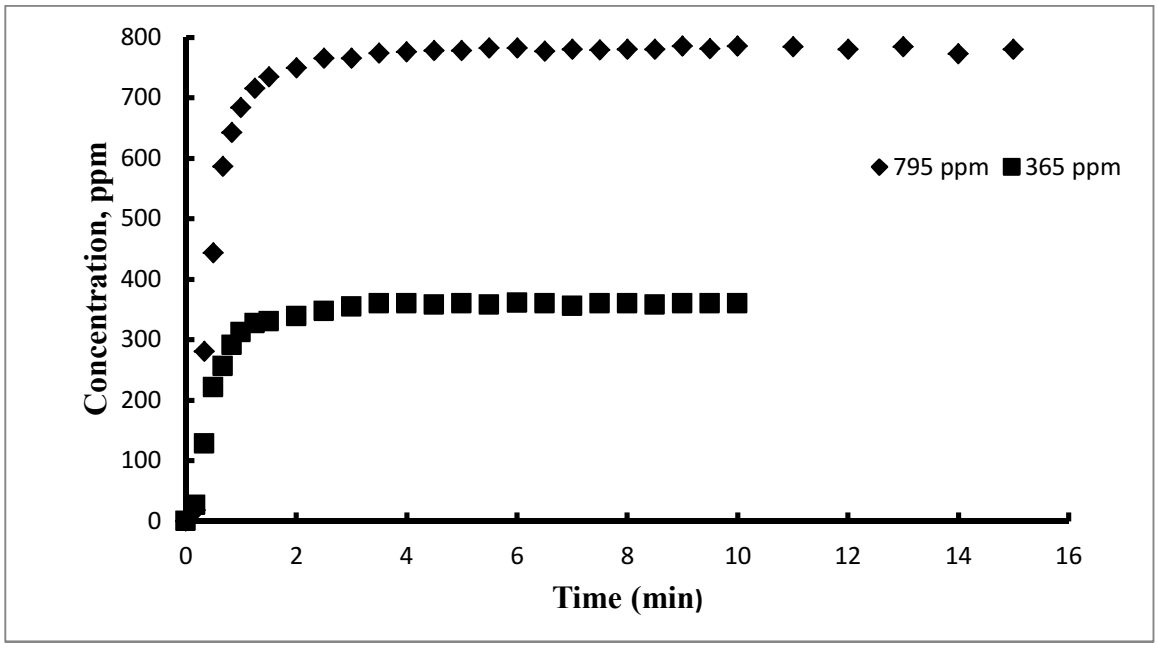

Fig 4.5.8: Effect of concentration at flow rate = 0.3L/min, Temp=40^0C and %RH= High

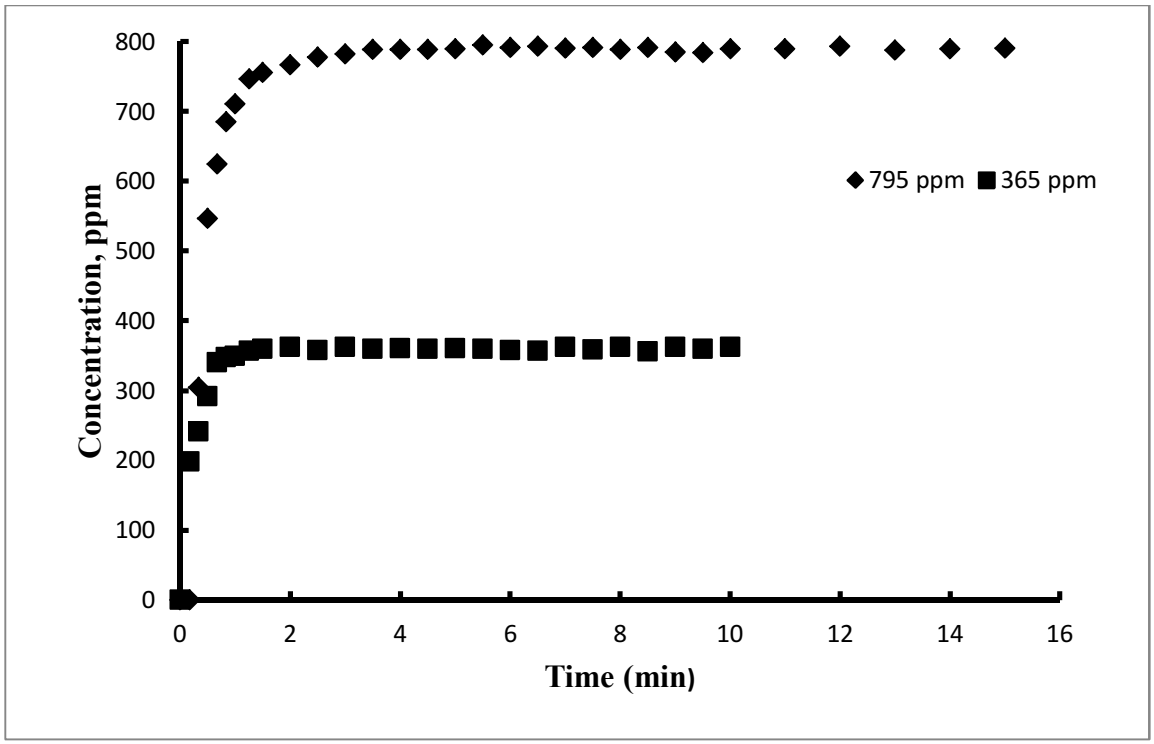

Fig4.5.9: Effect of concentration at flow rate = 1.0L/min, Temp=0^0C and %RH= Low

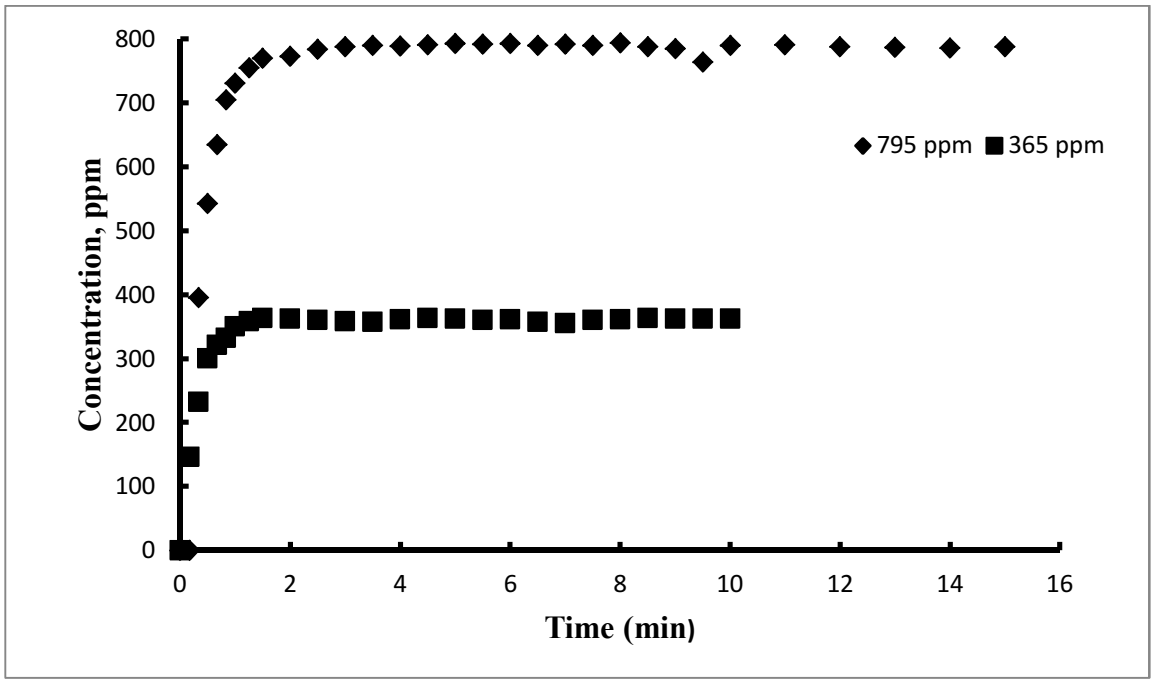

Fig 4.5.10: Effect of concentration @ flow rate =1.0L/min, Temp=40^0C and %RH= Low

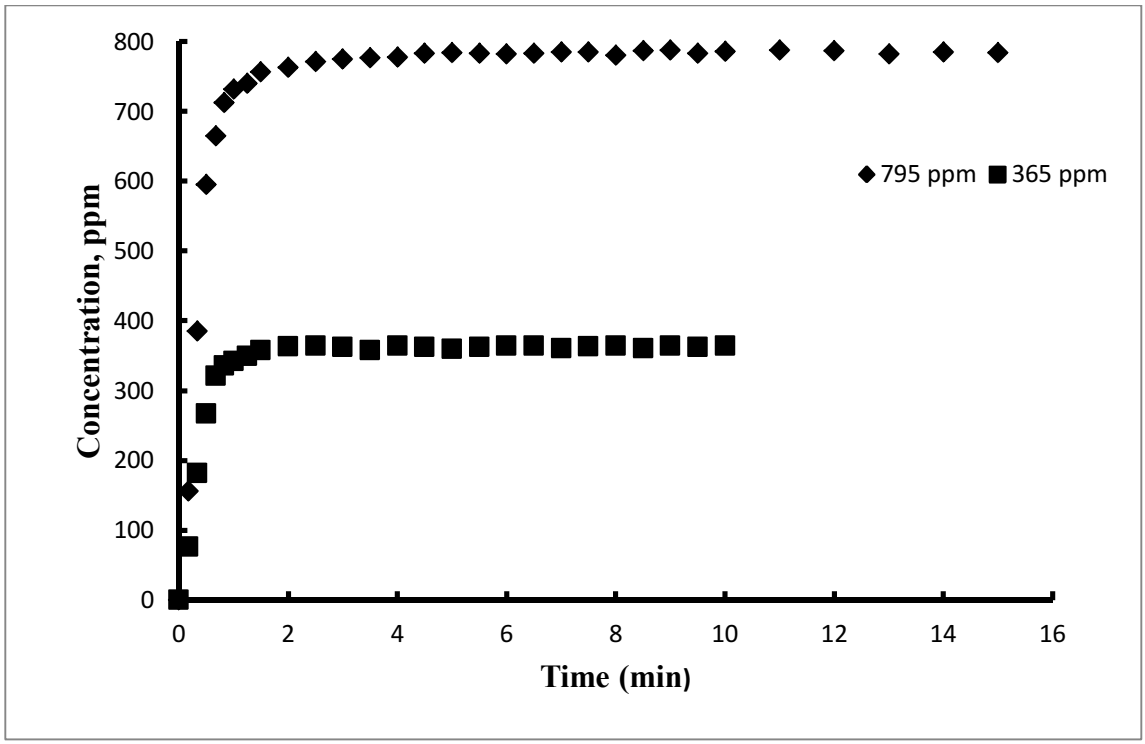

Fig 4.5.11: Effect of concentration at flow rate = 1.0L/min, Temp=0^0C and %RH= High

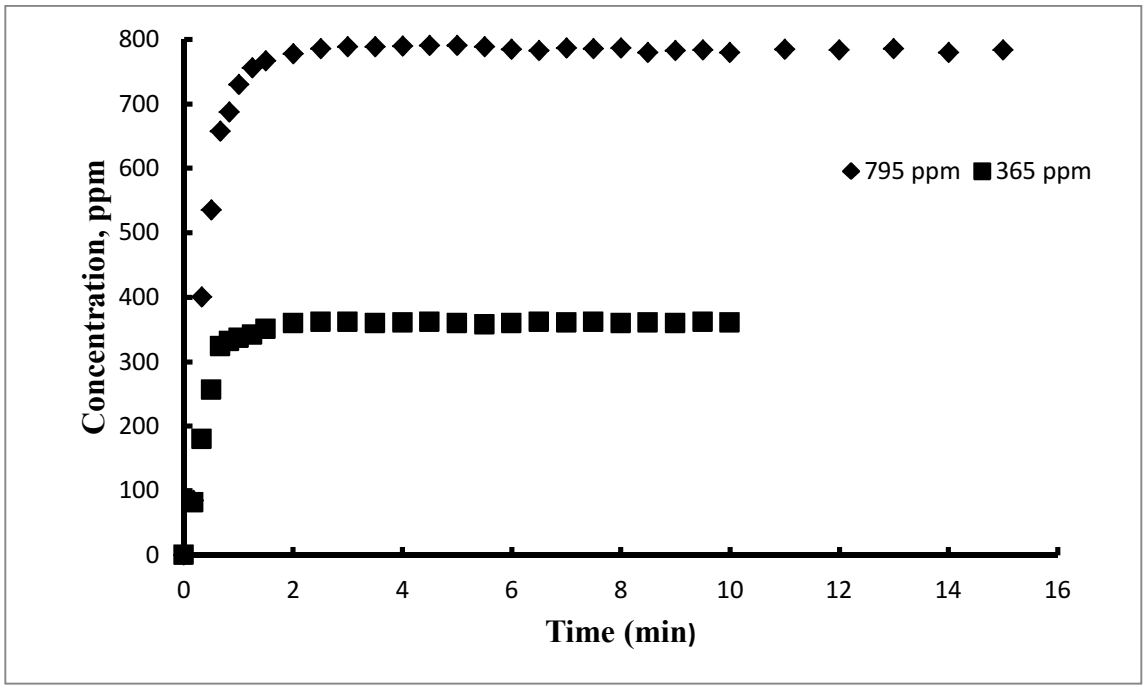

Fig 4.5.12: Effect of concentration at flow rate = 1.0L/min, Temp=40^0C and %RH= High

APPENDIX C: EFFECT OF FLOWRATE

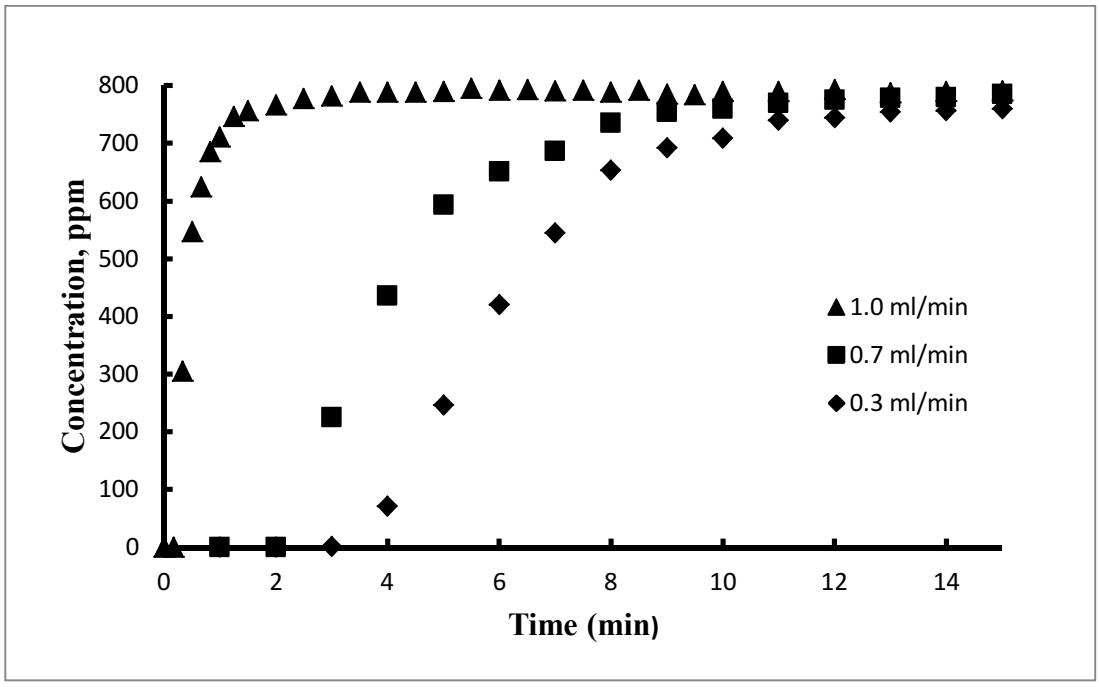

Fig4.6.1: Effect of flow rate at C= 795ppm, T= 0^0C and %RH= Low

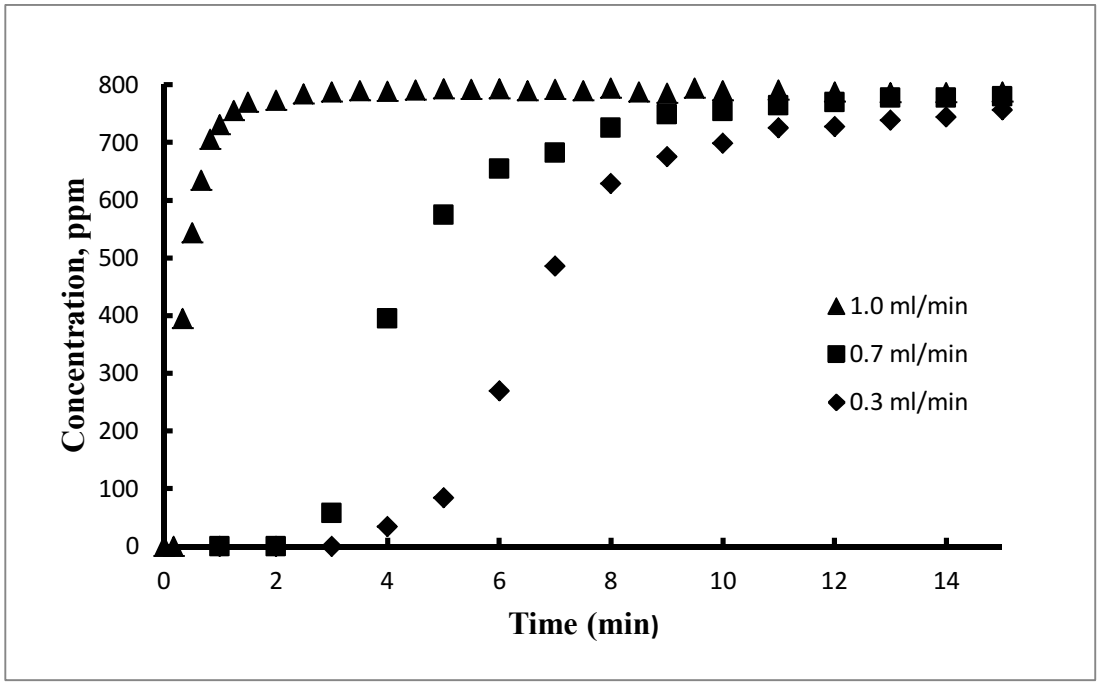

Fig 4.6.2: Effect of flow rate at C= 795ppm, T=40^0C and %RH= Low

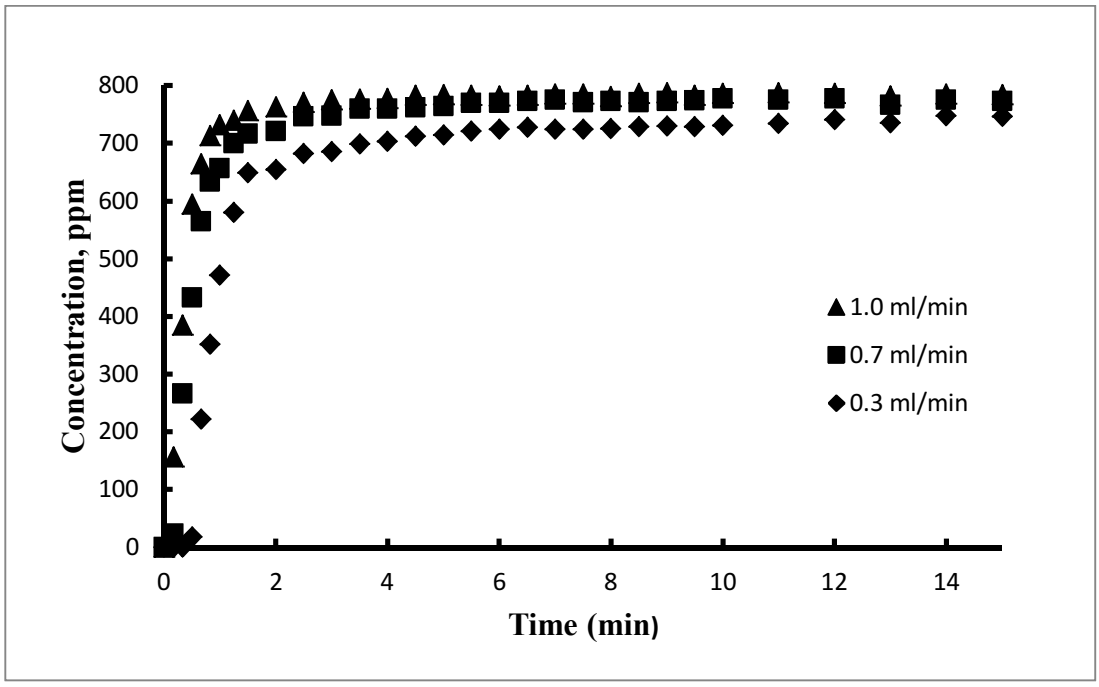

Fig 4.6.3: Effect of flow rate at C= 795ppm, T= 0^0C and %RH= High

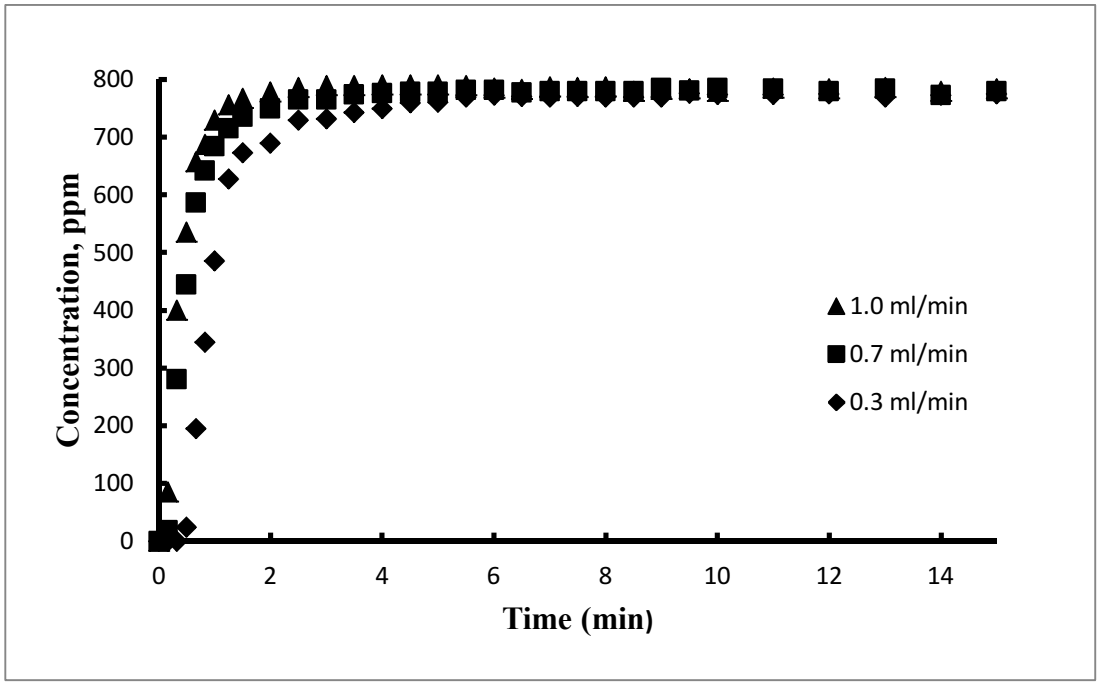

Fig 4.6.4: Effect of flow rate at C= 795ppm, T= 40^0C and %RH= High

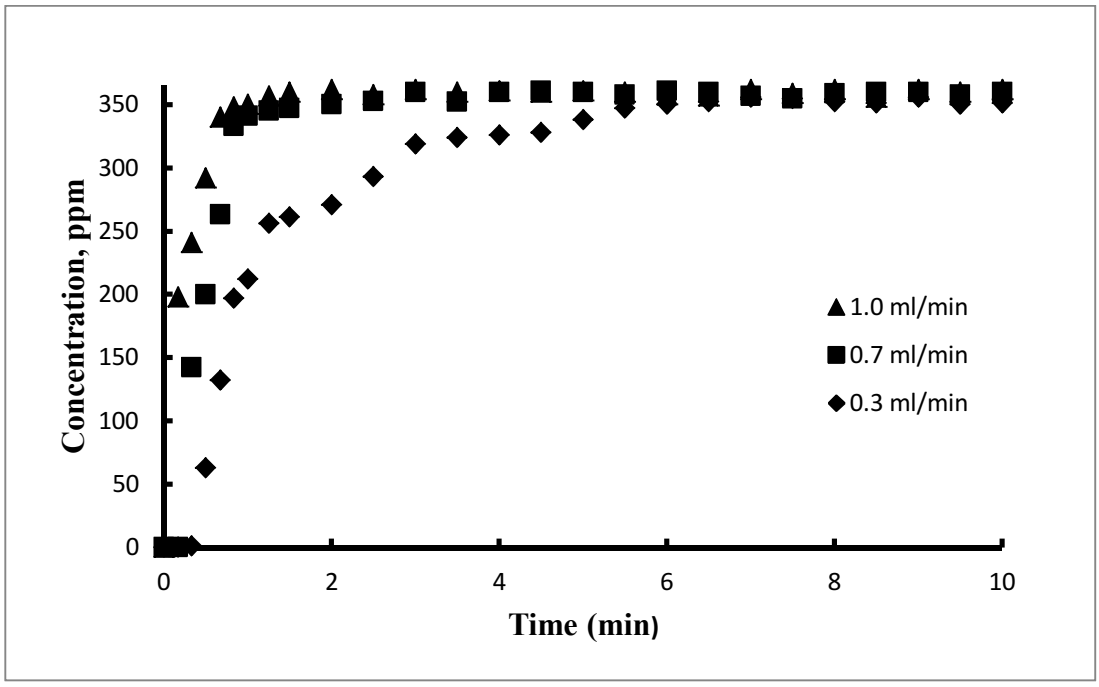

Fig 4.6.5: Effect of flow rate at C= 365ppm, T= 0^0C and %RH= Low

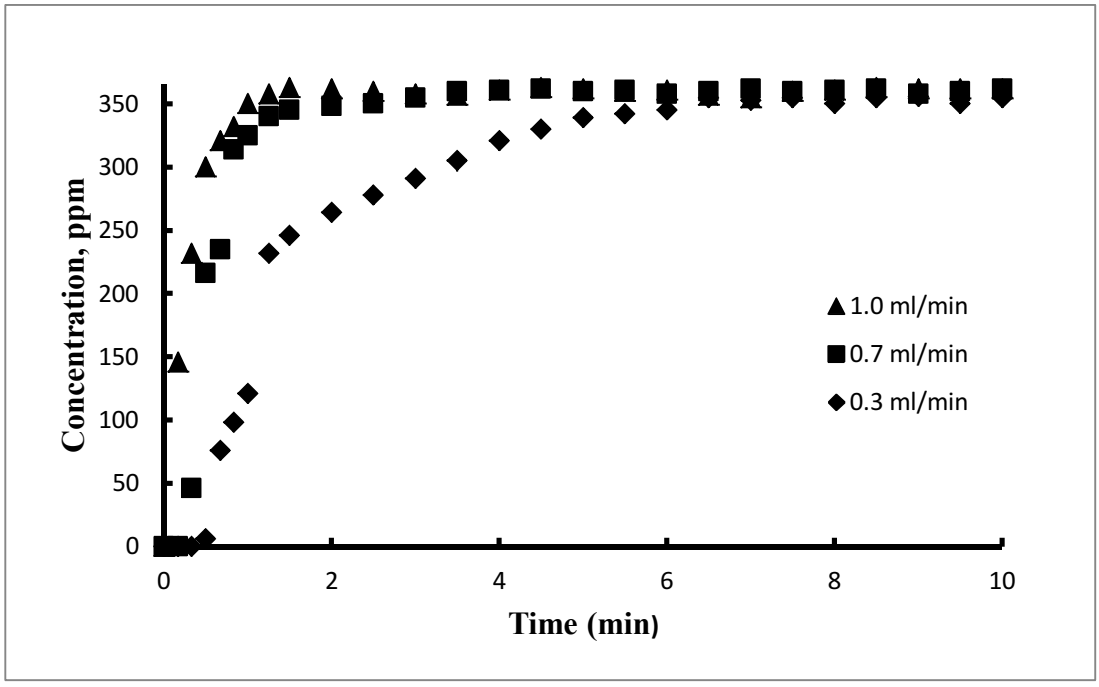

Fig 4.6.6: Effect of flow rate at C= 365ppm, T= 40^0C and %RH= Low

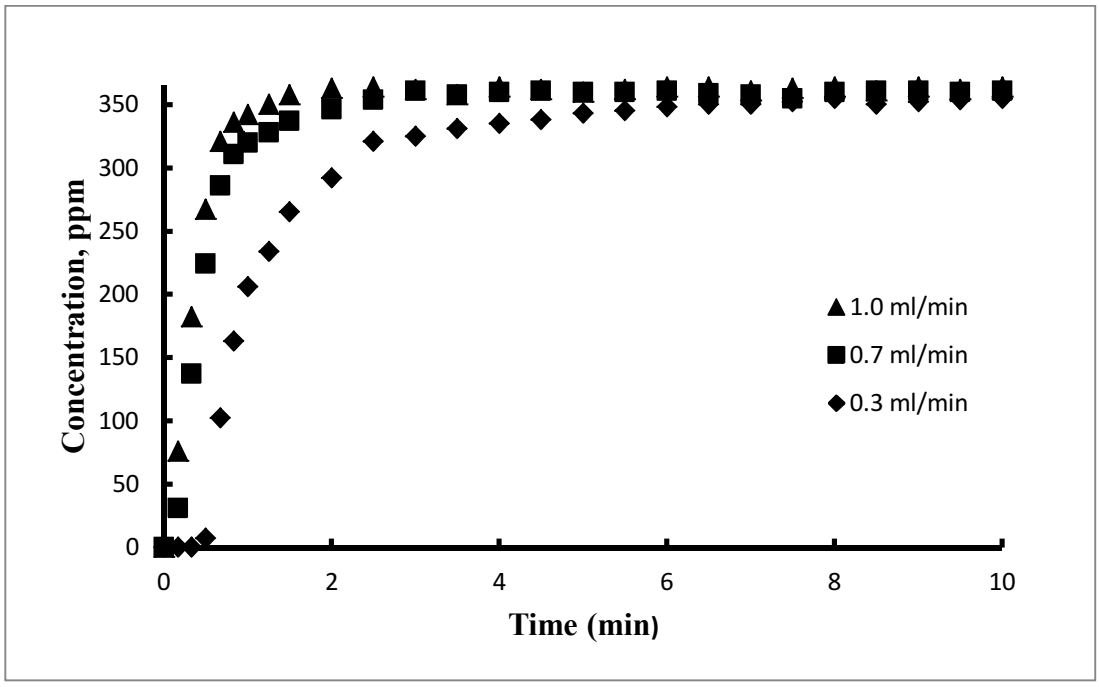

Fig 4.6.7: Effect of flow rate at C= 365ppm, T= 0^0C and %RH= High

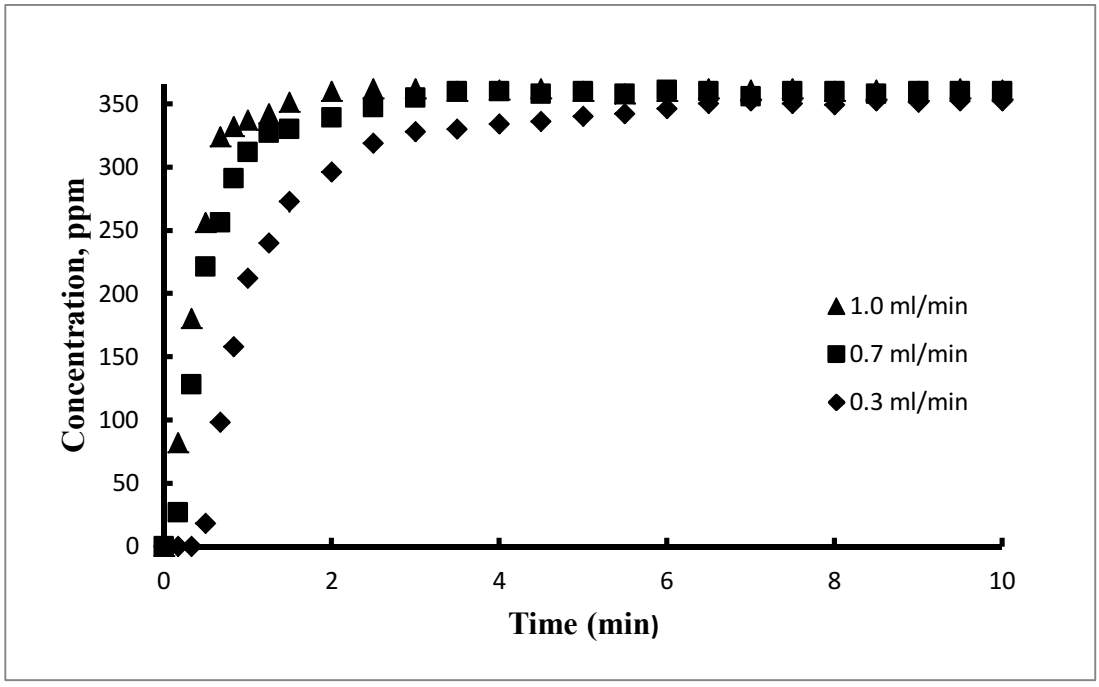

Fig 4.6.8: Effect of flow rate at C= 365ppm, T= 40^0C and %RH= Hig

APPENDIX D: EFFECT OF RELATIVE HUMIDITY

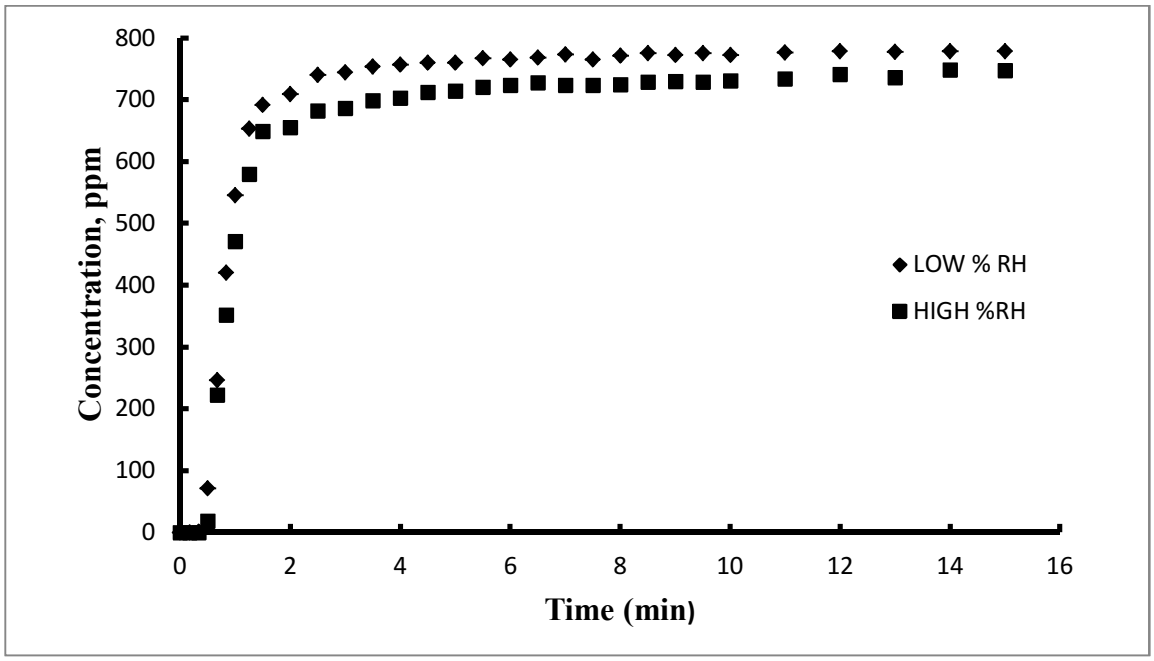

Fig 4.7.1: Effect of Humidity at Flow rate = 0.3L/min, Concentration = 795ppm and Temp = 0^0C

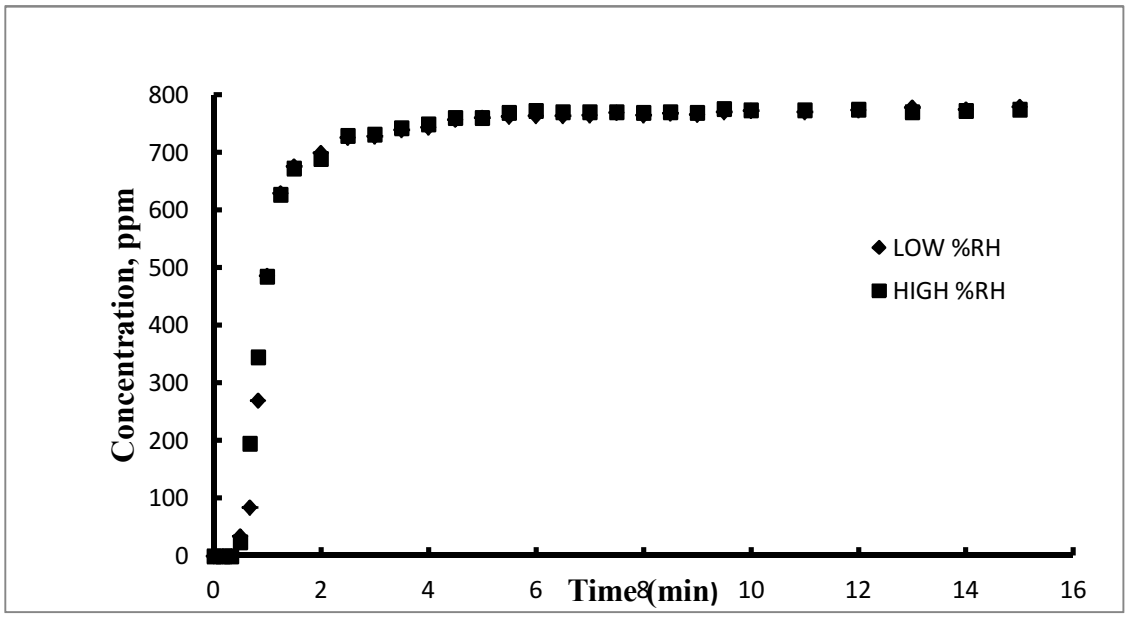

Fig 4.7.2: Effect of Humidity at Flow rate = 0.3L/min, Concentration = 795ppm and Temp =40^0C

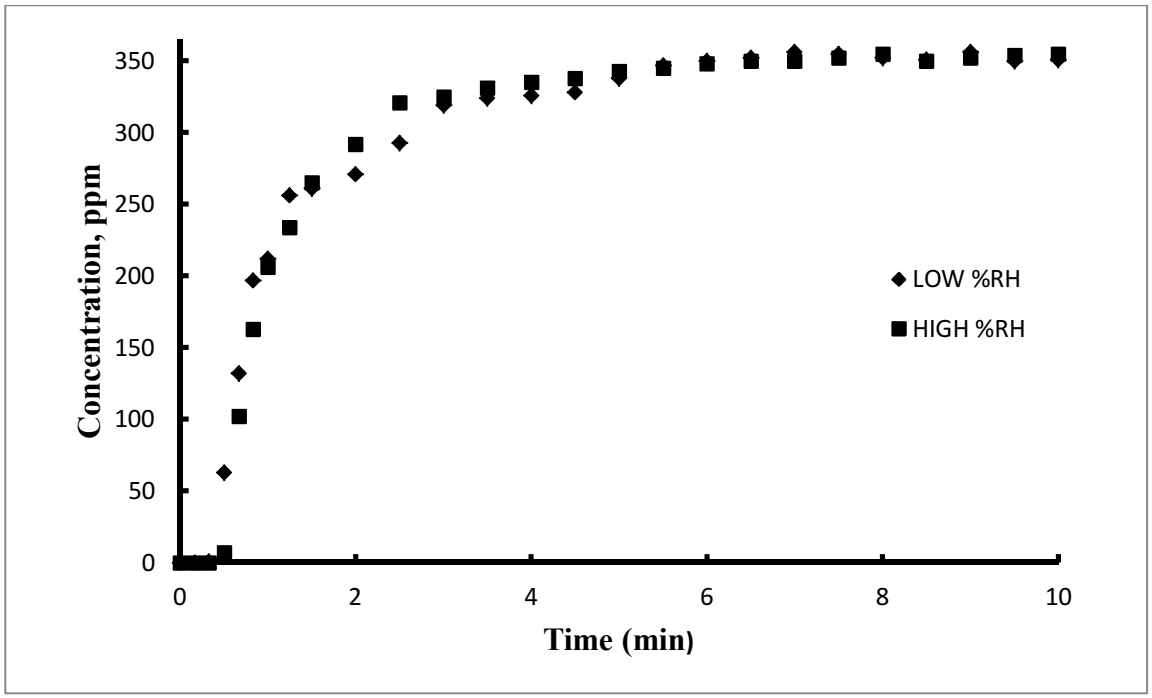

Fig 4.7.3: Effect of Humidity at Flow rate = 0.3L/min, Concentration = 365ppm and Temp = 0^0C

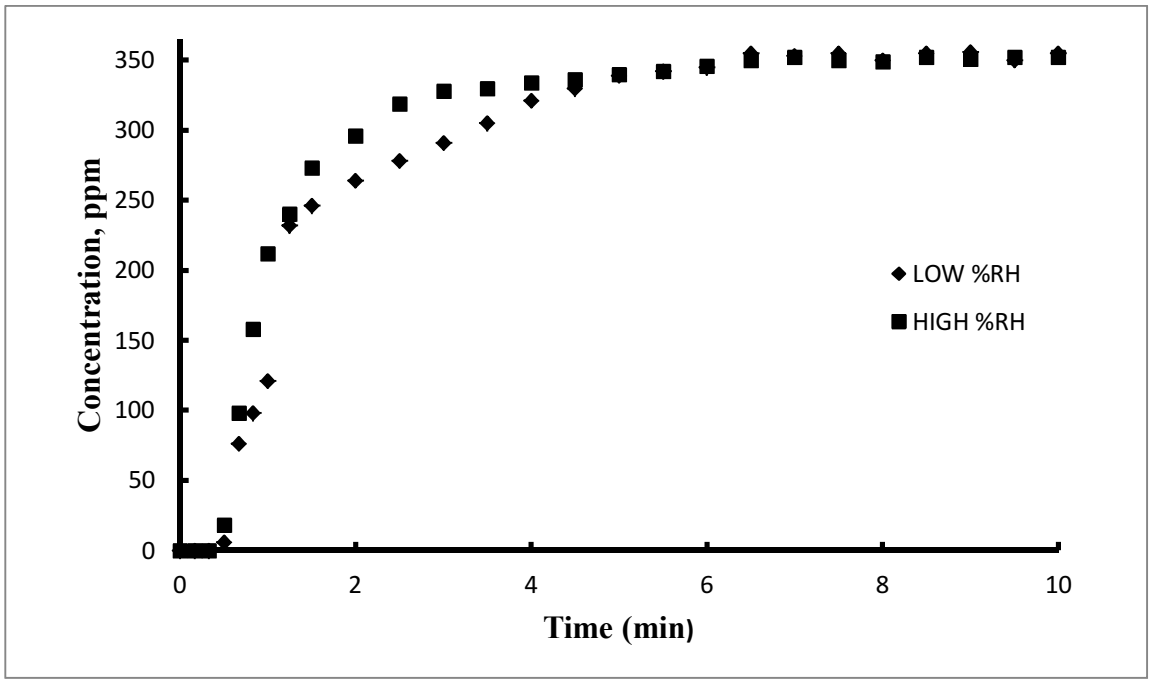

Fig 4.7.4: Effect of Humidity at Flow rate = 0.3L/min, Concentration = 365ppm and Temp = 40^0C

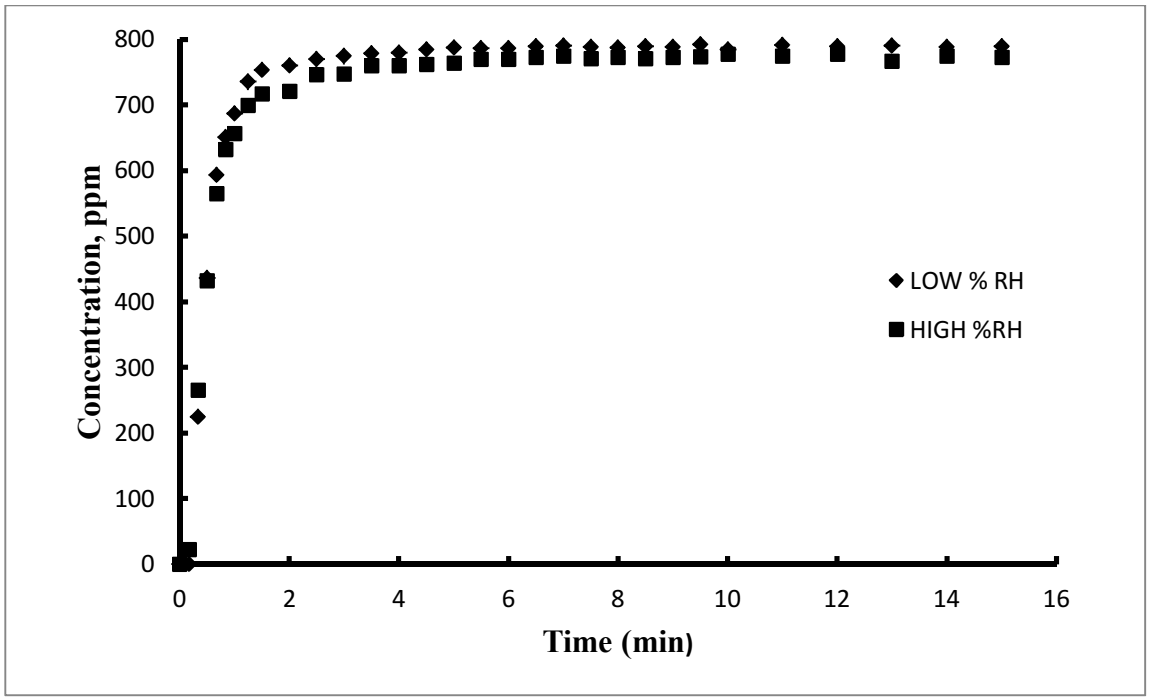

Fig 4.7.5: Effect of Humidity at Flow rate = 0.7L/min, Concentration = 795ppm and Temp = 0^0C

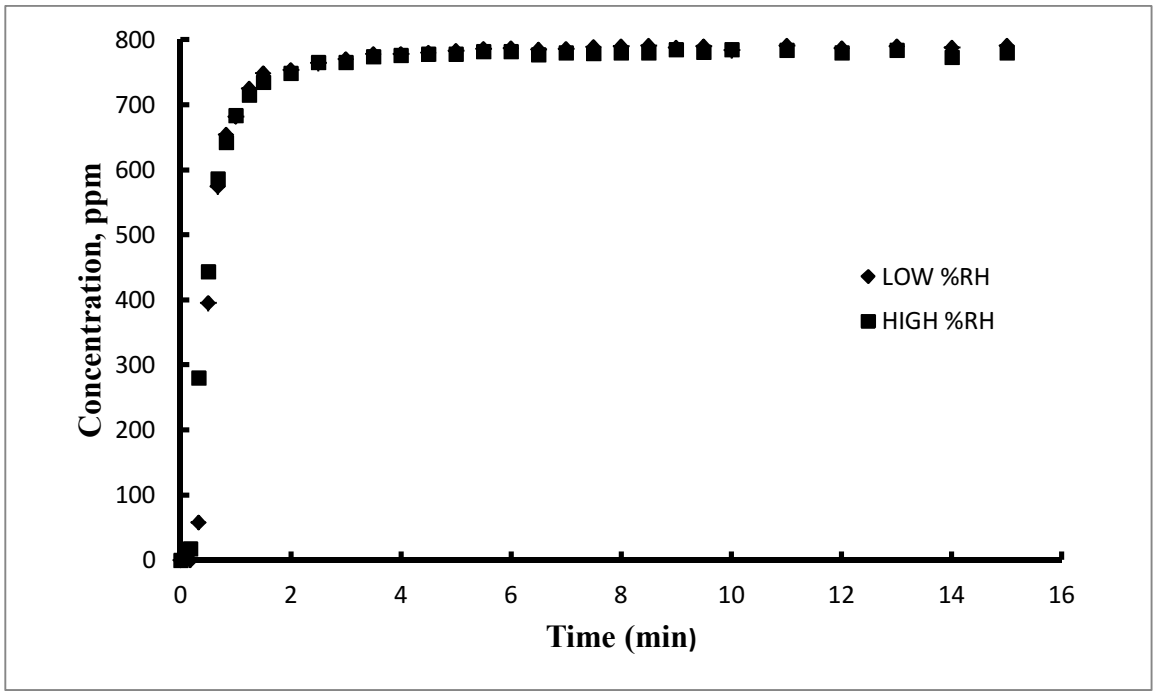

Fig 4.7.6: Effect of Humidity at Flow rate = 0.7L/min, Concentration = 795ppm and Temp = 40^0C

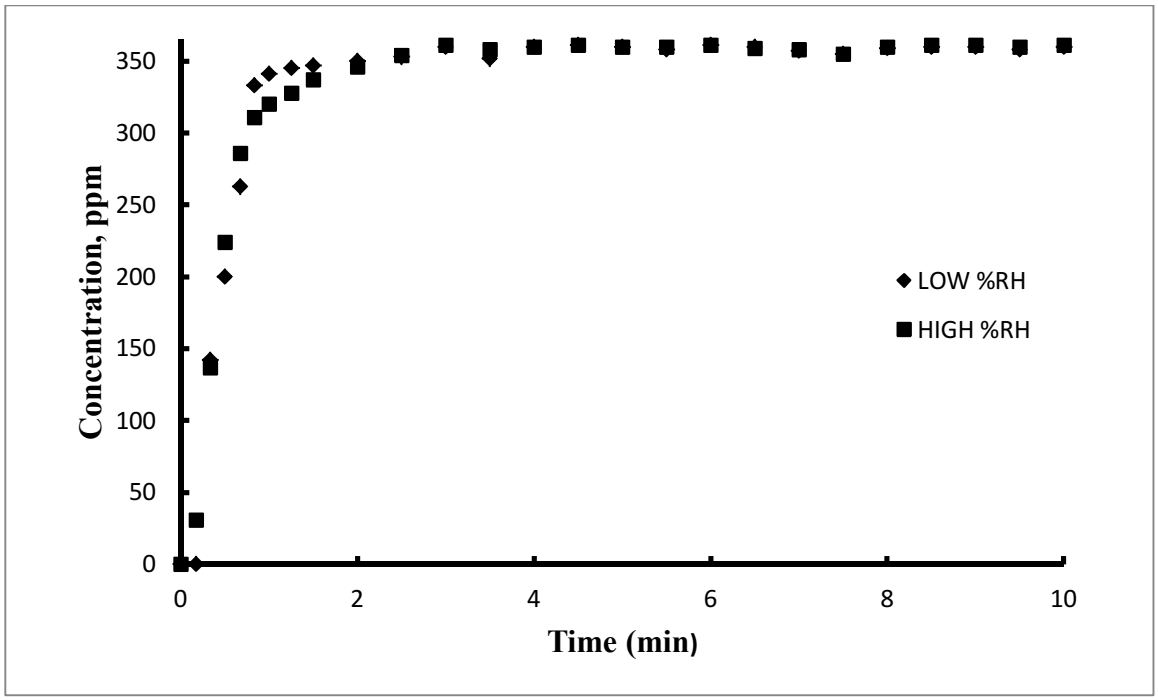

Fig 4.7.7: Effect of Humidity at Flow rate = 0.7L/min, Concentration = 365ppm and Temp = 0^0C

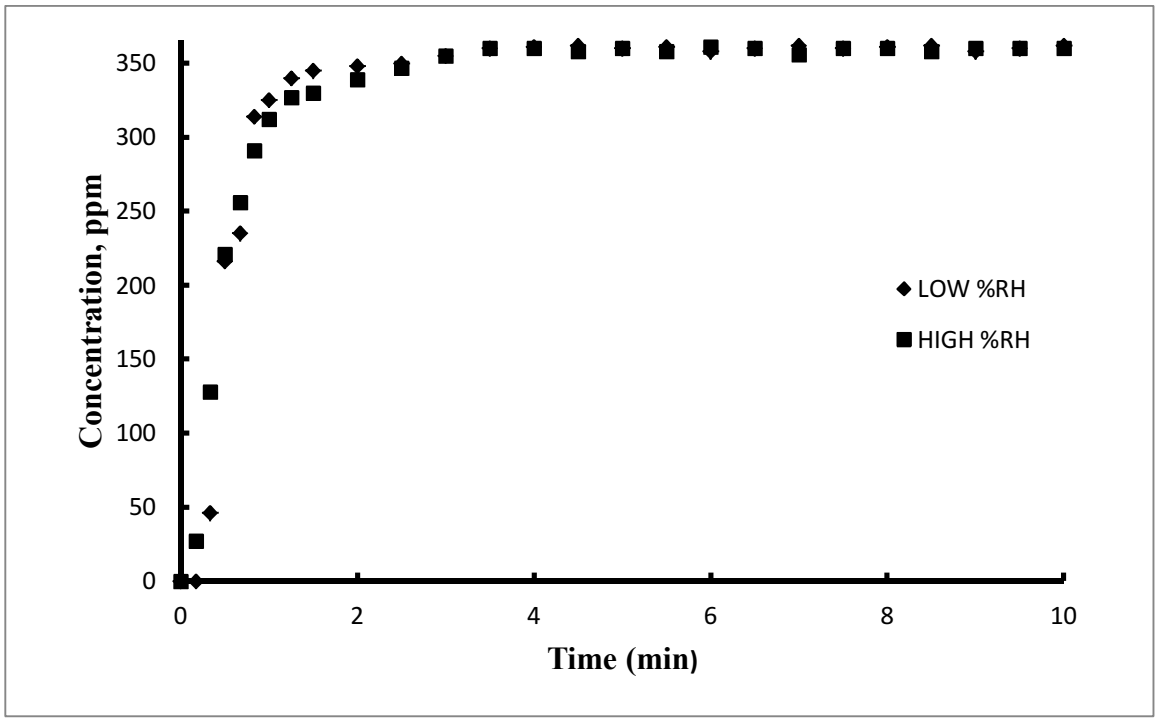

Fig 4.7.8: Effect of Humidity at Flow rate = 0.7L/min, Concentration = 365ppm and Temp = 40^0C

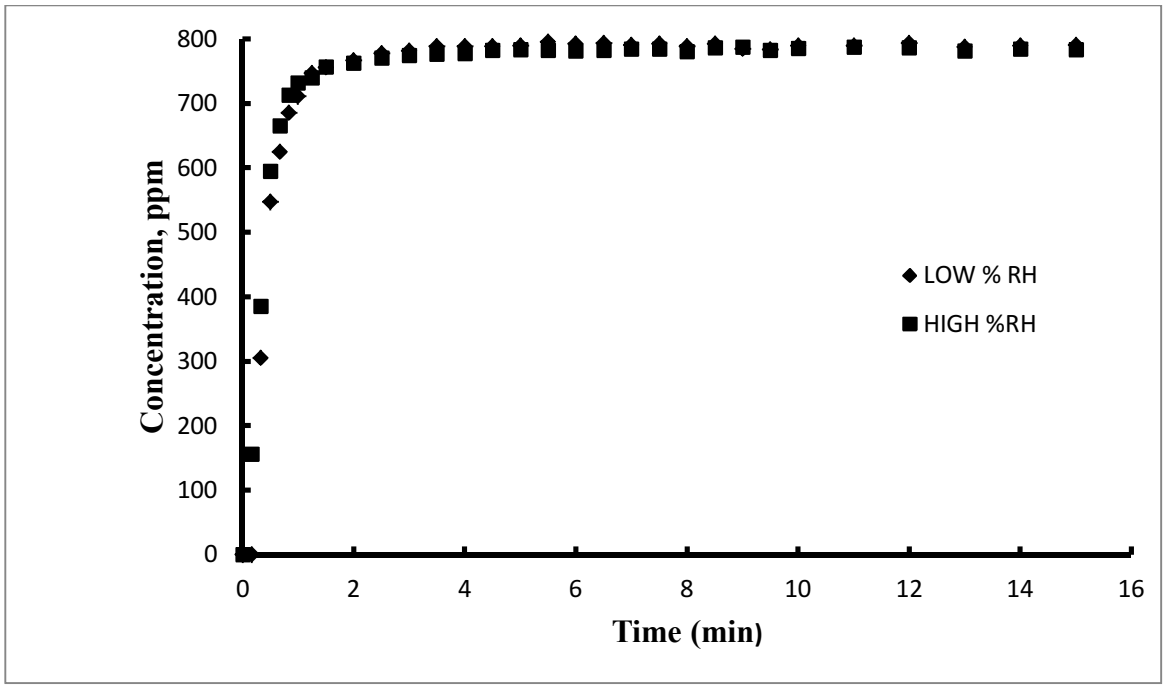

Fig 4.7.9: Effect of Humidity at Flow rate = 1.0L/min, Concentration = 795ppm and Temp = 0^0C

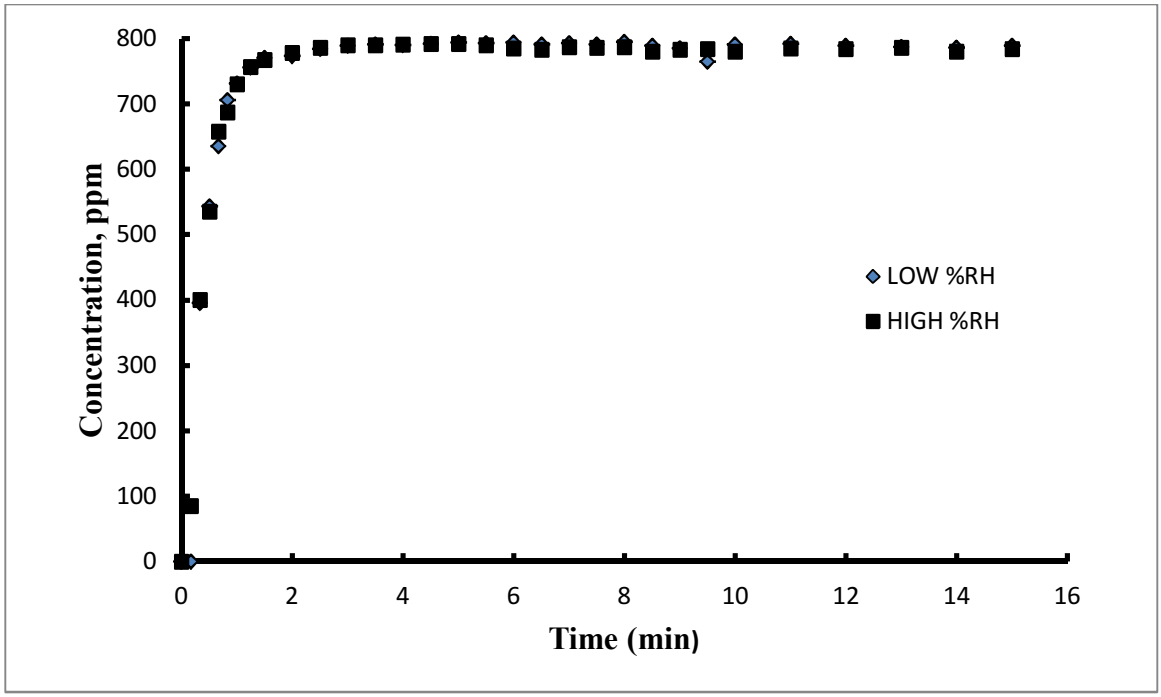

Fig 4.7.10: Effect of Humidity at Flow rate = 1.0L/min, Concentration = 795ppm and Temp = 40^0C

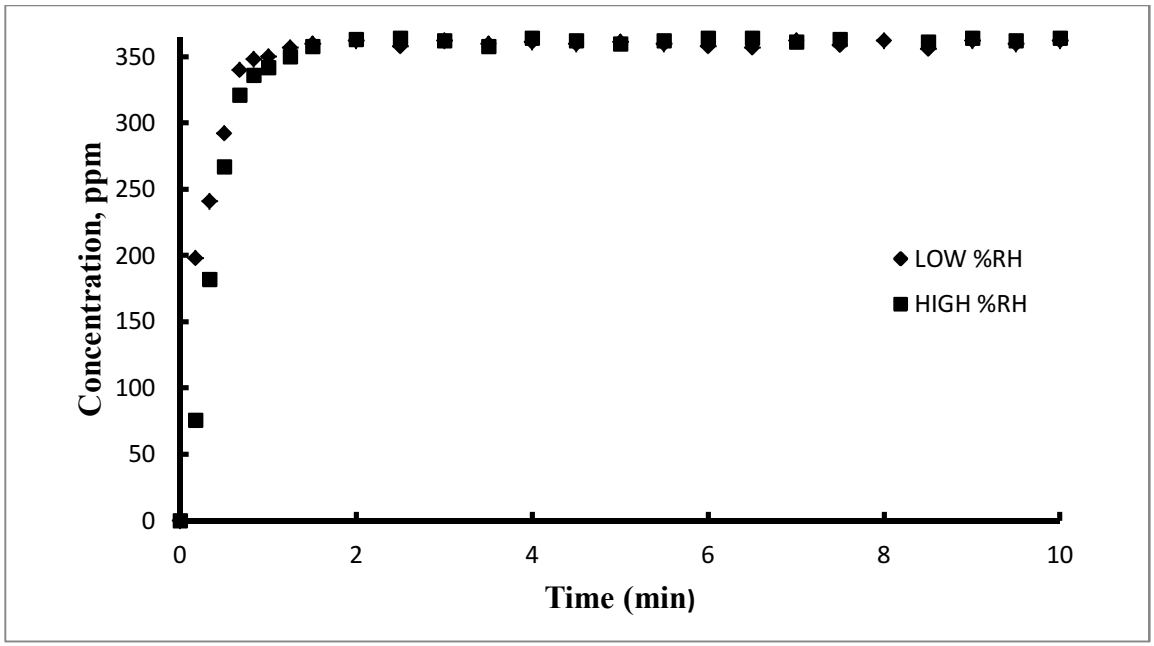

Fig 4.7.11: Effect of Humidity at Flow rate = 1.0L/min, Concentration = 365ppm and Temp = 0^0C

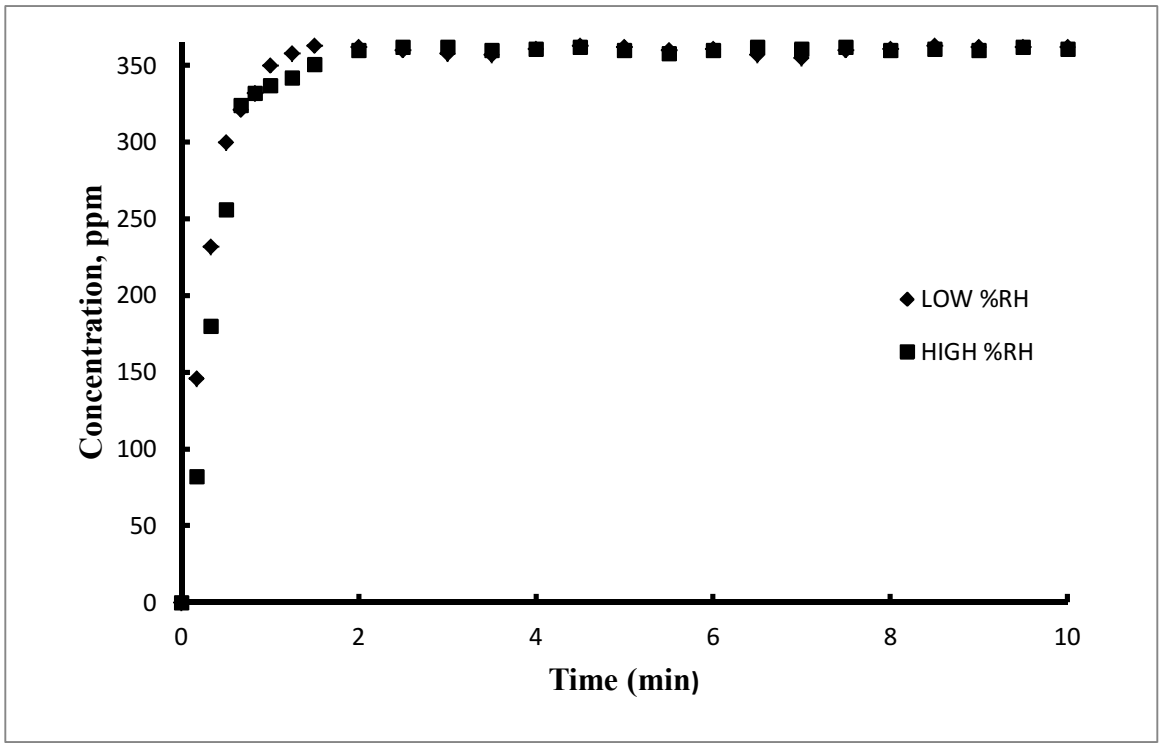

Fig 4.7.12: Effect of Humidity at Flow rate = 1.0L/min, Concentration = 365ppm and Temp = 40^0C

REFERENCES

[1] M S. Shafeeyan, W. M. Ashri Wan Daud, A. Houshmand and A. Shamiri (2010): A review on surface modification of activated carbon for carbon dioxide adsorption Journal of Analytical and Applied Pyrolysis 89: 143–151

[2] A.Arenillas, K.M. Smith, T.C. Drage and C.E. Snape: CO_2 capture using some fly ash-derived carbon materials Fuel 84 (2005) 2204–2210

[3] S. Kazama, T. Teramoto and K. Haraya: Carbon dioxide and nitrogen transport properties of bis (phenyl) fluorine based card polymer membranes. *Journal of Membrane Science* 2002, 207 (1) 91–104.

[4] CO_2Now,http://CO_2now.org/Current-CO_2/CO_2-Now/global-carbonemissions.html

[5] "Greenhouse Gases and Global Warming Potential Values", US Environmental Protection Agency, April 2002

[6] "Long term Reductions in Greenhouse gas Emissions in the UK", Inter-departmental Analyst Group, DTI, February 2002

[7] C.L. Leci: Financial implications on power generation costs resulting from the parasitic effect of CO_2 capture using liquid scrubbing technology from power station flue gases, Energy Conversion and Management Volume 37, Issues 6-8,(1996), Pages 915-921

[8] M.G. Plaza, C. Pevida, B. Arias, M.D. Casal, C.F. Martín, J. Fermoso and F. Rubiera .J. J. Pis, Different Approaches for the Development of Low-Cost CO_2 Adsorbents J. Environ. Eng. 135 (2009) 426–432.

[9] Satyapal .S, Filburn .T, Trela J. and Strange J. Energy Fuels 2001 (15) 250.

[10] I.A.W. Tan, A.L. Ahmad and B.H. Hameed: Enhancement of basic dye adsorption uptake from aqueous solutions using chemically modified oil palm shell activated carbon Colloids and Surfaces A: Physicochem. Eng. Aspects 318 (2008) 88–96

[11] Tomeczek .J. and Palugnoik H. (2002): Kinetics of mineral matter transformation during coal combustion. *Fuel,* Vol. 81 (10), 1251-1258.

[12] M. Ahmaruzzaman (2009): Role of Fly Ash in the Removal of Organic Pollutants from Wastewater *Energy & Fuels* 2009, *23,* 1494–1511

[13] Zou Yong, Vera G. Mata and Al´Irio E. Rodrigues: Adsorption of Carbon Dioxide on Chemically Modified High Surface Area Carbon-Based Adsorbents at High Temperature Adsorption 7, 41–50, 2001

[14] M.G. Plaza, C. Pevida, A. Arenillas, F. Rubiera and J.J. Pis: CO2 capture by adsorption with nitrogen enriched carbon Fuel 86 (2007) 2204–2212

[15] Mohammad Saleh Shafeeyan, Wan Mohd Ashri Wan Daud, Amir Hossein Houshmand, and Arash Arami-Niya: Ammonia modification of activated carbon to enhance carbon dioxide adsorption: Effect of pre-oxidation *Applied Surface Science* (2010), doi:10.1016/j.apsusc.2010.11.127

[16] M. Mercedes Maroto-Valer, Zhe Lu, Yinzhi Zhang and Zhong Tang: Sorbents for CO_2 capture from high carbon fly ashes, Waste Management 28 (2008) 2320–2328

[17] A.Boonpoke1, S. Chiarakorn, N. Laosiripojana, S. Towprayoon and A. Chidthaisong: Synthesis of Activated Carbon and MCM-41 from Bagasse and Rice Husk and their Carbon Dioxide Adsorption Capacity, Journal of Sustainable Energy & Environment 2 (2011) 77-81

[18] Carlos A. Grande and Alı´rio E. Rodrigues: Electric Swing Adsorption for CO2 removal from flue gases international journal of greenhouse gas control 2(2008) 194 – 202

[19] Youssef Belmabkhout, Guy De Weireld, and Abdelhamid Sayari: Amine-Bearing Mesoporous Silica for CO_2 and H2S Removal from Natural Gas and Biogas, Langmuir 2009, 25(23), 13275–13278

[20] Weitkamp, J. (2000). Zeolites and Catalysis, *Solid State Ionics*.131: 175-188.

[21] Zheng, F., Tran, D. N., Busche, B. J., Fryxell, G. E., Addleman, R. S., Zemanian, T. S., and Aardahl, C. L. (2005): Ethylenediamine-Modified SBA-15 as Regenerable CO_2 Sorbent. *Ind. Eng. Chem. Res.* 44: 3099-3105.

[22] M.J. Khan, R.A. Shawabkeh, A.A. Al-Juhani, A. Ul-Hamid and I.A. Hussein: Chemical modification of waste oil fly ash for improved mechanical and thermal properties of low density polyethylene composites, J. Polymer Research, *Volume 122, (2011), Issue 4, page 2486-2496*

[23] Binici H., Gemci R., Kucukonder .A. and Solak H.H: Investigating sound insulation, thermal conductivity and radioactivity of chipboards produced with cotton waste, fly ash and barite (2012) Construction and Building Materials, 30, pp. 826-832

[24] O' Flynn C.J., Fenton O., Healy and M.G.(2012): Evaluation of amendments to control phosphorus losses in runoff from pig slurry applications to land Volume 40, Issue 2, February 2012, Pages 164-170

[25] Tanigaki N., Manako K. and Osada M.: Co-gasification of municipal solid waste and material recovery in a large-scale gasification and melting system (2012) Waste Management, 32 (4), pp. 667-675

[26] Xu H., Shao Q., Zhou, J. and Ma X. : Study on preparation of water treatment ceramic particles by using sludge and fly ash and the ceramic particles' application (2012) Advanced Materials Research, 356-360, pp. 1876-1881.

[27] ACAA 2005, Coal Combustion Product Production and Survey, http://www.acaausa.org/PDF/2005CCP Production and Use Figures Released by ACAA.pdf (accessed 1.11.06)

[28] World Coal Institute, Electricity generated from coal, 2000, http://www.wci-coal.com

[29] P. Pengthamkeerati, T. Satapanajaru and P. Chularuengoaksorn (2008): Chemical modification of coal fly ash for the removal of phosphate from aqueous solution Fuel Volume 87, Issue 12, September 2008, Pages 2469–2476

[30] Widi Astuti, Agus Prasetya, Endang Tri Wahyuni, and Made Bendiyasa: The Adsorption of Lead from Aqueous Solutions Using Coal Fly Ash: Effect of Crystallinity, World Academy of Science, Engineering and Technology 78 2011 World Academy of Science, Engineering and Technology 78 -201

[31] Deb P.K., Rubin A.J., Launder A.W. and Mancy K.H., (1966): Removal of COD from wastewater by fly ash. In proc. 21st Ind. Waste conference, D.E. Bloodygood Ed. Published by Purdue University, W. Lafayette, Indiana. 848-860

[32] R. Sanz, G. Calleja, A. Arencibia and E.S. Sanz-Pe´ re: CO_2 adsorption on branched polyethyleneimine-impregnated mesoporous silica SBA-15, Applied Surface Science 256 (2010) 5323–532

[33] Reyad Shawabkeh, Adnan Al-Harahsheh, and Awni Al-Otoom: Copper and zinc sorption by treated oil shale ash Separation and Purification Technology 40 (2004) 251–257

[34] E. Demirbas and M.Z. Nas: Batch kinetic and equilibrium studies of adsorption of Reactive Blue 21 by fly ash and sepiolite Desalination 243 (2009) 8–21

[35] R. Shawabkeh and A. Harahsheh: H_2S Removal from Sour Liquefied Petroleum Gas Using Jordanian Oil Shale Ash Oil Shale, 2007, Vol. 24, pp. 109–116

[36] Maria Visa, Cristina Bogatu and Anca Duta: Simultaneous adsorption of dyes and heavy metals from multicomponent solutions using fly ash, Applied Surface Science 256 (2010) 5486–5491

[37] Akgerman A. and Zardkoohi M. (1996): Adsorption of phenol from wastewater by peat, fly ash and bentonite. *Journal of Chemical Engineering*, *Data,* 41, 185-187.

[38] Dinesh Mohan, Kunwar P. Singh, Gurdeep Singh, and Kundan Kumar: Removal of Dyes from Wastewater Using Fly ash, a Low-Cost Adsorbent *Ind. Eng. Chem. Res.* 2002, *41,* 3688-3695

[39] M.L. Gray, Y. Soong, K.J. Champagne, John Baltrus, R.W. Stevens Jr and P. Toochinda, S.S.C. Chuang: CO_2 capture by amine-enriched fly ash carbon sorbents Separation and Purification Technology 35 (2004) 31–36

[40] Samson Oluwaseyi Bada and Sanja Potgieter-Vermaak: Evaluation and Treatment of Coal Fly Ash for Adsorption, Leonardo Electronic Journal of Practices and Technologies (2008) p. 37-48

[41] Govindasamy Chandrasekar, Won-Jin Son and Wha-Seung Ahn: Synthesis of mesoporous materials SBA-15 and CMK-3 from fly ash and their application for CO2 adsorption, J Porous Mater (2009) 16:545–551

[42] M. Olivares-Marı´n, T.C. Drage and M. Mercedes Maroto-Valer: Novel lithium-based sorbents from fly ashes for CO2 capture at high temperatures International Journal of Greenhouse Gas Control 4 (2010) 623–629

[43] Janek Reinika, Ivo Heinmaaa, Uuve Kirsoa, ToivoKallasteb, Johannes Ritamakie, Dan Bostromc, Eva Pongraczd, Mika Huuhtanene, William Larssong, Riitt Keiskie, Krisztian Kordasf and Jyri-Pekka Mikkolag: Alkaline modified oil shale fly ash: Optimal synthesis conditions and preliminary tests on CO_2 adsorption Journal of Hazardous Materials 196 (2011) 180– 186

[44] Yamin Liu, Qing Ye, Mei Shen, Jingjin Shi, Jie Chen, Hua Pan, and Yao Shi: Carbon Dioxide Capture by Functionalized Solid Amine Sorbents with Simulated Flue Gas Conditions Environ. Sci. Technol. 2011, 45, 5710–5716

[45] Vivek Kumar, Nitin Labhsetwar, Siddharth Meshram, and Sadhana Rayalu: Functionalized Fly Ash Based Alumino-Silicates for Capture of Carbon Dioxide Energy Fuels 2011, 25, 4854–4861

[46] Honghong Yi, Hua Deng, Xiaolong Tang, Qiongfen Yu, Xuan Zhou and Haiyan Liu: Adsorption equilibrium and kinetics for SO_2, NO, CO_2 on zeolites FAU and LTA Journal of Hazardous Materials 203– 204 (2012) 111– 117

[47] Reyad Shawabkeh, Muhammad J. Khan, Abdulhadi A. Al-Juhani, Hamad I. Al-Abdul Wahab and Ibnelwaleed A. Hussein: Enhancement of surface properties of oil fly ash by chemical treatment Applied Surface Science 258 (2011) 1643– 1650

[48] A. Palomo, M.W. Grutzeck and M .T. Blanco: Alkali activated fly ashes cement for the future, Cem. Concr. Res. 29 (8) (1999) 323–1329.

[49] Gyu Hwan and Chong Rae Park: Preparation and characteristics of rice straw-bases porous carbon with high adsorption capacity. Fuel (2002) 327

[50] A. Ferna´ndez-Jime´nez and A. Palomo: Composition and microstructure of alkali activated fly ash binder: Effect of the activator Cement and Concrete Research 35 (2005) 1984 – 1992

[51] A. Palomo, S. Alonso, A. Ferna´ndez-Jime´nez, I. Sobrados and J. Sanz: Alkaline activation of fly ashes. A 29Si NMR study of the reaction products, J. Am. Ceramic Soc. 87 (6) (2004) 1141– 1145

[52] A. Ferna´ndez-Jime´nez and A. Palomo: Alkali activated fly ashes Structural studies through Mid-Infrared Spectroscopy'' Microporous and Mesoporous Mat. *Volume 86, Issues 1–3*, *28 November 2005*, *Pages 207-214*.

[53] X. Zhaohui and X. Yunping, *Cement & Concrete Research*, 31, 1245 (2001)

[54] Sang-Sook Park and Hwa-Young Kang: Characterization of fly ash-pastes synthesized at different activator conditions *Korean J. Chem. Eng.*, 25(1), 78-83 (2008)

[55] Van J.G. S. Jaarsveld and Van J. S. J. Deventer, *Miner. Eng.*, 10, 659 (1997)

[56] M.M. Bekheita, N. Nawara, A.W. Addison, D.A. Abdel-Latifa and M. Moniera: Preparation and characterization of chitosan-grafted-poly(2-amino-4,5-pentamethylene-thiophene-3-carboxylic acid N-acryloyl-hydrazide) chelating resin for removal of Cu(II), Co(II) and Ni(II) metal ions from aqueous solutions International Journal of Biological Macromolecules 48 (2011) 558–565

[57] Y. Jiang, E.R. Elswick and M. Mastalerz: Progression in sulfur isotopic compositions from coal to fly ash: examples from single-source combustion in Indiana, International Journal of Coal Geology 73 (2008) 273.

[58] R.A. Shawabkeh: Synthesis and characterization of activated carbo-aluminosilicate material from oil shale, Microporous and Mesoporous Materials 75 (2004) 107

[59] G.H. Oh, C.H. Yun and C.R. Park, Role of KOH in the one-stage KOH activation of cellulosic biomass, Carbon Sci. 4 (4) (2003) 180–184

[60] Xiaoping Zhanga, Xin Zhaoc, Jiaqi Hu, Chaohai Weia and Hsiaotao T. Bib: Adsorption dynamics of trichlorofluoromethane in activated carbon fiber beds Journal of Hazardous Materials 186 (2011) 1816–1822

[61] M.S. Chiou and H.Y. Li: Adsorption behavior of reactive dye in aqueous solution on chemical cross-linked chitosan beads Chemosphere 50 (2003) 1095–1105

[62] X.P. Zhang, S.X. Chen and X.T. Bi: Application of wave propagation theory to adsorption breakthrough studies of toluene on activated carbon fiber beds, Carbon 48 (2010) 2317–2326

[63] R. Leyva-Ramos, P.E. Diaz-Flores, J. Leyva-Ramos and R.A. Femat-Flores: Kinetic modeling of pentachlorophenol adsorption from aqueous solution on activated carbon fibers, Carbon 45 (2007) 2280–2289.

[64] Cheng, Q., Pavlinek, V., Li, C., Lengalova, A., He, Y., and Saha, P. (2006): Synthesis and Characterization of New Mesoporous Material with Conducting Polypyrrole Confined in Mesoporous Silica. *Mater. Chem. Phys.* 98: 504-508.

[65] A.C. Lua and Q.P. Jia: Adsorption of phenol by oil–palm-shell activated carbons in a fixed bed, Chem. Eng. J. 150 (2009) 455–461.

[66] Jingjing Peia and Jianshun S. Zhang: Determination of adsorption isotherm and diffusion coefficient of toluene on activated carbon at low concentrations Building and Environment 48 (2012) 66-76

[67] Z. W. Chen and M. Chanda, J. Polym. Material 2002, 19, 381

[68] Sunho Choi, Jeffrey H. Drese and Christopher W. Jones: Adsorbent Materials for Carbon Dioxide Capture from Large Anthropogenic Point Sources ChemSusChem 2009, 2, 796 – 854

[69] M. B. Yue, Y. Chun, Y. Cao, X. Dong and J. H. Zhu, Adv. Funct. Mater. 2006, 16, 1717

[70] Monier, M. and D. A. Abdel Latif : Adsorption of Hg^{2+}, Cu^{2+} and Zn^{2+} ions from aqueous solution using formaldehyde cross-linked modified chitosan-thioglyceraldehyde Schiff's base (2012) International Journal of Biological Macromolecules, 50 (3), pp. 773-781.

[71] *Reyad Shawabkeh:* Equilibrium study and kinetics of Cu2+ removal from water by zeolite prepared from oil shale ash Process, Safety and Environmental Protection 87 (2009) 261–266

[72] C. Namasivayam and D. Kavitha1: Removal of Congo Red from water by adsorption onto activated carbon prepared from coir pith, an agricultural solid waste Dyes and Pigments 54 (2002) 47–58

[73] I.A.W. Tan, B.H. Hameed and A.L. Ahmad: Equilibrium and kinetic studies on basic dye adsorption by oil palm fibre activated carbon Chemical Engineering Journal 127 (2007) 111–119

[74] V.K. Gupta, I. Ali,b Suhas, and Dinesh Mohan: Equilibrium uptake and sorption dynamics for the removal of a basic dye (basic red) using low-cost adsorbents Journal of Colloid and Interface Science 265 (2003) 257–264

[75] I.A.W. Tan, A.L. Ahmad and B. H. Hameed. Adsorption of basic dye on high-surface-area activated carbon prepared from coconut husk: Equilibrium, kinetic and thermodynamic studies Journal of Hazardous Materials 154 (2008) 337–346

[76] Zou, W., Han, R., Chen, Z., Jinghua, Z. and Shi, J., (2006): Kinetic study of adsorption of Cu (II) and Pb (II) from aqueous solutions using manganese oxide coated zeolite in batch mode. Colloids and Surfaces A: Physicochemical and Engineering Aspects, 279(1–3): 238

[77] Yahya S. Al-Degs a, Musa I. El-Barghouthi a, Amjad H. El-Sheikh and Gavin M. Walker: Effect of solution pH, ionic strength, and temperature on adsorption behavior of reactive dyes on activated carbon Dyes and Pigments 77 (2008) 16-23

[78] Faust S and Aly O: Adsorption processes for water treatment. Butterworth Publishers; 1987

[79] Monier, M. and D. A. Abdel Latif: preparation of cross-linked magnetic chitosan-phenylthiourea resin for adsorption of Hg(II), Cd(II) and Zn(II) ions from aqueous solutions (2012) Journal of Hazardous materials 209-210(2012) 240-249.

[80] M. Monier, N. Nawar and D.A. Abdel-Latif: Preparation and characterization of chelating fibers based on natural wool for removal of Hg(II), Cu(II) and Co(II) metal ions from aqueous solutions Journal of Hazardous Materials 184 (2010) 118–125

[81] Y. Jiang, E.R. Elswick and M. Mastalerz: Progression in sulfur isotopic compositions from coal to fly ash: examples from single-source combustion in Indiana, International Journal of Coal Geology 73 (2008) 273

[82] G.G. Stavropoulos and A.A. Zabaniotou: Production and characterization of activated carbons from olive-seed waste residue, Microporous Mesoporous Mater. 82 (2005) 79–85.

[83] R.L. Tseng, S.K. Tseng and F.C.Wu: Preparation of high surface area carbons from Corncob with KOH etching plus CO2 gasification for the adsorption of dyes and phenols from water, Colloids Surf. A 279 (2006) 69–78.

[84] Singh B.K. and Nayak P.S. (2004): Sorption equilibrium studies of toxic nitro-substituted phenols on fly ash. *Adsorption Science and Technology*, Vol. 22, 295-310.

[85] Singh, P.K., Mohan, D., Singh, G. and Kumar, K. (2002). Removal of dyes from wastewater Using fly ash, a low-cost adsorbent, *Industrial and Engineering Chemistry Research*, Volume 41, 3688-3695.

[86] A. Dabrowski, Adsorption-from theory to practice, Advances in Colloid and Interface Science, 93 (2001) 135-224

[87] Zhang, X., Schubert, S., and Agar, D. W. (2005). Studies on the Kinetics of Carbon Dioxide absorption with Immobilised Amines (IA) *Chem. Eng. J.* 107: 97-102.

[88] Maroto-Valer .M.M., Tang Z. and Zhang Y., 2005: CO_2 capture by activated and impregnated anthracites. Fuel Processing Technology 86(14–15), 1487–1502

[89] Xu, X., Song, C., Andresen, J. M., Miller, B. G., and Scaroni, A. W. (2002). Novel Polyethylenimine-Modified Mesoporous Molecular Sieve of MCM-41 Type as High-Capacity adsorbent for CO2 Capture. *Energy & Fuels* 16: 1463-1469

[90] L. B. Adams, C. R. Hall, R. J. Holmes, R. A. Newton, Carbon 1988, 26, 451

[91] S. K. Verma, J. Walker, P. L., Carbon (1992), volume 30, 8

VITAE

NAME:	Ali Lawan Yaumi
DATE OF BIRTH:	31st March 1982
PLACE OF BIRTH:	Maiduguri, Nigeria.
NATIONALITY:	Nigerian
PRESENT ADDRESS:	Chemical Engineering Department King Fahd University of Petroleum and Minerals P.O Box 8595, Dhahran, 31261, Saudi Arabia
PERMANENT ADDRESS:	C/o Alh Lawan Yaumi, Kashim Ibrahim College of Education, P.M.B 1469 Maiduguri, Borno State
EMAIL:	aliyaumi001@yahoo.com
MOBILE NUMBER	+2348037387456
EDUCATIONAL QUALIFICATIONS:	**M. Sc.** ***(Chemical Engineering)*** May, 2012 King Fahd University of Petroleum and Minerals, Dhahran, Saudi Arabia. **B. Eng (*Chemical Engineering)*** February, 2008 University of Maiduguri, Borno State, Nigeria.